

Optimization of sizing, modeling and power
converter for Hybrid Renewable Power system
in remote locations for desalination
Applications

by

R. NAGARAJ

ENGG 02201104041

Indira Gandhi Centre for Atomic Research

A thesis

Submitted to

The Board of Studies in Engineering Sciences

In partial fulfillment of requirements for the Degree of

DOCTOR OF PHILOSOPHY

of

HOMI BHABHA NATIONAL INSTITUTE



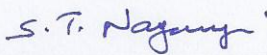
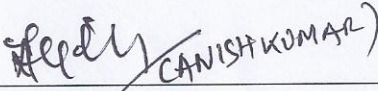
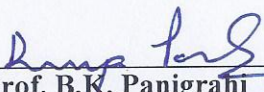

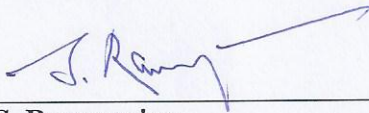
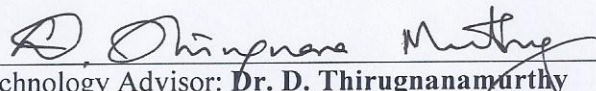
July 2019

Homi Bhabha National Institute

HomiBhabha National Institute¹

Recommendations of the Viva Voce Committee

As members of the Viva Voce Committee, we certify that we have read the dissertation prepared by Mr. R. NAGARAJ entitled "Optimization of sizing, modeling and power converter for Hybrid Renewable Power system in remote locations for desalination Applications" and recommend that it may be accepted as fulfilling the thesis requirement for the award of Degree of Doctor of Philosophy.

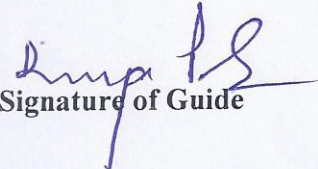
	9/7/19
External Examiner - Prof. S.T. Nagarajan, Elec. Engg. Dept, Delhi Tech. University.	Date:
 CANISH KOMAR	9/7/19
Chairman - Prof. M. Saibaba	Date:
	9/7/19
Guide / Convener - Prof. B.K. Panigrahi	Date:
	9/7/2019
Member 1- Prof. B.P.C. Rao	Date:
	
Member 2- Prof. S. Rangarajan	Date: 09.07.2019
	
Technology Advisor: Dr. D. Thirugnanamurthy	Date: 9.7.19

Final approval and acceptance of this thesis is contingent upon the candidate's submission of the final copies of the thesis to HBNI.

I/We hereby certify that I/we have read this thesis prepared under my/our direction and recommend that it may be accepted as fulfilling the thesis requirement.

Date: 9/7/19

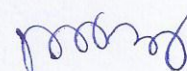
Place: Kallakur


Signature of Guide

Statement by Author

This dissertation has been submitted in partial fulfillment of requirements for an advanced degree at Homi Bhabha National Institute (HBNI) and is deposited in the Library to be made available to borrowers under rules of the HBNI.

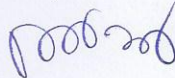
Brief quotations from this dissertation are allowable without special permission, provided that accurate acknowledgement of source is made. Requests for permission for extended quotation from or reproduction of this manuscript in whole or in part may be granted by the Competent Authority of HBNI when in his or her judgment the proposed use of the material is in the interests of scholarship. In all other instances, however, permission must be obtained from the author.



R. NAGARAJ

Declaration

I, hereby declare that the investigation presented in the thesis has been carried out by me. The work is original and has not been submitted earlier as a whole or in part for a degree / diploma at this or any other Institution / University.



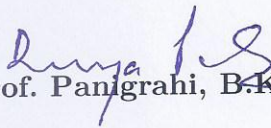
R. NAGARAJ

CERTIFICATE

I hereby certify that I have read thesis dissertation prepared under my direction and recommend that it may be accepted as fulfilling the dissertation requirement

Date: 9/7/19

Place: Kalpakkam


[Prof. Panigrahi, B.K.]

Guide & Convenor

List of Publications

Journal

1. Nagaraj R, D.Thirugnanamurthy, M.M. Rajput, M.Sai Baba, “Brackish Water RO plant as a variable load for Renewables based Hybrid Power System for increased power output”, *Int. J. Desalination and Water Treatment, Taylor & Francis (Desalination) Publication, Vol.88 (2017)* pp:33-40 ISSN: 1944-3994, doi: 10.5004/dwt.2017.21414.
2. Nagaraj R, D.Thirugnanamurthy, M.M. Rajput, M.Sai Baba, “Modelling of High Step-up Converter in closed loop for Renewable Energy Applications”, *Int. J. Environment, Development and Sustainability, Springer Link Publishers, 2017, Vol.19, Issue : 6, pp: 2475 – 2485, ISSN : 1387-585X, doi: 10.1007/s10668-016-9866-8.*
3. Nagaraj R, D.Thirugnanamurthy, M.M. Rajput, B.K. Panigrahi, “Techno-economic analysis of hybrid power system sizing applied to small desalination plants for sustainable operation”, *Int.J. of Sustainable Built Environment (2016), Elsevier Publishers, , 2016, Vol.5, Issue 2, ISSN: 2212-6090, pp 269-276, doi: 10.1016/j.ijsbe.2016.05.011*
4. Nagaraj R, D.Thirugnanamurthy, M.M. Rajput, “Modeling of Renewables based Hybrid Power System with Desalination Plant load using Neural Network”, *Int. J. Distributed Generation & Alternative Energy, Taylor & Francis Publication, Dec 2018, Vol.34(1), ISSN 2156-3306.*
5. Nagaraj R, Swaminathan P, “Feasibility Analysis of Eco-Friendly Hybrid Power Based R.O. for Remote Locations”, *Int. J. of Environmental Sciences, 2012, Vol.1, No. 2, ISSN: 2301-3656, pp 226 -232.*

Conferences:

1. Nagaraj, R., "Renewable energy based small hybrid power system for desalination applications in remote locations," IEEE Xplore Power Electronics, vol., no., pp.1-5, ISSN: 2160-3162, Print ISBN: 978-1-4673-0931-8, Dec 2012, DOI: 10.1109/IICPE.2012.6450437.
2. Nagaraj R, Dr. Panigrahi B.K., et.al., “Techno-economic Analysis of Hybrid Power System Sizing Applied to Small Desalination Plants”, International Conference on Innovative Technologies and Management for Water Security INDACON14 during Feb 2014 at NIOT, Chennai

3. Nagaraj R, Invited talk on “Fast forward solar energy utilization using intelligent control techniques“ 10-11 Oct 2014 at Mewar University, Chittorgarh, Rajasthan.
4. Sujatha, K.; Nagaraj, R.; Ismail, M.M., "Real time supervisory control for hybrid power system," IEEE xplore - Green Computing, Communication and Conservation of Energy, vol., no., pp.415-418, Dec. 2013, doi: 10.1109/ICGCE.2013.6823471
5. R. Nagaraj, Dr. B.K. Panigrahi, T. Prabakaran, K. Linish, Vishnu Pandey, M.M.Rajput, Dr. P.K. Tewari, “Size Optimization and Simulation studies of Renewable sources based Co-generation systems with BWRO plant as energy storage alternative”, Trombay Symposium on Desalination and Water Reuse’15(TSDWR2015), Jan 22-23, 2015 at Homi Bhabha Centre for Science Education, TIFR, Mumbai organized by Indian Desalination Association.
6. R. Nagaraj, K. Linish et.al. “Integrated water and power generation using renewable energy based hybrid power systems”, National seminar cum workshop on water and energy: Sustainability and security for future needs (WAVE-2012), Mumbai, Sep 2012

Acknowledgements

As a first person, I would like to express my sincere gratitude to my guide Prof. B.K. Panigrahi whose enlightening guidance, critical observations and intellectual support have enriched me throughout my research work.

I wish to record my sincere thanks to Shri. M.M. Rajput, Head, NDDP, BARC for having permitted me to pursue this course and research work.

I gratefully acknowledge the contributions of the members of Doctoral Committee for their critical review and suggestions during the progress review and pre-synopsis viva- voce. I would like to make a special mention about Chairman Prof. M. Sai Baba, Prof. B.P.C Rao and Prof. S. Rangarajan for their intriguing questions during reviews and other personal meetings. Searching answers for the questions raised formed the basis of many of my publications. I record my sincere gratitude to my technology advisor Dr. D. Thirugnanamurthy for his valuable contributions in the research work and thesis preparation. I wish to record my sincere thanks to Prof. G. Sasikala, Dean, Engg. Sciences for her constant support.

Special thanks are due to Dr. Anees, Dr. Gurpreet kaur and Smt. Jemima Ebenezer for their patient review of thesis and Shri. Jegadeesan who helped in formatting the thesis.

Acknowledgements are due to my colleagues of NDDP, BARC for their constant support throughout the research work.

Finally, I express my gratitude to my parents, wife and children, who have always shown keen interest in my progress of work and for being source of inspiration and pillar of support for my life.

CONTENTS

	Page No.
SYNOPSIS	i
LIST OF FIGURES	xii
LIST OF TABLES	xv
LIST OF ABBREVIATIONS	xvi

Table of contents

1	INTRODUCTION	1
1.1	Introduction.....	1
1.2	Energy scenario.....	1
1.2.1	Primary energy sources	2
1.2.2	Remaining reserves of fossil fuel	3
1.2.3	Environmental impacts of energy	3
1.3	Water scenario.....	4
1.4	Desalination	7
1.1	Energy Implications of Desalination	9
1.2	Energy-Water nexus	9

1.3	Energy-related risks to water security	11
1.3.1	Limited or unreliable and affordable energy for extraction of water	11
1.3.2	Water for energy production and related problems.....	12
1.3.3	Pollution of water due to energy-related activities.....	12
1.4	LITERATURE SURVEY.....	13
1.4.1	Renewables based desalination.....	13
1.4.2	Solar PV based Desalination.....	17
1.4.3	Wind energy based Desalination	17
1.4.4	Desalination Costs.....	18
1.4.5	Challenges	20
1.4.6	Hybrid renewables based desalination	20
1.4.7	Motivation and objectives:.....	24
1.5	Thesis organization.....	26
2	SIZE ANALYSIS AND OPTIMIZATION OF RENEWABLE HYBRID POWER SYSTEMS.....	27
2.1	Introduction.....	27
2.1.1	Energy storage systems: (ESS).....	28
2.1.2	Reverse Osmosis (RO) desalination using solar PV and wind Energy	29
2.2	Hybrid Solar PV-Wind power scheme	30
2.3	Modeling the renewable energy systems.....	31
2.3.1	Solar Photovoltaic.....	31
2.3.2	Wind energy.....	34
2.3.3	Energy storage battery.....	35

2.3.4	Assumptions.....	36
2.4	Cost Model of solar PV, wind and battery system	36
2.5	Techno-economic analysis of hybrid power system	38
2.6	Data.....	39
2.7	Simulation methodology	39
2.8	Results and discussions	42
2.8.1	Monthly distribution of power generation	44
2.8.2	Analysis of Cost of Energy Vs. Energy production	46
2.8.3	Availability of power Vs. Cost of Energy	47
2.9	Brackish Water RO plant as a variable load for Renewables based Hybrid Power System for increased power utilization	50
2.10	Simulation Methodology with desalination plant as load.....	50
2.11	Results and discussions	52
2.11.1	Cost of Water for various combinations of PV and wind capacities.....	57
2.12	Conclusion	61
3	MODELING OF RENEWABLES BASED HYBRID POWER SYSTEM WITH DESALINATION PLANT LOAD USING NEURAL NETWORK	63
3.1	Introduction.....	63
3.2	Introduction to ANN	63
3.3	Modeling the Biological Neuron.....	65
3.4	Building Blocks of ANN	67
3.4.1	Network Architecture.....	67
3.4.2	Setting the weights.....	69

3.4.3	Activation Functions.....	69
3.5	Advantages of ANN:.....	70
3.6	ANN Vs Traditional statistical methods.....	70
3.7	Back Propagation Network (BPN)	71
3.7.1	Architecture	71
3.7.2	Training Algorithm	72
3.8	Modeling hybrid Solar PV-Wind Power Scheme	76
3.9	Proposed Neural Network Model	77
3.9.1	Training	79
3.9.2	Validation and Verification:	81
3.9.3	Verification	83
3.9.4	Neural network model	84
3.10	Conclusion	86
4	HIGH STEP-UP CONVERTER IN CLOSED LOOP FOR RENEWABLE ENERGY APPLICATIONS.....	87
4.1	Introduction.....	87
4.2	Background.....	87
4.3	Description and modeling of the High Step-up Converter	89
4.4	Results - MATLAB Modeling and Simulation.....	97
4.5	Performance with variation in input voltage:	101
4.6	Experimental details and setup	105
4.7	Errors associated with measurements:	109
4.8	Experimental results	110

4.9	Conclusion	113
5	CONCLUSIONS AND FUTURE SCOPE OF WORK	114
5.1	Summary of major findings.....	115
5.2	Major contributions:	117
5.3	Directions for future scope of work	118
	REFERENCES	120
	Appendix - A.....	136
	Appendix - B.....	147

SYNOPSIS

Introduction:

The energy consumption keeps on growing with the increase in world population as well as the living standard. In spite of improvements in energy efficiency, the demand has increased. This demand at present and in future is for electrical power generation. The fossil fuel prices have to eventually increase due to its limited availability causing that the policymakers have to look for other sustainable sources of energy. Wind and solar photo voltaic are the most promising renewable sources, in addition to hydroelectric power sources which have been traditionally exploited.

Water is a critical resource and water security is a necessary criterion for a country's sustainable development. A huge gap exists between the demand and availability of fresh water. Desalination of seawater/saline groundwater is the option available to fill the gap between the availability and demand for fresh water. A variety of desalination processes have been developed. All these processes demand a significant amount of energy. There are many parts of the country which does not have the conventional source of power and costs of extending the electricity grid to these places are very high. Fortunately, there are many parts of the country that have water shortage but have exploitable renewable sources of energy that could be used to drive desalination processes. Renewable energy systems utilize sources available locally and freely for production of energy. Producing the fresh water at source using desalination technologies that are driven by renewable energy systems is a viable solution to

the water scarcity at remote locations and islands that are characterized by both lack of adequate potable water and access to conventional energy sources like heat and electricity grid.

Renewable energy sources have the inherent problems of intermittency, uncertainty, and low availability which makes the power supply more unreliable. Huge energy storage systems like batteries are to be employed to increase the availability. Photovoltaic (PV) and wind power are complementary because sunny days mostly have very low wind while the cloudy days and nights are more likely to have strong winds. Therefore, hybrid PV-Wind systems can have higher availability and reliability than systems based on individual PV or wind sources. Therefore, this study is orientated towards hybrid PV-Wind systems suitable for small-scale desalination plants. The desalination plant can act as a variable load and can effectively attack the problem of intermittency and variability of renewable power.

The performance of the hybrid power system largely depends on the proper combination of capacities of the individual system like PV and wind generator. The power generation depends on instantaneous solar irradiation and the wind speed also. On the other hand, the load requirement variations also affect the overall generation. This makes it necessary to study the overall annual power generation for various combinations of PV-Wind capacities under varying load conditions. Also, there is a need to develop high efficient power converter that can take multiple renewable energy inputs with a closed loop controller. Further, there is a need to develop a comprehensive model for annual power generation for

the PV-wind hybrid system for a particular site (e.g. Kalpakkam) and the annual water production under a given site conditions to assess the feasibility.

Thesis organization

A general introduction and literature survey along with motivation of the work and objectives are given in Chapter 1. Chapter 2 presents the modeling of the hybrid power system and analysis with various capacities of the same. Chapter 3 deals with the Neural Network based modeling of the hybrid power system. Chapter 4 explains the development of a power converter for the multiple renewable energy sources. The last chapter summarizes the overall conclusions and salient findings of the entire study and scope of further works. The contents of the individual chapters are given below.

Chapter 1: Introduction

This chapter gives a brief introduction to the energy requirement and status of renewable energy systems. The nexus between energy and water is also explained. The need for co-generation of power and water is emphasized. The uncertainties in renewable energy supply due to its intermittent nature is explained. The requirement of the hybrid power system and the present status is also presented. The need for selection of a proper combination of renewable energy capacities and the effect of load variations are also discussed. Finally, the motivation for the study and the objectives of the studies are stated.

Chapter 2: Modeling and Size Optimization Analysis of Hybrid Power System

This chapter deals with the system under study and analysis on the combination of capacities of the system. A methodology of selection of the capacities of various power sources of the hybrid power system is developed for obtaining the optimum configuration. The optimum configuration can be chosen based on our objectives.

A hybrid PV-Wind energy conversion system (with battery storage) and desalination plant as the load are proposed in this study as a small-scale standalone system. The main energy sources for the system are wind and PV generators, while the battery bank works as an energy storage backup source. The system taken for modeling is, intended to be used for water pumping system of the desalination plant.

The modeling of solar PV system is carried out. The equivalent circuit of solar PV system is discussed. The basic equations governing the power generated are explained. Maximum Power Point Tracking (MPPT) algorithm is implemented to maximize the power output from the PV cells with varying radiations. From this, the output power can be calculated. At each point of output power, the maximum power is measured by using the Perturb & Observe (P&O) method which is used to determine the value of reference current to adjust the output power toward the maximum point.

Similarly, the modeling of wind generator system was also carried out. The output of a wind turbine depends primarily on the wind velocity. The input to

the wind model is the average wind velocity for the hour and the generator constants which depend on the capacity of the generator chosen. From this, the power output of the wind generator is determined.

The modeling of the battery system is also done on the basis of charging power received, discharged capacity and efficiency of the battery.

The cost model of the various energy sources is developed considering the capital cost per kW capacity. The annualized capital costs are calculated by using the capital recovery factor which is calculated by taking the life span of systems and the interest rate into account. Also, the operation and maintenance costs are included in the model. The annual total cost of the hybrid power system for a particular set of capacities of solar PV, wind, and battery is finally calculated by summation of the individual costs. Thus the entire system under study is modeled.

The selection of capacities of solar PV, wind generator, and battery greatly affects the total power generated in a particular year, capital cost and the Operation & Maintenance cost of the system. This has got a direct bearing on the Cost of Energy per unit of power generated (COE) and the availability of power for the load. Hence an in-depth techno-economic analysis of the combination of different renewables is necessary to obtain enough understanding of the system. The entire hybrid power system is modeled in MATLAB software. The main objective of the model is to analyze the various combinations of solar PV, wind generator and battery capacities with respect to total power generation, availability and cost of energy per unit.

The simulation is carried out for various combinations of solar PV capacities, wind generator capacities, and battery capacities. The hourly solar irradiance data measured in kWh/m²/day and wind speed data in m/s are given as inputs for simulation. The above data is used to calculate the power output available from PV and wind sources using the models. The power generated is calculated for every hour of the day for a complete year (8760 hours). The hybrid power system shall be designed to feed power to a brackish water desalination plant of 24 m³/day capacity.

It is observed that the desalination plant caters the need of both the variable load and the energy storage requirements of the renewable power systems. This helps to extract maximum possible power generation from the system. Hence the hybrid PV-wind system is more economical and reduces the need for high battery storage capacities. For an objective of around 6000 kWh per year power production, the best option is the combination of 8 kW Solar PV , 1 kW Wind and 1.5 kW storage battery for obtaining energy at cost of INR 12.73 per kWh with an availability of 40% . For lowest cost of energy / kWh, we can select a combination of 5 kW Solar PV, 1 kW Wind and 0.5 kW battery. With the above combination, we get the lowest cost of energy at INR 11.32 per kWh, but the total power produced in the year is around 5000 kWh with an availability of only 29%. For application of this hybrid power system for desalination purpose that requires a variable load of 2 kW, the necessity of energy storage battery is reduced. There is an average increase of around 25% in utilization of power generated. In the case of desalination plant as load, the hybrid power system can

produce and store water in suitable tanks and hence the availability factor is not a major concern. For an objective of lower cost of water, we can select the combination of 5 kW solar PV, 1 kW wind and 0.5 kW battery to produce a total of 6906 m³ of product water at a cost of INR 80 per 1000 liters. This comes with an availability of plant of around 28% which can be compensated by selecting suitable storage tanks.

Similarly, for a high production of water at around 7500 m³, we can select the combination of 10 kW solar PV, 2 kW wind and 0.5 kW storage battery to produce water at a cost of INR 116 per 1000 liters of water and the availability is around 54%. The cost economics is highly viable in remote locations and islands where there is no availability of conventional grid power and water.

Chapter 3: Neural Network Modeling of Annual Power Generation

The estimation of total annual power generation of a particular combination of hybrid power system is an elaborate process and hence there is a need for a model to make a quick estimation of the annual power generation. This chapter deals with modeling of hybrid renewable power system using Artificial Neural Network (NN).

The configuration and the power generation data developed in Chapter 2 is chosen for neural network modeling. A neural network model is developed for the above system with solar PV, wind generator and battery capacity as inputs and total power (kWhr) production per year as the output. The neural network has three layers viz. input layer, a hidden layer, and the output layer. The input

layer is composed of three nodes as inputs: solar PV capacity, wind generator capacity, storage battery capacity. The hidden layer is made up of five nodes whose activation function is the hyperbolic tangent sigmoid transfer function. The output layer is composed of one node, and this represents the required output (i.e.) the estimated total kWhr produced for the year for a given set of capacities as input. The input comprising of 400 data set is used for training of the chosen neural network. The weight values are adjusted using this data set during training according to the error calculated using the training algorithm. The input weight matrix, bias and weight matrix for hidden layer and the bias for the output layer are calculated. The chosen architecture converged in 217 iterations. The trained model was validated and verified using 60 data sets. The NN model fitted with very high regression values above 0.99 indicating the accuracy of the NN model. With the model, the total kWh produced in a given year for a given capacity of solar PV, wind generator, and battery capacity is estimated.

Chapter 4: High step-up converter in closed loop for Renewable energy applications

Since a majority of small scale renewable energy sources (RES) including the solar PV modules gives the output voltage in the range of around 15 – 40 V DC, the output needs to be stepped up to suit the load requirements using a high voltage gain converter. The renewable sources inherently generate sudden variations in input voltage, a good output voltage profile even during such random variations in input conditions is essential. Such power converter enables deployment of hybrid renewable systems for standalone desalination applications.

This chapter presents prototype development of a high step-up converter configuration with closed loop control. The converter topology is explained and the design of the circuit is elaborated. The converter for hybrid power system that can handle two input sources is developed and tested.

A 100 W high step up dc-dc converter prototype with two input sources is developed. The converter is designed in closed loop to deliver an output voltage of around 200 V with variable input voltage in 15 V to 40 V range. The proposed configuration is suitable for application for renewable sources based systems.

The circuit components and parameters are designed from the design equations Eq. 4.1 to Eq. 4.7. The turns ratio (n) of coupled inductor is chosen to be 5 for a moderate duty cycle of 0.4 to 0.6 to obtain the desired voltage ratio in the range of 8 to 17. The inductance of coupled reactor is designed for a value of 30 μ H. Other capacitors and resistor values are also chosen using the design equations. The transfer function is derived for closed loop operation of the designed circuit. The controller is tuned and the proportionality constant K_p and integral constant K_i values are set at 9.1 and 1.7 respectively. We obtained the stable performance with less than 17% peak overshoot and rise time of less than 0.2 ms. The designed circuit is subjected to both steady and random input voltage variations and the output voltage is found to be within $\pm 5\%$ range.

Chapter 5: Conclusions and Future scope of work

This chapter summarizes the findings and proposes lines of future work that will be of important to this technology. The hybrid renewable power system for

desalination applications in remote locations and islands is developed. The following is the summary of the work.

1. A methodology of selection of the capacities of various power sources of the hybrid power system is developed for obtaining the optimum configuration. The optimum configuration can be chosen based on the requirement.
2. From the results obtained, we can see that addition of capacities of PV panels or Wind turbines or storage capacities separately does not help in reduction of the cost of energy. But, when the capacities of Solar PV and Wind turbines are supplemented with each other, we find that we are able to maintain the total kWh produced per year to meet the load requirements.
3. For a requirement of around 6000 kWh per year power production, the best option obtained is the combination of 8 kW Solar PV , 1 kW Wind and 1.5 kW storage battery for obtaining energy at cost of INR 12.73 per kWh with an availability of 40% .
4. If the requirement is only the lowest cost of energy / kWh, we can select a combination of 5 kW Solar PV, 1 kW Wind and 0.5 kW battery. With the above combination, we get the lowest cost of energy at INR 11.32 per kWh, but the total power produced in the year is around 5000 kWh with an availability of only 29%.
5. In the case of desalination plant as load, the hybrid power system can produce and store water in suitable tanks and hence the availability factor is not a major concern. The necessity of energy storage battery is also reduced. For application of hybrid power system for desalination purpose that requires a load of 2 kW, there is an average increase of around 25% in utilization of power generated, when used for desalination plant.

6. For lower cost of water, we can select the combination of 5 kW solar PV, 1 kW wind and 0.5 kW battery to produce a total of 6906 m³ of product water at a cost of INR 80 per 1000 liters. This comes with an availability of plant of around 28% which can be compensated by selecting suitable storage tanks.
7. Similarly, for a high production of water at around 7500 m³, we can select the combination of 10 kW solar PV, 2 kW wind and 0.5 kW storage battery to produce water at a cost of INR 116 per 1000 liters of water and the availability is around 54%.
8. A neural network model is proposed for the above system with Solar PV, Wind generator and battery capacities as inputs and total kWh production per year as the output. The proposed three layer architecture is trained to obtain the required performance optimization. The network estimates the total power generated per year for a given capacity of Solar PV, Wind generator and Battery. The developed model predicts the unknown test data with regression of 0.99.
9. A prototype power converter configuration for the renewable energy application is developed. The circuit components and parameters are fixed from the design. The turns ratio (n) of coupled inductor is chosen to be 5 for a moderate duty cycle of 0.4 to 0.6 to obtain the desired voltage ratio in the range of 8 to 17. The transfer function is derived for closed loop operation of the designed circuit. We obtained the stable performance with less than 17% peak overshoot and rise time of less than 0.2 ms. The designed circuit is subjected to both steady and random input voltage variations and the output voltage is found to be within $\pm 5\%$ range.

The renewable energy based hybrid power system will be the future of power solution for remote and isolated locations. Also, such systems with specific load applications can be developed and brought into the market with some more study and testing.

List of Figures

<i>Figure 1.1 Global Energy consumption in TWh/year from 1965 to 2015 /</i>	<i>2</i>
<i>Figure 1.2 Years of fossil fuel reserves left</i>	<i>3</i>
<i>Figure 1.3 Global water distribution</i>	<i>5</i>
<i>Figure 1.4 Water stress map of India</i>	<i>6</i>
<i>Figure 1.5 Schematic representation of desalination system</i>	<i>8</i>
<i>Figure 1.6 A typical solar PV - wind hybrid power system</i>	<i>21</i>
<i>Figure 1.7 Solar resource map of India</i>	<i>22</i>
<i>Figure 1.8 Wind resource map of India./</i>	<i>23</i>
<i>Figure 2.1 Schematic diagram of a typical Hybrid power system</i>	<i>30</i>
<i>Figure 2.2 Schematic representation of a PV cell</i>	<i>32</i>
<i>Figure 2.3Trend line showing total power produced (in kWh) / per year for various combinations of capacities</i>	<i>43</i>
<i>Figure 2.4 Individual PV & wind power generation - Monthly distribution</i>	<i>44</i>
<i>Figure 2.5 Monthly power generation of solar PV and wind</i>	<i>45</i>
<i>Figure 2.6 Comparison of trend of Cost of Energy and Units produced for various sizing combination of energy sources</i>	<i>46</i>
<i>Figure 2.7 Effect of availability and Cost of energy [in Indian Rupees (INR)] colour coded with total power produced per year.</i>	<i>48</i>
<i>Figure 2.8 3-D Plot showing cost of energy / unit, % availability and total units produced / year.</i>	<i>49</i>
<i>Figure 2.9 Proposed methodology of simulation</i>	<i>51</i>
<i>Figure 2.10 Plot showing increase in kWh /year produced with BWRO plant as load</i>	<i>55</i>
<i>Figure 2.11Daily water production throughout the year (in m³ /day)</i>	<i>56</i>

<i>Figure 2.12</i> Cost of Water Vs % Plant Operation Hours	59
<i>Figure 3.1</i> A simple Artificial Neural Network	64
<i>Figure 3.2</i> A simple model of Biological Neuron	66
<i>Figure 3.3</i> Some Artificial Neural Network Connection Structures	68
<i>Figure 3.4</i> Architecture of Back Propagation Network	72
<i>Figure 3.5</i> Proposed neural network architecture for estimation of total kWh produced per year	78
<i>Figure 3.6</i> Regression plots of neural network model for training datasets	80
<i>Figure 3.7</i> Validation checking of the neural network model	82
<i>Figure 3.8</i> Regression plots of neural network model for validation datasets	83
<i>Figure 3.9</i> Regression plots of neural network model for verification testing and overall datasets	84
<i>Figure 4.1</i> Schematic of renewables based generation system with a high step-up converter	90
<i>Figure 4.2</i> Circuit configuration of high step-up converter	91
<i>Figure 4.3</i> Diagram indicating the current and voltage polarities under steady state	92
<i>Figure 4.4</i> Voltage gain for various duty ratios with different values of n	93
<i>Figure 4.5</i> High step up dc-dc converter PV system in closed loop with PI controller.	96
<i>Figure 4.6</i> Model of high step-up DC-DC converter with closed loop PI controller	97
<i>Figure 4.7</i> Step response and Bode Plot for the converter in closed loop	99
<i>Figure 4.8</i> Output voltage waveforms of MOSFET and diodes of High step-up DC-DC converter using PI controller	100
<i>Figure 4.9</i> Output current waveforms of capacitors and diodes of High step-up DC-DC converter using PI controller	101
<i>Figure 4.10</i> Output voltage response for steady change in Input voltage	102

<i>Figure 4.11 Output voltage response for Random Input voltage</i>	_____ 103
<i>Figure 4.12 Hybrid power converter with two inputs</i>	_____ 104
<i>Figure 4.13 Block diagram of the hybrid power converter</i>	_____ 105
<i>Figure 4.14 Photograph of experimental setup</i>	_____ 107
<i>Figure 4.15 Snapshot of DSO displays showing output voltages at various input conditions</i>	_____ 111
<i>Figure 4.16 DSO waveforms of input and output voltages and currents</i>	___ 112

List of Tables

<i>Table 2.1 Symbols used in solar PV model equations</i>	33
<i>Table 2.2 Symbols used in wind model equations</i>	35
<i>Table 2.3 Symbols used in Cost model</i>	37
<i>Table 2.4 Simulation input parameters</i>	40
<i>Table 2.5 Partial list of different configurations of hybrid power systems along with their key performance indicators</i>	41
<i>Table 2.6 Partial list of different configurations of hybrid power systems and kWh/year generated with constant load and BWRO plant load</i>	53
<i>Table 2.7 Symbols used in Cost model</i>	58
<i>Table 2.8 Simulation input parameters</i>	58
<i>Table 3.1 Associated Terminologies of Biological and Artificial Neural Net</i>	67
<i>Table 3.2 Values of Weight matrices and biases</i>	85

List of Abbreviations

AC	Alternating Current
ANN	Artificial Neural Network
ARIMA	Autoregressive Integrated Moving Average
BWRO	Brackish Water Reverse Osmosis
COE	Cost of Energy
DC	Direct Current
DG	Diesel Generator
DSO	Digital Storage Oscilloscope
ESR	Equivalent Series Resistance
ESS	Energy Storage System
INR	Indian Rupees
IW	Input Weights
LED	Light Emitting Diode
LW	Hidden Layer Weights
MED	Multi Effect Distillation
MOSFET	Metal Oxide Semiconductor Field Effect Transistor
MPP	Maximum Power Point
MPPT	Maximum Power Point Tracking
NN	Neural Network
NOCT	Normal Operating Cell Temperature
O&M	Operation and Maintenance
P	Proportional
P&O	Perturb and Observe

PI	Proportional Integral
PID	Proportional Integral Differential
PV	Photo Voltaic
RES	Renewable Energy System
RO	Reverse Osmosis
STC	Standard Test Conditions

Chapter 1

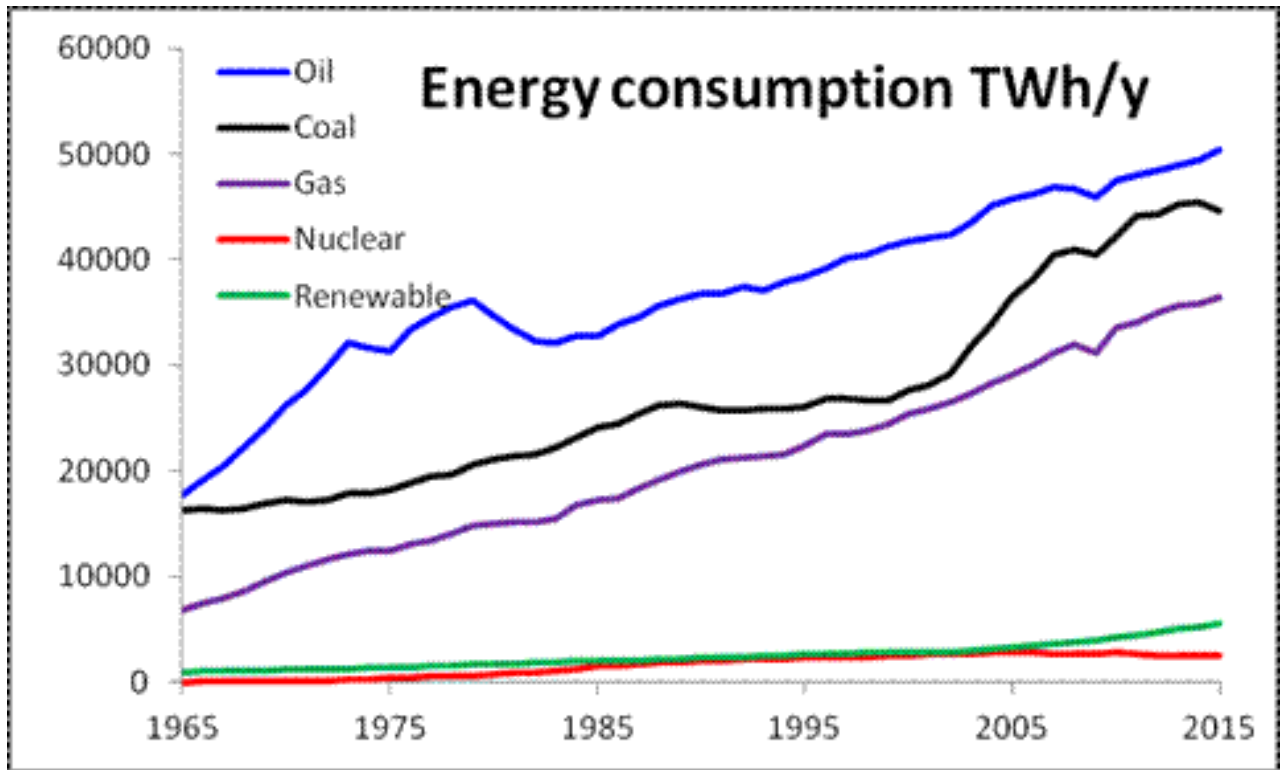
1 INTRODUCTION

1.1 Introduction

Chapter 1 presents a brief introduction to the global energy scenario and renewable energy sources. The global water scenario is also discussed particularly with reference to the availability of fresh water and the desalination process used to augment freshwater resources. The nexus between the water and the energy is also discussed. The availability and accessibility of energy sources are analyzed stressing on the use of locally available renewable energy sources.

1.2 Energy scenario

The rapid industrialization spread throughout the world during the late sixties and early seventies. The global population also doubled from 3.7 billion in the 1970 to 7.4 billion in 2015. The economic growth was largely due to mass consumption and increase in affordability for goods by the middle classes especially in growing economies like India and China. This process increased the hunger for energy than ever before which was completely catered by the fossil fuels [1] . The world total energy consumption is an index used for accessing the economic growth. The energy consumption in per year from 1965 is shown in Figure 1.1



*Figure 1.1 Global Energy consumption in TWh/year from 1965 to 2015 [1]
We can observe that the energy consumption goes on increasing year after year. The share of renewables are increasing at a faster rate during the last decade.*

1.2.1 Primary energy sources

The energy consumed is derived from the primary supply sources of energy like coal, natural gas, oil, nuclear, hydro and other renewables. The world primary energy consumption, even till date is predominantly fed by oil at 33%, closely followed by coal at 30% and natural gas at 24%. The hydro electric energy and nuclear energy contributes a decent 7% and 4% respectively. The remaining 2% is catered by the new and renewable energy sources like solar, wind and biomass [1] [2].

1.2.2 Remaining reserves of fossil fuel

The fossil fuels are exhaustible in nature. From the trend of consumption, we can observe that we are increasing the usage of these reserves continuously and eventually we may be left out without these sources.

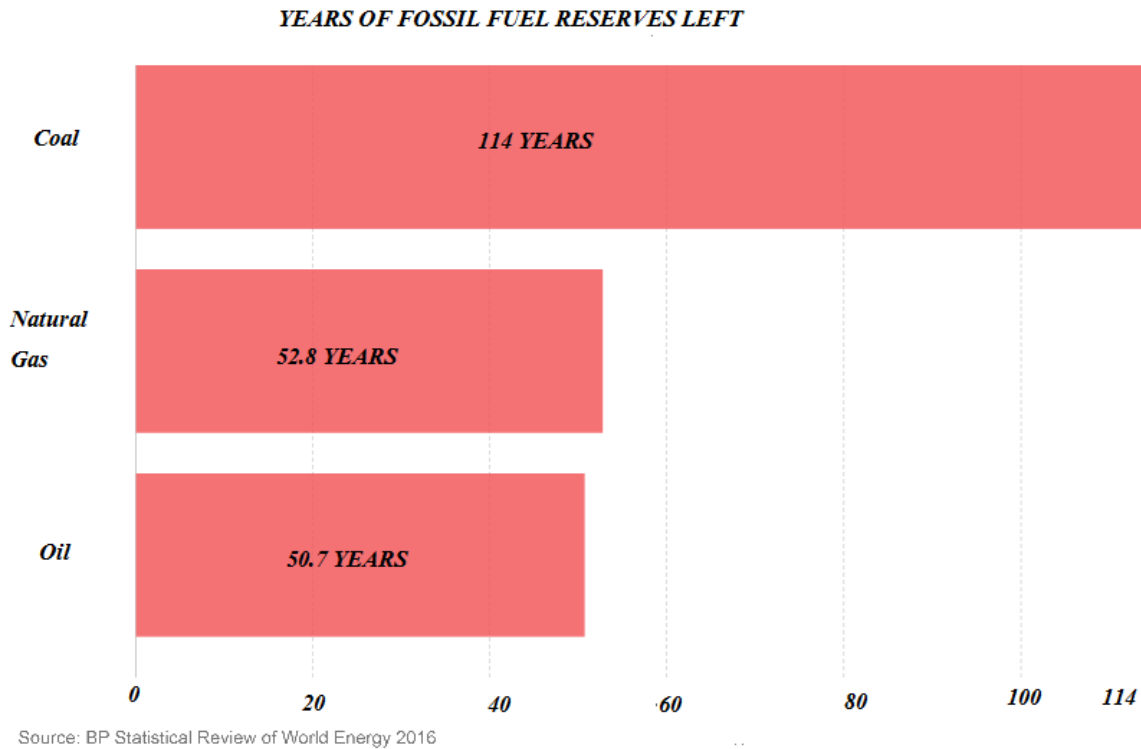


Figure 1.2 Years of fossil fuel reserves left [1]

The above graph illustrates that the world cannot depend on fossil fuels for long.

Figure 1.2 shows the total remaining years for which we will have fossil fuel reserves throughout the world. The oil and natural gas gets exhausted by another half a century and the coal for slightly above a century.

1.2.3 Environmental impacts of energy

The major environmental impacts of energy production and consumption are global warming and climate change. All fossil fuels emit greenhouse gases. This is coupled with deforestation for extraction of fossil fuels. On the other end, the consumption of energy in the industries also generate greenhouse gases. So, the complete dependence on fossil fuels is going to aggravate the problem of global warming and climate change.

The hydro power does not directly contribute to the global warming, but its environmental impacts are largely ecological. This needs a lot of land to be submerged in water for building dams and often require relocation of human beings and other living organisms. The nuclear power can produce electricity in large scale and does not contribute to carbon emission. The environmental impact from the nuclear power is lower than fossil fuels.

The renewable energy sources like the wind and solar have got the lowest environmental impacts. Wind turbines have the lowest carbon emission levels of 12 g CO₂ equivalent per kWh of electricity generated as against 820 g CO₂ equivalent per kWh in case of coal. As far as ecological impact is concerned, the solar and wind farms can be made alongside the agricultural lands. Wind farms need only foundation arrangement and rest land can be used for agriculture. [3]

1.3 Water scenario

Water is distributed in various forms across the earth. Most of the water is available in oceans, and an only tiny portion of 2.5 % is present as fresh water. Hence, the bulk of the water on Earth is saline, with a salinity of 35,000 ppm on an average (35 grams of salts in 1 kg of seawater). Freshwater is defined as water that has a salinity of less than 1 percent that of the oceans - i.e., below around

350 ppm and water around this salinity is only fit for human and animal consumption and also for most of the other uses. Out of the available fresh water, a major fraction is locked in the form of glaciers, ice caps and snow leaving behind only a tiny percentage of water for use [4].

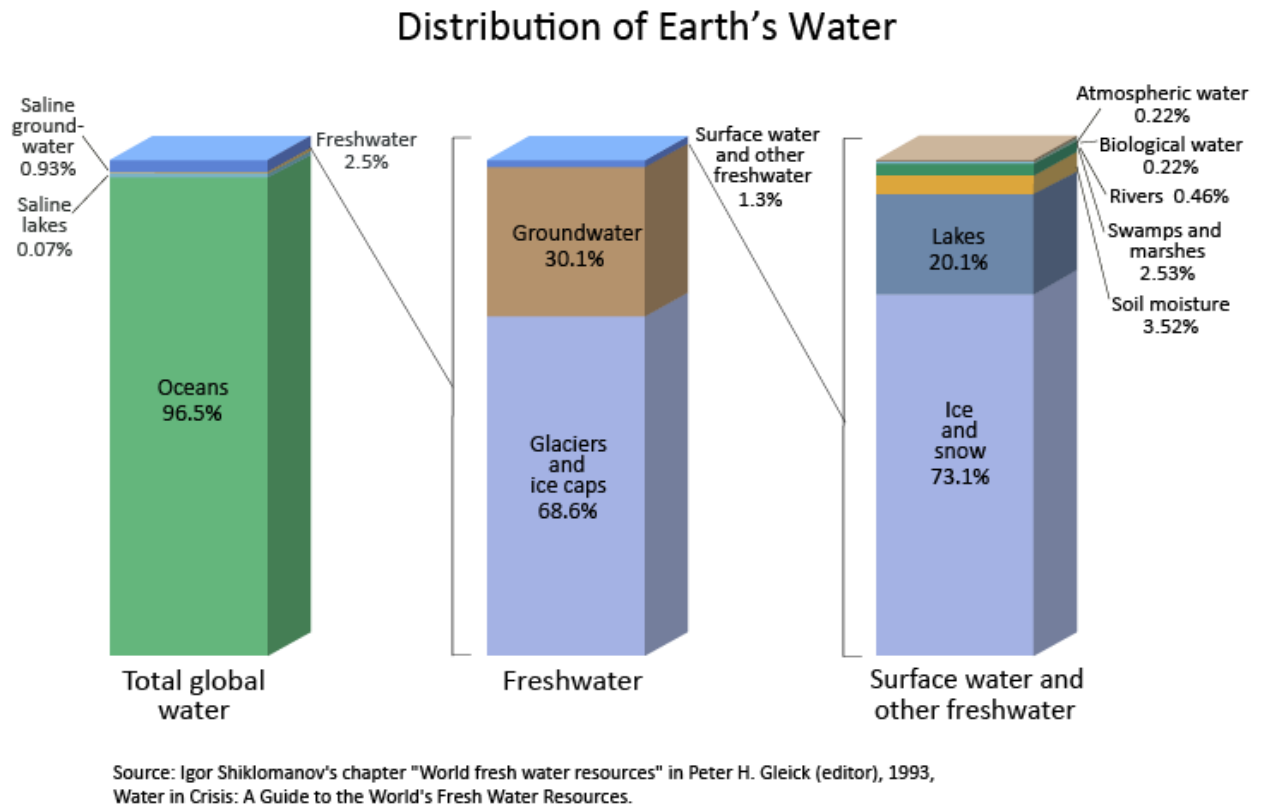
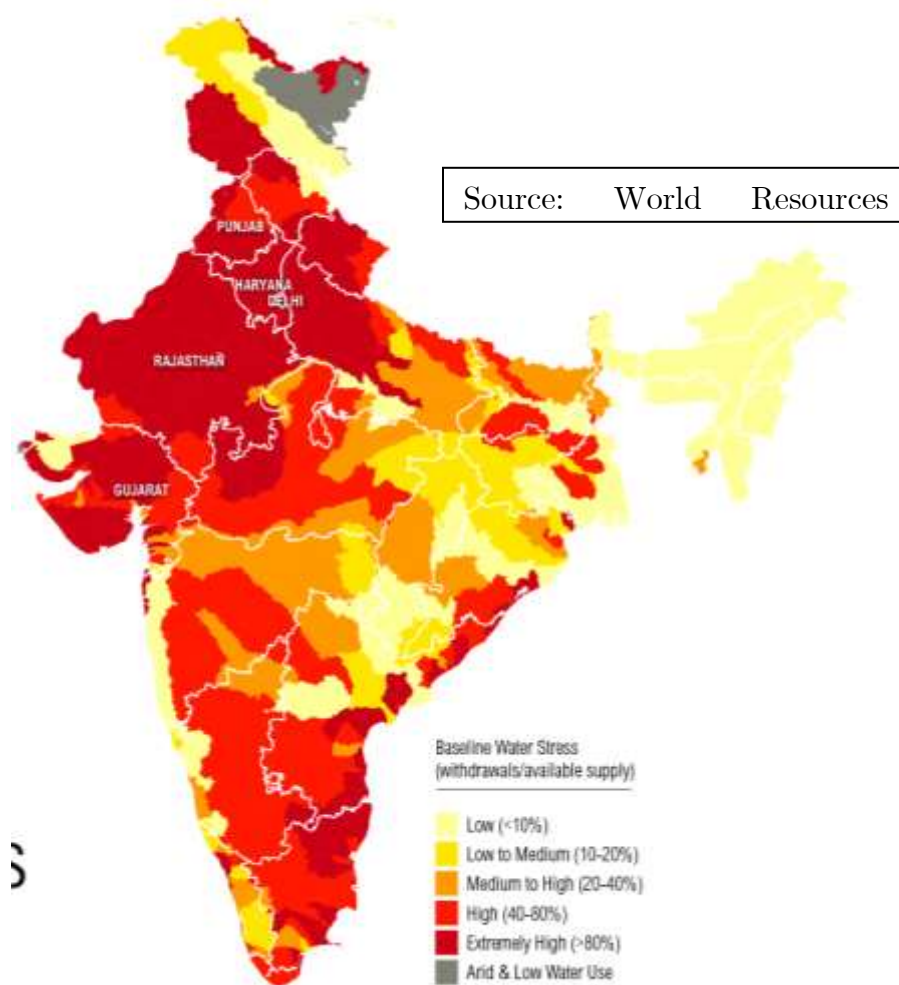


Figure 1.3 Global water distribution [4]

The distribution of, already limited fresh water, makes it more scarce.

Figure 1.3 represents the distribution of global water in a lucid manner. The available fresh water is also highly skewed both spatially and temporally. All the parts of the planet are not equally distributed with fresh water resulting in regions of acute water scarcity.



*Figure 1.4 Water stress map of India [http://www.wri.org]
We can observe that most of the places in India are already water stressed.*

The availability of the water is not evenly distributed throughout the year, and hence there are periods in a year when water shortages are very common. Also, even if the fresh water is available, the quantity and quality of the fresh water is another issue. Hence there is inherent uncertainty in access to the fresh water.

The water scenario of India is shown in Figure 1.4. Water stress is estimated based on the withdrawals of water against the availability. If the withdrawals are lower than the availability, the region is classified as low water stress, and then the water stress increases with increase in withdrawals [5]. We can observe that most of the regions come under high and extremely high water stress.

1.4 Desalination

The demand for fresh water continues to grow with ever-increasing population, rapid industrialization, and economic growth. On the other hand, the availability of directly usable natural water keeps on shrinking. The disturbances created by global warming and climate change, exploitation of natural resources all contribute to the problem. The problem is more prominent in partially arid climates and also in islands and some coastal regions. Hence, desalination of the locally available salt water of any quality is seen as an option to supplement the demand gap for freshwater supplies. The schematic representation of desalination system is shown in Figure 1.5.

Desalination processes extract fresh water from the saline water leaving behind the brine which will be of higher salt concentration than the input saline water. There is an energy input in some form or other to carry out this process. [6]

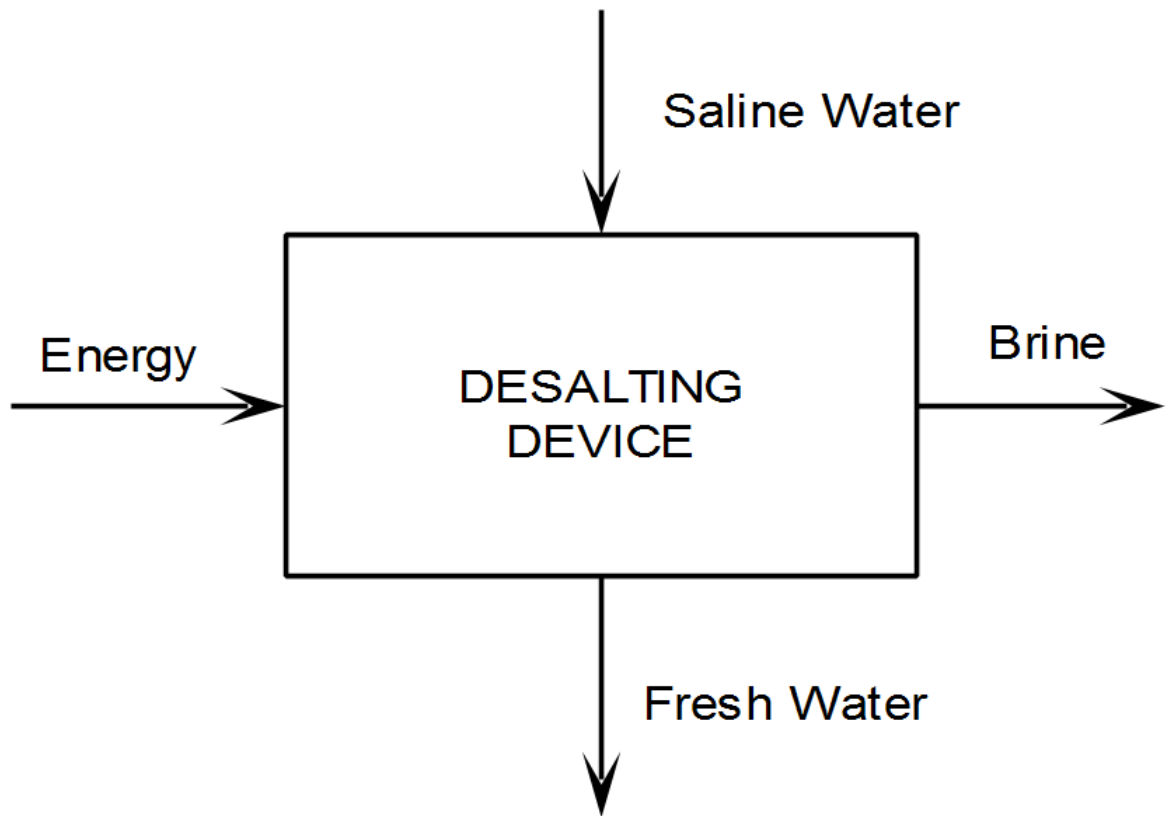


Figure 1.5 Schematic representation of desalination system

There are basically two broad categories of desalination technologies based on the type of energy primarily used. Thermal desalination uses thermal energy to heat saline water and condense the vapours to produce water of high quality. The membrane desalination is basically a pressure driven process. The salt water is pressurized to the required level and passed through the membrane to produce the product water which is usually of potable water quality. This consumes mainly electrical energy for the pumps used to produce the required pressure. [7]

1.1 Energy Implications of Desalination

Desalination process is highly energy-intensive, and the major input is energy in different forms. Membrane-based desalination processes (Reverse Osmosis - RO) needs energy in the form of electricity whereas thermal based desalination processes (Multi-stage flash -MSF, Multi-effect distillation - MED) requires primarily thermal energy, but also needs significant electricity for pumping needs. Even though the energy required for desalination is site-specific, on an average, we can say that the seawater desalination using multistage flash technology needs approximately 290 kJ/kg of thermal energy in addition to 2.5–3.5 kWh electrical energy per 1000 liter of product water, whereas huge capacity reverse osmosis process consumes about 3.5–5.0 kWh of electrical energy alone per 1000 liter of product water [8]. Considering the average energy requirement of various desalination processes and the global desalination capacity of around 65 million m³/day, the energy requirement works out to be approximately 200 million kWh per day and keeps growing every year [9] [10]

1.2 Energy-Water nexus

Water and energy systems have become increasingly interdependent and are tightly intertwined these days. Water is used in almost all stages of energy production, particularly in electricity generation. Energy is invariably required to produce or extract, transport over long distances and deliver water at the essential quality for various human uses. At the back end, energy is also required to treat waste waters before sending back to the environment. [11] Historically, the interactions between energy and water have not been properly addressed. They were considered based on region or based on the technologies. Throughout

the world, energy systems were developed separately, and water systems were managed separately. These two were treated independent of each other [12]. But the fact remains that the energy and water flows are intrinsically connected with each other. The inherent properties and characteristics of water make it an ideal choice to be used for producing energy. On the other hand, the energy is required to treat, distribute water for human use and again put the water back into the cycle. Thermoelectric power generation draws huge quantities of water for cooling purposes and in turn, dissipates back tremendous amounts of energy on account of its inherent inefficiencies involved the conversion of thermal energy to electricity. The quality and quantity of intensity of water use and energy dissipated vary with generation and cooling technology [13]. In addition, water treatment and distribution for drinking water supply and municipal wastewater also require energy [14].

Water and energy needs will be governed by growth in population and also migration patterns. The changes in the type of fuels used and energy technologies adopted also shape the water and energy needs. For example, if the population increases in a region, the demand for both water and energy is set to increase. This can be triggered by an increase in production of locally available energy resource like coal, oil. As a consequence, the requirement of water also increases. Hence both water and energy need to be managed as a whole. While many of the forces affecting the water-energy nexus are cannot be controlled directly, this interconnection can be effectively managed to a certain extent by proper planning considering various available technology choices, fixing proper share for various energy sources and also planning the site of these projects [15].

1.3 Energy-related risks to water security

Most of the present day water distribution and water production systems consume energy in the form of electricity. Also, there are specific requirements due to infrastructure and site-specific conditions that make these water systems depend on the fossil fuels sources directly for extraction and distribution of water. The form of energy that is utilized and its abundance or scarcity can increase the water security of that region or can cause danger to water security. In addition, most of the conventional energy sources are likely to contaminate the already scarce surface water and also the water table, in certain cases [16]. There are certain major problems that are identified in the literature, and they are briefed in the following paragraphs. These points are important and very much relevant for policy makers and government planners.

1.3.1 Limited or unreliable and affordable energy for extraction of water

The quality of water for various tail end-users are not same and are very much different from one another. Such variable quality requirement calls for a various degree of treating the water. The processes and methods employed also depends on the source of raw water. Consequently, the quantity and the form of energy needed for the treatment of water also varies to a great extent. For instance, the underground water can be directly pumped for agricultural uses and hence only pumping power is required either in the form of electricity or diesel. On the contrary, desalination processes to produce potable water from either brackish water or water from sea sources, need significant energy, both for pumping purposes and for core process activities [17]. Also, the cost of energy is the most

significant component in extraction of water and amounts to approximately one-third of the total O&M component [17]. Hence, the supply of water is governed by the availability and affordability of energy. The energy source, if directly drawn from hydrocarbon fuels, is highly susceptible to ever-changing price trend. As a consequence, the energy cost becomes un-affordable and project can become unviable. This can ultimately affect the availability of water. Parts of the country and certain geographic locations which predominantly depend on desalination as the major source for drinking water are more likely to be affected by the input energy costs [9] [18].

1.3.2 Water for energy production and related problems

Water has become a limited resource in most parts of the world. Water is essential for energy production, agriculture and of course, to cater drinking water needs. Policymakers often face problems in allocation and re-allocation of the water resources for its various uses. Particularly in case of developing nations that witness large scale requirements of energy production face this dilemma wherein some amount of water allocated for other purposes have to be diverted for energy production. Thus water has become a very important factor in determining health and day to day livelihood of the society [19] [20].

1.3.3 Pollution of water due to energy-related activities

Usage of fossil fuels increases the danger of contamination the available water sources. The water resources are affected in terms of its quality and also are harmful to flora and fauna in that region. Even the very extraction of fossil fuels can cause pollution to the water. The coal is extracted in coal mines. The huge

mine dumps that are left over residues from the mines have a lot of polluting things that diffuses slowly into the underground and contaminate the water. When the gas is being drilled, spillages and major leakages release heavy metals to the surface, polluting the water. [21] [22] Also, at deep levels underground, water is highly salty, and when released into the surface contaminates the surface water. In addition to this, the fractional distillation of gas can pollute underground, and river waters are rendering it useless for human and animal purposes and even industrial purposes [17] [23] [24] [25] [26] [27].

1.4 LITERATURE SURVEY

The literature survey presents the literature survey on renewables based desalination systems. The availability and accessibility of energy sources are analyzed stressing on the use of locally available renewable energy sources. The options available for desalination systems based on these renewable energy sources are explained. The present technology status and barriers in renewable energy based desalination systems are analyzed. The hybrid power system based on renewable sources is presented as a technology option. The motivation of the research work is drawn from the present barriers in design and implementation of the above system, and the research objectives are set.

1.4.1 Renewables based desalination

Desalination is an energy-intensive process. Mostly, energy supply is from fossil fuel sources, and they are highly vulnerable to every changing global market conditions and also the inherent logistical supply issues to remote places and island communities. Hence it is an obvious fact that they are not sustainable.

Until now, most of the desalination plants are located in regions where energy availability is high, and costs of energy are low. [28] At present, close to only one percent of the water produced by various technologies is powered by solar, wind, biomass and other similar new energy sources. The renewable energy option is now being adopted in various applications making it a regular energy source, and due to this increase in the scale of utility, the cost of these energy sources are likely to decline in the near future [29]. This makes the renewable energy a more viable option. The demand for desalinated water is growing with the growth in the economy and energy-importing countries like India, China, and other small islands; there is a vast scope for renewable energy-powered desalination systems worldwide [30].

Designers need to consider these different technology options for desalination, and their decisions shall be based on the available renewable energy sources at a given site. For example, thermal desalination is a viable option with high potential for solar energy. Membrane desalination can also be considered with electricity from solar photovoltaic panels. This is a good solution for arid regions that have extensive solar energy potential. Wind energy could be considered for membrane desalination projects locations with good wind potential and in coastal areas/islands. [31] [32]

The desalination itself is still a costly process, and declining renewable energy deployment costs are most likely to bring the overall cost down in the recent future. Such a configuration is of particular interest for remote locations and island communities with small populations where infrastructure for drinking water and electricity generation, transmission and distribution is either inadequate or absent. [33]

Hence the water needs and various renewable energy sources available shall be mapped for a country. This mapping provides a clear roadmap for taking policy decisions about concluding on renewable powered desalination plants in years to come. Such mapping and subsequent planning would enable a self-sustained model of development for packets of society that mainly look upon desalination systems as the major source for potable and useful applications. Renewable energy-powered desalination can enable a continued and sustained growth, particularly in the countries that depend on desalinated water for supporting local communities and other productive uses like irrigation. On the whole, such option may be viewed as a self-sustainable model of investment which brings down various costs like ecological and operation related. Government planners shall also consider the above option and assess the overall life-cycle costs of various technologies available at the time of planning their capacity, related infrastructure, and water supply need on a sustainable basis [34].

Energy storage systems are also required for the renewable energy system to increase the availability. For example, thermal storage systems with concentrated solar plates, when used for desalination, can significantly help in reduction of the fossil fuels use and hence the associated CO₂ emissions. Similarly, other renewable energy sources, like solar PV and wind power, when associated with energy storage systems, can offer significant contributions. In this context, this thesis proposes desalination itself to be a more useful and viable method to store renewable electricity, under varying conditions of operation. The same is elaborated in Chapter 3

Thus, the renewable energy sources based desalination can offer a sustainable method to produce fresh water. With the scenario where fossil fuel prices continue to increase, and the cost of renewable energy technologies continue to come down, it is expected that the above option will become economically attractive. Particularly in case of remote locations, with a low density of population and absence of infrastructure for power and water, renewable energy with desalination is most likely to be the cost-effective solution. At present, less than 1% of the desalination capacity is based on renewable energy sources, and this does not truly reflect its advantages. The membrane-based reverse osmosis and the thermal technology based multistage flash and multi-effect desalination systems contribute to above 60 % of the renewables based desalination plants. Among the renewable sources, solar photovoltaic tops with above 40 % of the total power produced. Solar thermal-based systems and wind energy follow it. The best-suited combination of the renewables coupled with a suitable desalination technology can be the solution to achieve energy security and water security, in an economical, efficient and an environmentally friendly method. The techno-economic feasibility of renewable desalination system needs an elaborate assessment considering various inputs. The site selected for the plant, the renewable resources availability throughout the year, various parameters of input raw water like the salt content, suspended solid content and the amount of fresh water required along with its quality, the availability of conventional electricity, all needs to be taken into consideration. Apart from these, the problems related to the day-to-day running of the plant, transportation option for raw water, and requirement of pre-treatment are additional the factors to be taken into consideration for the decision-making process. Some technology solutions are more suitable for larger plant capacities, and others are for small-scale applications.

1.4.2 Solar PV based Desalination

The reverse osmosis and the electrodialysis desalination systems directly need energy only in the form of electricity. Hence, they are a natural choice for getting coupled with photovoltaic panels. Among the above mentioned processes, the electrodialysis is used for the production of high purity water and reverse osmosis is used to produce potable water. Some demonstration scale PV-RO plants have been installed in remote locations up to 10 m³ per day capacity [35]. Cost economics is still a major challenge due to higher costs of PV and storage battery. [36] The unreliable solar resource is also a problem. The lifespan of the battery system is very crucial and depends upon operating conditions and meticulous maintenance. Any revolution in storage device would lead to the large-scale deployment of PV based systems. [37] [38]

1.4.3 Wind energy based Desalination

The wind turbine can provide power output both as mechanical and electrical. The electrical energy generated can be used for reverse osmosis and electrodialysis plant. The mechanical power output can be directly utilized for mechanical vapor compression systems without converting into electrical energy. The seacoast zones are generally with high wind potential and are the most resourceful locations for setting up of wind turbine based systems. Wind-powered reverse osmosis plants with sea water as input have been installed for demonstration purposes at few places up to capacities of 50 m³ per day. The hour-to-hour variation and seasonal variation is a problem of wind power systems similar to solar-based systems.

Storage systems like batteries can also increase the availability but comes with its own cost and maintenance issues.

Hence, combining with other renewable sources can address the problem of intermittency. Also, desalination can act as a buffer and double up as an energy storage method during high resource availability periods [39] .

1.4.4 Desalination Costs

The operational cost of desalination plant comprises of cost of energy, cost of chemicals consumed, cost of workforce and cost of maintenance/spares. Energy cost is the single major component of the running cost of desalination at around 40%. Hence, the cost of energy dictates the overall cost of desalination. Energy cost, thus, decides the economic viability of the desalination plant [40].

It is very difficult to compare various desalination technologies as a whole. Such a comparison has to be site specific. Several factors that govern the cost of desalination are unique to that particular site. [41] The source of raw water, transfer of the raw water up to the desalination plant, distribution of final product water to the point of use, disposal of reject water and the cost of locally available energy, all are unique to the site selected. All these factors have got a significant impact on the final cost. [42]

The reverse osmosis and multistage flash processes are the most used and commercially well-established technologies to date. The initial investment of higher for MSF plant due to elaborate design and fabrication involved in the plant equipment. The operational costs of RO plant are more due to the

complexity involved in the process. The initial investment towards capitals is in the range of 800 – 1500 US dollars on an average [43]. The range is wide due to the variation of prevailing labor costs at site and interest rates in the country. The cost of running the plant is slightly above two percent per year of the initial investment cost. [44]

The overall cost shows a decreasing trend in the past decade, particularly for RO plants. This is largely due to improvements in technology and reduction in the cost of membranes. Still, desalination is a viable option for nations with middle-income levels. It proves to be a costly proposition in case of developing nations. The typical cost figures are in the range of 1 to 2 US dollars per 1000 liters of product water. The economies of scale, coupled with other positive factors, if available, can bring it down as much as 0.5 US dollars per 1000 liters of product water [23]. The above costs are based on desalination plants with grid power electricity at costs around 5 US cents per unit.

In the first instance, the renewables based desalination appears to be more expensive as compared to the grid power based desalination plants. This is true for places where already established energy infrastructure is present. But locations that are very remote and islands with small communities lack such infrastructure. Extending the energy supply to such areas is definitely not going to be an economical option and sometimes may not be technically feasible also. The renewables powered desalination systems have got their scope at these places. Such plants will be sustainable and economically more viable than any other technology.

1.4.5 Challenges

Coupling of the desalination plant with the renewable energy sources brings in a lot of challenges. The variable and intermittent nature of renewable sources make it very difficult to decide on the capacity of the system as a major design problem. Similarly, the management of power generated from the source to the load and the storage system is a difficult technical task. Both these things bring economic issues as a challenge. Advances in technologies aimed at improving the availability of energy at lower costs and better energy storages. A complete survey to create a database of available renewable energy resources in all regions is the primary challenge. The variability of these resources creates the problem of availability of energy source. This, in turn, affects the reliability of the system. The technological challenge involved is to freeze a design under varying input resources. The design of capacities has got a direct bearing on the cost of the system and hence the final cost of water produced which is a highly sensitive issue. A synchronized effort is required in the energy and water industry for addressing these challenges. The developing nations need to attend the problem of high initial cost and availability of skilled workforce to operate the plants [45] [28].

1.4.6 Hybrid renewables based desalination

The hybrid power system is basically combination of two or more sources of power generation systems together. The locally available renewable energy sources are the natural choice for creating the hybrid power system. [46] Most probably, the solar photovoltaic (PV) systems are employed in association with wind energy systems. Such hybrid energy configurations offer a better of energy security to the region as it uses the energy mixed from various sources. [47] [48]

Nevertheless, it comes with its own complications. This is normally accompanied by energy storage systems like batteries to ensure maximum supply reliability and availability. [49] Figure 1.6 shows a general schematic of the typical solar PV – wind generator based hybrid power system.

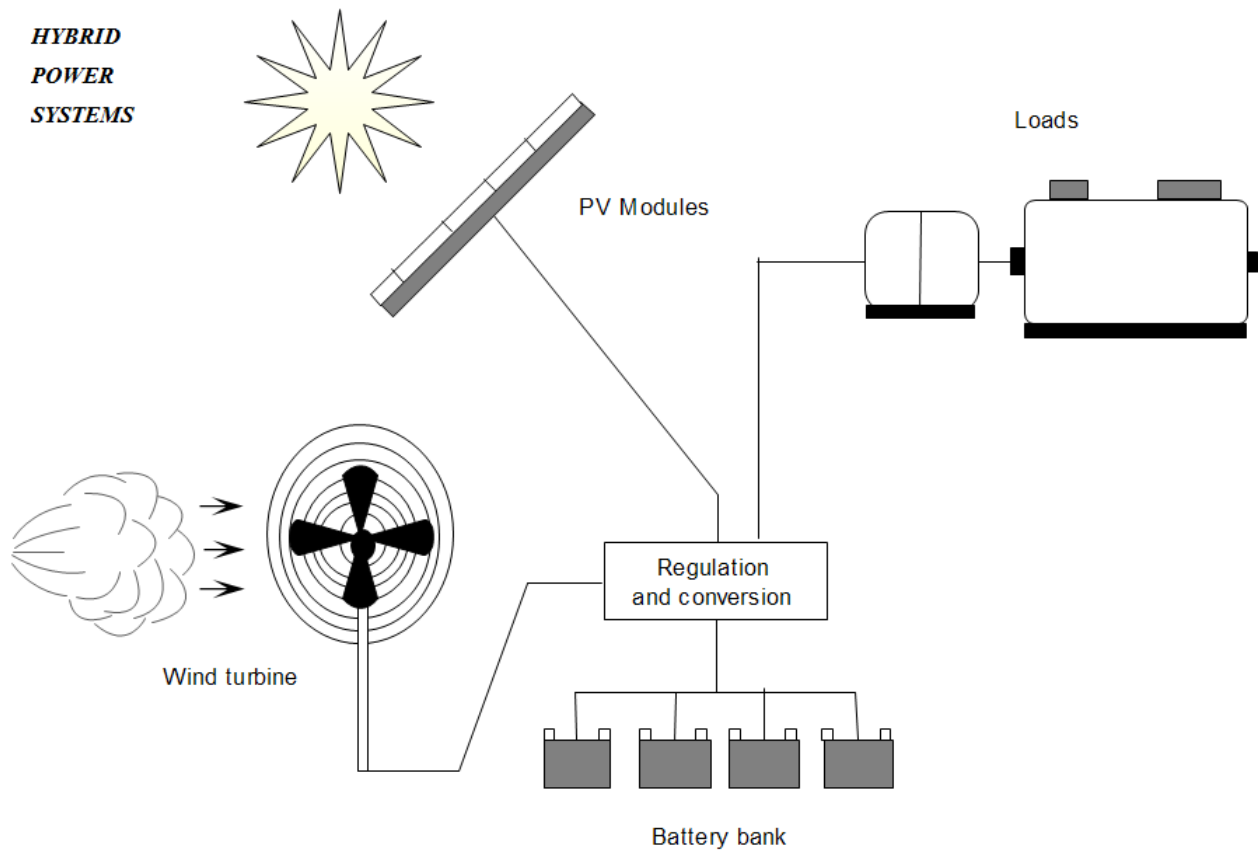


Figure 1.6 A typical solar PV - wind hybrid power system

The above hybrid power system has solar PV and wind generator as renewable sources. Battery is used for energy storage. The regulation and conversion of power is handled by power electronic circuitry.

The system consists of solar Photo Voltaic (PV) modules, wind generator as sources for renewable power generation. There is a battery bank for storage of

energy. These are all connected to a power conversion system. This takes power for either or both the sources, charges the battery and feeds power to the load.

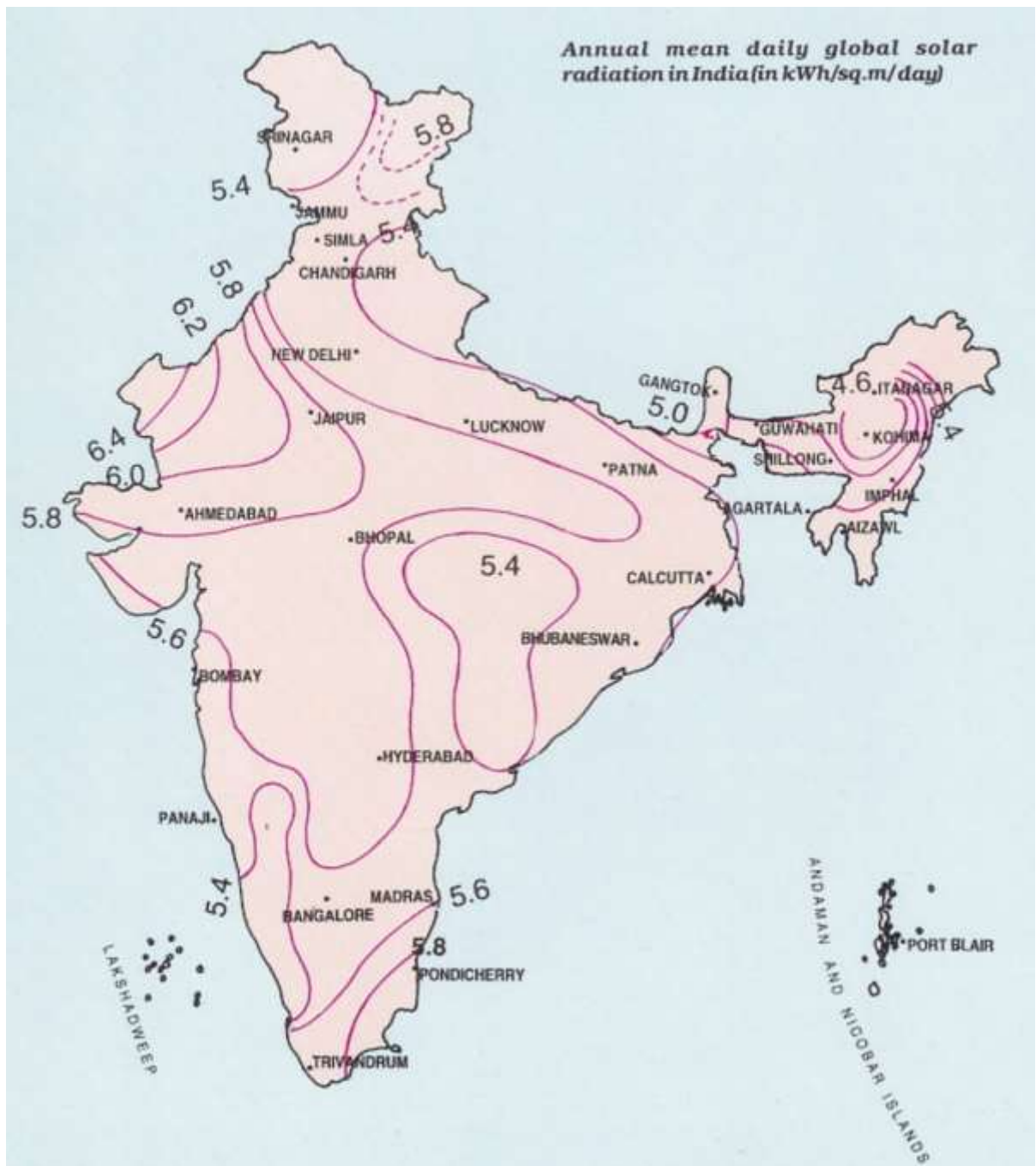


Figure 1.7 Solar resource map of India [www.mnre.nic.in]

We can see that most of the parts of India has an average solar irradiation of above 5 kWh/m²/day.

The solar and wind power availability throughout India are shown in Figure 1.7 and Figure 1.8. We can observe that an average of 5 kWh solar resource is available per m² area on a typical day. Parts of the country like Tamil Nadu, Gujarat, Rajasthan and even some places in Jammu & Kashmir has got around 6 kWh/m²/day of the resource.

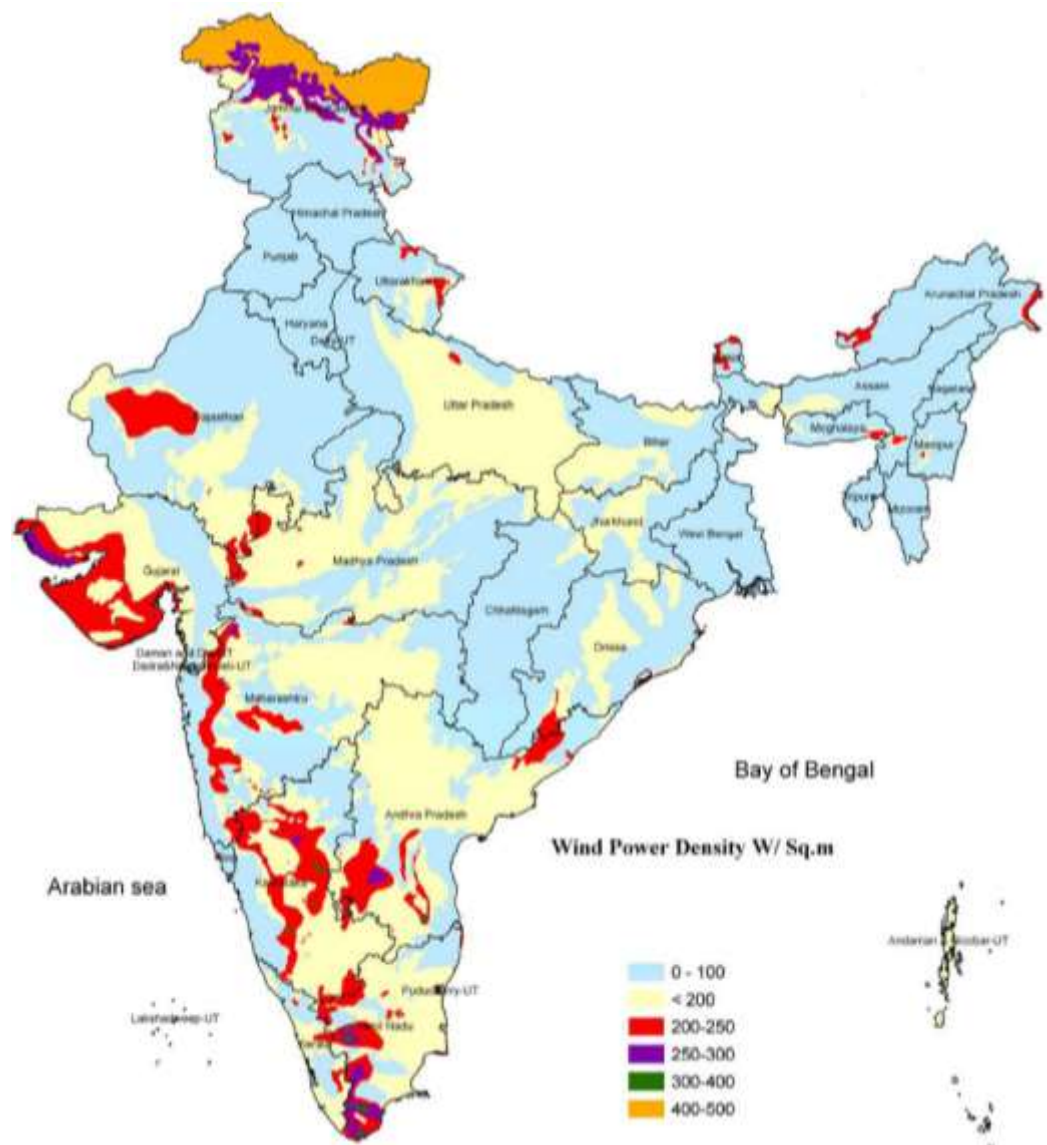


Figure 1.8 Wind resource map of India. [www.niwe.res.in]

Almost half of regions in India has got a moderate wind power potential with wind power density around 200 W/m².

Similarly, there are regions of high wind resources like Tamil Nadu, Gujarat having around 200 W/m². Most of these resources have been commercially exploited for power generation purposes. The next concentration is in the medium resource regions where the current potential is very high. The solar power is available not more than 10 hours a day, but the wind power is exploitable through most of the hours. This paves the way for venturing into medium wind resource area also in hybrid power mode along with the solar PV. This characteristic makes conditions favorable for solar PV – wind hybrid power system along with small energy storage batteries. [50]

1.4.7 Motivation and objectives:

Renewable energy sources have the inherent problems of intermittency, uncertainty, and low availability which makes the power supply more unreliable. Huge energy storage systems like batteries are to be employed to increase the availability. Photovoltaic (PV) and wind power are complementary because sunny days are generally accompanied by very low wind and cloudy days and night times are likely to have strong winds. Therefore, hybrid PV-wind systems can have higher availability and reliability than systems based on individual PV or wind sources. Thus, this study is orientated towards hybrid PV-wind systems suitable for small-scale desalination plants that are to be applied in remote locations and islands.

Use of hybrid PV-Wind systems for desalination has a unique advantage of reduction in energy storage battery capacity resulting in increased utilization of power generated and reduced cost.

Hence the performance of the hybrid power system largely depends on the proper combination of capacities of the individual system like PV and wind generator. The power generation depends on instantaneous solar irradiation and the wind speed. On the other hand, the load requirement variations also affect the overall generation. This makes it necessary to study the overall annual power generation for various combinations of PV-wind capacities under varying load conditions.

There is a need to develop a comprehensive model for annual power generation. Also, the performance of the system with desalination plant as a load and the annual water production need to be assessed under given site conditions in order to access the techno-economic feasibility. Also, there is a need to develop high efficient power converter that can take multiple renewable energy inputs with a closed loop controller.

From the literature survey and current status of the technology, the following are the derived objectives taken for the study:

- Modeling of hybrid renewable power system with PV-wind coupled with the desalination plant for remote locations and islands.
- Calculate the overall annual power generation for the selected site.
- Size optimization analysis for various combination of PV-wind capacities.
- Method of identifying combination of solar and wind capacities for various objectives like cost of energy, total power generation and availability.
- Analysis of the size optimization study for a desalination plant load.

- Neural Network based modeling of total annual power generation for various combinations.
- Development and testing of a power converter that can take multiple renewable energy source inputs.

1.5 Thesis organization

The thesis is organized into five chapters, viz. introduction with the review of the literature, size optimization of PV-wind hybrid power system, Neural network modeling of PV-wind system and Power converter for the hybrid power system. A general introduction is given in chapter 1 and literature survey along with motivation of the work and objectives are explained in Chapter 2. Chapter 3 presents the modeling of the hybrid power system and sizing analysis of the same. Chapter 4 deals with the Neural Network based modeling of the hybrid power system. Chapter 5 explains the development and testing of the high-efficiency power converter for the multiple renewable energy source inputs. The last chapter summarizes the overall conclusions and salient findings of the entire study.

Chapter 2

2 SIZE ANALYSIS AND OPTIMIZATION OF RENEWABLE HYBRID POWER SYSTEMS

2.1 Introduction

The energy and water scenario and their nexus was discussed in Chapter 1. Water and energy are the basic needs that control the lives of humanity and also promote civilization. Water, energy, and environment are essential inputs for the sustainable development of society [51]. The availability of fresh water is an important issue in many areas of the world. The ocean is the only perennial source of water. Their main problem is obviously its high salinity [52]. The removal of salinity is accomplished by several desalination methods. But, all the desalination processes require significant quantities of energy. Ironically most of the places that are water stressed are also energy stressed. The cost of extending grid power may be prohibitively high in those cases. Rural / Remote locations like hills and islands multiply the problem to a larger magnitude [53]. These remote parts do not have access to the conventional source of power. Use of renewable sources like solar, wind, Biomass and other locally available energy sources is the only solution. Fortunately, most of such locations have exploitable renewable sources of energy that could be used to drive desalination processes [54]. Renewable energy systems utilize sources available locally and freely for production of energy. Production of fresh water using desalination technologies driven by renewable energy systems is thought to be a viable solution to the water scarcity at remote areas, which is characterized by

lack of potable water and conventional energy sources like heat and electricity grid. Also, they are environmental friendly [55]. Desalination systems cannot be compared with conventional systems in terms of cost without taking site-specific factors into consideration. They are suitable for certain locations and will certainly emerge as widely feasible solutions in due course of time [56] [57] [58] [59] [60] [61] [62] [63].

But the renewable sources are of intermittent nature and have poor availability. Hence, it is practically difficult to produce water with a single source of energy. Naturally, combining two or more sources of energy, known as hybrid power system along with energy storage devices, is the next available option.

2.1.1 Energy storage systems: (ESS)

The power system is expected to perform well in terms of its reliability and availability leading to better energy security. Hence various energy storage systems (ESS) like the pumped energy storage, battery storage and fuel cells are to be employed to meet the objective [64] [65] [66]. The storage devices help in managing the load, apart from carrying out the basic function of storing the energy. There is always a need to balance between the load end requirements and the generation instantaneously [67] [68] [69]. When the demand exceeds the supply, ESS supplies the additional power required. Another important application is the meeting up of peak demand. Very short time spike load requirements can be met out by the ESS [70] [71]. Also energy storage systems helps in reducing the capacity of DG sets and can cater power back up requirements for emergency loads. Future energy storage systems are expected to contribute for easier transition to smart grid networks [72] [73] [74].

2.1.2 Reverse Osmosis (RO) desalination using solar PV and wind Energy

The energy storage systems takes away a portion of generated energy for energy conversion purposes during the process of storage and again during usage. Hence, it is necessary to utilize the surplus energy generated instantaneously to make a final product which can be stored. This eliminates the energy wastage due to conversion efficiency both during storage phase and also during reuse of stored energy for end use. This increases the net overall energy available for the load.

A suitably sized reverse osmosis plant finds its application under such circumstances. RO is the desalination process with the minimum energy requirements [75] [76] [77] [78] [79]. The RO plant is considered as a load because the plant can run as and when enough power is available from any of these sources, produce water and stored in tanks. The plant can operate at various capacities and hence it serves as a variable load. With this, we can keep the capacity of energy storage system like batteries to a minimum and hence increase efficiency and reduce costs.

This chapter presents the techno-economic analysis of various sizing combinations of systems with solar Photovoltaic, wind energy and storage batteries for a constant load. The components of the hybrid power system is modeled using MATLAB to simulate the performance of the system for different combinations of capacities. [63]

The second section of this chapter also discusses the hybrid power system coupled with a brackish water reverse osmosis desalination plant working as the variable

load. This configuration of small capacity hybrid power system can be employed for supplying electricity and clean water in islands and remote locations.

2.2 Hybrid Solar PV-Wind power scheme

The complementary features of wind and solar resources make the use of hybrid wind–solar systems to drive a desalination unit a promising alternative as usually when there is no sun and the wind is stronger and vice versa [80]. It should be noted, however, that there will be conditions when both solar and wind energy is not available. This implies that the load operates only partially when the energy is available unless some storage device is used. Batteries are one such storage devices but are usually expensive [54] [56].

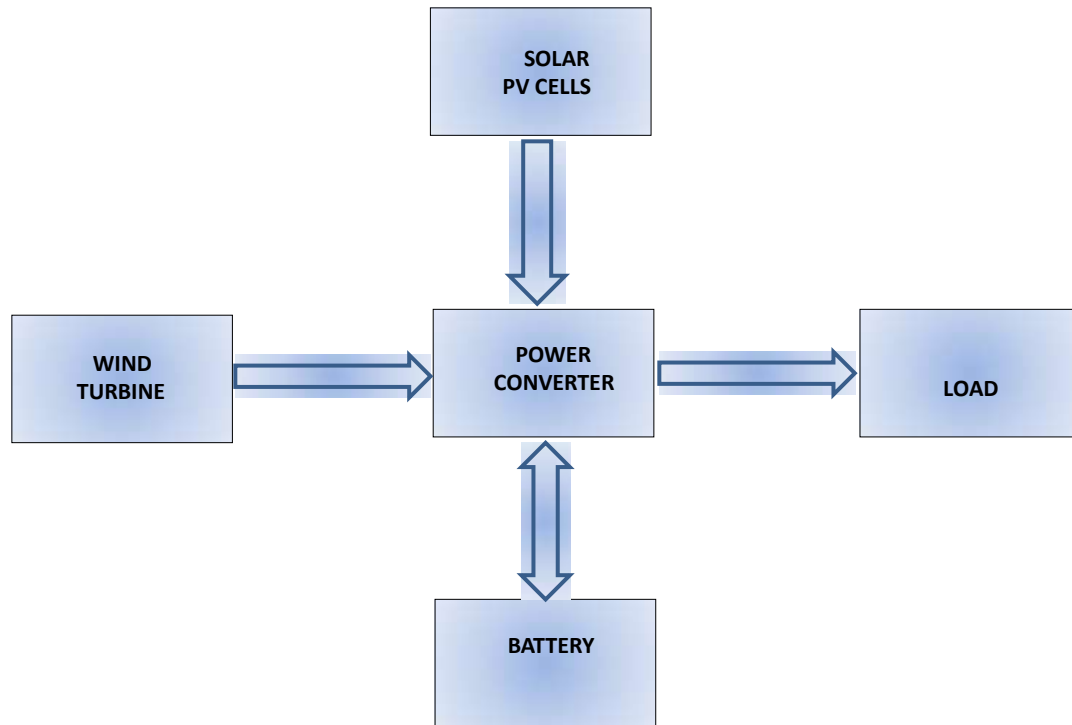


Figure 2.1 Schematic diagram of a typical Hybrid power system

The basic components of the hybrid system are the wind generator and the PV system. Others are additional/auxiliary components which help for the full-time functioning of the hybrid system. Figure 2.1 shows schematic of the hybrid system with the desalination plant as a load.

2.3 Modeling the renewable energy systems

There are a variety of renewable energy sources identified and utilized at various levels. The renewable energy sources encompasses solar energy, which includes thermal collectors, solar ponds and photovoltaic, wind energy and geothermal energy. In this section, we will discuss about solar photovoltaic and wind energy.

2.3.1 Solar Photovoltaic

Photovoltaic effect was discovered in selenium way back in 1839. The photovoltaic (PV) process absorbs the energy in sunlight and converts the energy directly to the form of electricity. A typical photovoltaic cell comprises of a minimum two thin layers of semiconductor and the most common semiconductor used is silicon. [81] This junction of semiconductor is the source that harvests the energy in light and creates charged particles in the material. Metal contacts are provided on either side of the layer to conduct these generated electrical charges in the form of direct current. The schematic representation of a PV cell is given in Figure 2.2

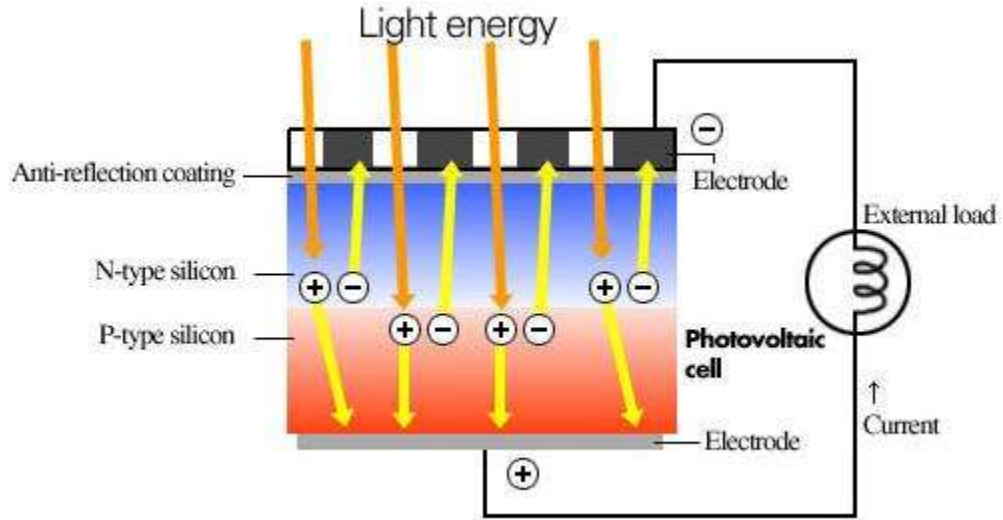


Figure 2.2 Schematic representation of a PV cell

The Luque and Hegedus model of PV cell is given by the equation below and Table 2.1 gives the description of symbols used [82] [83].

$$I = I_{SC} \left[1 - \exp \left(\frac{V - V_{oc} + I R_s}{V_t} \right) \right] \quad \dots \text{Eq. (2.1)}$$

$$I_{sc} = I_{sc}^* \frac{G}{G^*} \left[1 + \frac{dI_{sc}}{dT_c} (T_c - T_c^*) \right] \quad \dots \text{Eq. (2.2)}$$

$$T_c = T_a + C_t G_{eff} \quad \dots \text{Eq. (2.3)}$$

$$C_t = \frac{NOCT (^{\circ}C) - 20}{800 W/m^2} \quad \dots \text{Eq. (2.4)}$$

$$V_{\alpha} = \left[V_{\alpha}^* + \frac{dV_{\alpha}}{dT_c} (T_c - T_c^*) \right] \left[1 + \sigma_{\alpha} \ln \left(\frac{G_{eff}}{G_{\alpha}} \right) \ln \left(\frac{G_{eff}}{G^*} \right) \right] \quad \dots \text{Eq. (2.5)}$$

$$R_s = \frac{V_{\alpha}^* - V_M^* + V_t \ln \left(1 - \frac{I_M^*}{I_{sc}^*} \right)}{I_M^*} \quad \dots \text{Eq. (2.6)}$$

$$P_v(t) = N_p v V_m(t) I_m(t) \quad \dots \text{Eq. (2.7)}$$

PV equipment is basically a static system and has no moving parts and hence requires minimal maintenance. Also, it has a long life. It generates electricity directly without producing any sorts of emission of the greenhouse gases, and its operation is practically silent.

Table 2.1 Symbols used in solar PV model equations

Symbol	Description
I_{sc}	is the short circuit current
V_{oc}	is the open circuit voltage
V_t	is the thermal voltage
R_s	is the series resistance
STC	is standard test conditions
I_{sc}^*	is the short circuit current of the module at STC
V_{oc}^*	is the open circuit voltage of the module at STC
G^*	is the Irradiance at STC
T_a	is the ambient temperature
T_c	is the operating temperature of the module above ambient

T_c^*	is the temperature of the module at STC
NOCT	is normal operating cell temperature
$\frac{dI_{sc}}{dT_c}$ and $\frac{dV_{oc}}{dT_c}$	are temperature coefficient of current and voltage
σ_{oc}	is the empirically adjusted parameter equal to -0.04
G_{oc}	is the empirically adjusted parameter taken as equal to the value of G^*
V_M^*	is the maximum voltage of the module at STC
I_M^*	is the maximum current of the module at STC.

2.3.2 Wind energy

Wind energy is created by the pressure differences in the atmosphere due to solar power. The wind turbine technology is highly mature and already deployed in commercial scale in sites of high wind energy potential. In future, small wind turbines are expected to play the crucial role in distributed and decentralized energy systems. The production can be improved by using novel control strategies and better energy storage systems.

The wind energy is modeled using the equation Eq. 2.8. Table 2.2 gives the description of symbols used.

$$P_w(t) = \begin{cases} 0 & (v < v_{in}) \\ a_1 v^2 + b_1 v + c_1 & (v_{in} \leq v < v_1) \\ a_2 v^2 + b_2 v + c_2 & (v_1 \leq v < v_2) \\ a_3 v^2 + b_3 v + c_3 & (v_2 \leq v < v_{out}) \\ 0 & (v > v_{out}) \end{cases} \quad \dots \text{Eq.(2.8)}$$

Table 2.2 Symbols used in wind model equations

Symbol	Description
$P_W(t)$	is the hourly output power of wind generator at wind speed v
v	is wind speed at the projected height
V_{in} and V_{out}	are cut-in and cut-off wind speed of the wind generator respectively

2.3.3 Energy storage battery

The modeling of battery storage system is required to track the amount of energy stored in the system at a given point of time during the simulation. For estimating the state of charge of the battery, we need to know the power generation from the renewable sources during the hour, the load requirements and the state of charge at the start of the hour. The state of charge at a given hour $E_b(t)$ is given by the equation

$$E_b(t) = E_b(t-1) + [E_{ch}(t) * \eta_{ch}] - [E_{dis}(t) * \eta_{dis}] \quad \dots \text{Eq.(2.9)}$$

where $E_b(t-1)$ denotes the state of charge in the preceding hour, $E_{ch}(t)$ and $E_{dis}(t)$ are the charge and discharge quantities of energy storage, η_{ch} and η_{dis} are the charging and discharging efficiencies respectively. The charging and discharging efficiencies of the lead-acid storage battery is approximately 90%.

2.3.4 Assumptions

In modelling the technologies, the technical performance, economical assessment and the data pertaining to site chosen are crucial factors that can affect the performance of the hybrid power system model.

1. Weather data is assumed to be constant within each 1 hour time step.
2. The steady state of technical parameters is assumed. The output of solar PV and the wind generator depends only on meteorological data. The battery charging and discharging efficiencies are also fixed. The capacity of the battery is assumed to be constant over its life cycle.
3. The applied weather data is for the design year and similar trend is expected to continue.
4. Maintenance and operation costs depend largely on the installed capacity.

2.4 Cost Model of solar PV, wind and battery system

The cost model of the various energy sources is developed considering the capital cost per kW capacity. The annualized capital costs are calculated by using the capital recovery factor which is calculated by taking the lifespan of systems and the interest rate into account. Also, the operation and maintenance costs are included in the model. The annual total cost of the hybrid power system for a particular set of capacities of solar PV, wind and battery is finally calculated by summation of the individual costs.

The formulae used for the cost model is as given below. Table 2.3 lists the description of symbols used.

$$ACC = CC \times CRF \quad \dots \text{Eq.}(2.10)$$

$$\begin{aligned} ATC = C(PV) \times [ACC(PV) + AMC(PV)] + C(W) \times [ACC(W) + AMC(W)] \\ + C(B) \times [ACC(B) + AMC(B)] \quad \dots \text{Eq.}(2.11) \end{aligned}$$

Table 2.3 Symbols used in Cost model

Symbol	Description
CC	Capital cost/kW (in INR – Indian Rupees)
CRF	Capital recovery factor
ACC	Annualized capital cost (in INR)
AMC	Annual O&M cost (in INR)
ATC	Annualized Total cost (in INR)
C(PV)	PV Capacity (in kW)
C (W)	Wind plant capacity (in kW)
C (B)	Battery capacity (in kW)
COE	Cost of Energy / kWh (in INR)

A brackish water RO desalination plant is connected as a load to the hybrid power system. This plant produces drinking water when the power available (both generated and stored put together) is sufficient to operate the plant. The water produced will increase up to its rated capacity if the power produced is also more. Hence the load can handle variation in the power generation due to the

renewable sources. The RO plant indirectly stores power produced in the form of product water thereby eliminating the need for having higher capacities of expensive batteries.

2.5 Techno-economic analysis of hybrid power system

The selection of capacities of solar PV, wind generator, and battery greatly affects the total power generated in a particular year, capital cost and the operation & maintenance cost of the system. This has got a direct bearing on the cost of energy per unit of power generated (COE) and the availability of power for the load. The percentage availability is defined the time period in a year, the instantaneous power output from the hybrid power system is sufficient enough to operate the RO plant.

A hybrid power system can be designed with a particular combination of solar PV capacity, wind generator capacity, and battery capacity. Due to the intermittent nature of renewable sources, selection of capacity of any particular renewable energy resource based system may lead to component over-sizing and unnecessary operational and lifecycle costs. Also, the total power generated may be reduced, and hence the availability will reduce, and cost of producing energy per unit will increase. Hence a proper combination of capacities of solar PV, wind, and battery is crucial to achieving the required objective.

Hence an in-depth techno-economic analysis of the combination of different renewables is necessary to obtain enough understanding of the system. We have modeled the entire hybrid power system in MATLAB using the equations (2.1) to (2.11). The main objective of the model is to analyze the various combinations of

solar PV, wind generator and battery capacities with respect to total power generation, availability and cost of energy per unit.

2.6 Data

The hybrid power system design options are analyzed for the selected site, Kalpakkam. Kalpakkam is situated in South India and has the following latitude and longitude:

Latitude: 12°34' North

Longitude: 80° 10' East

The solar irradiation data is measured by using the 'Online solar Radiation Meter' installed at the site, and the wind data is extracted from the meteorological data available at IGCAR, Kalpakkam.

2.7 Simulation methodology

We have used the hourly solar irradiance data measured in kWh/m²/day and wind speed data in m/s as inputs for simulation. The above data is used to calculate the power output available from PV and wind sources using the models as described in Section 2.3. The power generated is calculated for every hour of the day for a complete year. The hybrid power system shall be designed to feed power to a constant load requirement of 2 kW. When the power generated at a particular instant is sufficient to feed the load, the power is fed to the load. If the power generated is more than the load requirement, surplus power is used to charge the storage battery bank and the state of battery charge is monitored. When the power generated is less than the load requirement of 2 kW, battery supplements the additional requirement. If the available battery storage and

power generated are not sufficient for load, the load is disconnected, and the batteries are charged from the generated power.

The above simulation is carried out for various combinations of solar PV capacities (1 kW to 10 kW), wind generator capacities (1 kW to 10 kW) and battery capacities (0.5 kW to 2 kW). Capital cost, O&M cost (@ 2% of capital cost), interest rate (10 %) and project lifetime (for solar PV, wind, and batteries) are considered for calculation of cost economics. Table 2.4 gives the various input parameters used for simulation.

Table 2.4 Simulation input parameters [84] [85] [86] [87]

Parameter	Unit	Solar Photovoltaic	Wind Generator	Batteries
Capital Cost	Indian Rupees/kW (INR/kW)	50000	180000	10656
Lifespan	Years	20	20	5

Table 2.5 Partial list of different configurations of hybrid power systems along with their key performance indicators (Complete table given in Appendix – A)

Solar PV Capacity (in kW)	Wind Gen. Capacity (in kW)	Storage battery capacity (in kW)	Cost of Energy per Unit (in Indian Rupees – INR)	% Availability of power for the year	Total power Produced for the year (in kWh)
7	1	2	12.63	41.4	5664
8	1	1.5	12.73	40.0	5974
8	1	2	13.00	42.3	5954
9	1	2	13.45	43.4	6196
6	2	1.5	16.04	41.1	5548
8	2	1	16.18	41.1	6140
8	2	2	16.65	46.1	6138
10	2	1	16.87	43.0	6586
9	2	2	16.99	46.8	6360
10	2	1.5	17.09	45.3	6586
10	2	2	17.30	47.6	6586
6	3	2	18.68	47.4	6166
5	3	1.5	18.74	42.9	5756
9	3	1	18.77	44.8	6926
8	3	2	18.94	49.5	6700
9	3	1.5	18.97	47.8	6926
5	3	2	18.98	46.0	5756
10	3	1	19.05	45.7	7132
9	3	2	19.18	50.4	6926
10	3	1.5	19.25	48.5	7132
10	3	2	19.45	51.1	7132
4	3	1.5	19.71	40.7	5174
7	4	2	21.52	51.2	6776
9	4	2	21.85	52.9	7210
10	4	2	22.10	53.5	7396
7	5	2	24.08	53.4	7082
9	5	2	24.29	55.0	7504
10	5	2	24.45	55.6	7696

2.8 Results and discussions

The output of the simulation gives data on total power generation in kWh /year, cost of energy per unit and the % availability of power throughout the year for 400 combinations of solar PV, wind generator and battery capacity for the ranges mentioned in Section 2.7.

Table 2.5 lists the partial results of different configurations of hybrid power systems along with their key performance indicators. The table of complete results is given in Appendix - A.

Figure 2.3 shows the total units produced per year for various combinations of solar PV, wind and battery capacities. For a particular solar PV capacity, the total power generated / year increases with increase in wind generator and battery capacities. When the next solar PV capacity is chosen, and the wind generator and battery capacities are started from minimum values, the total power generated / year drops down. The trend continues and thus forms a sawtooth pattern. The net increase in total power generation due to increase in wind generator and storage battery capacities starts to saturate with higher solar PV capacities.

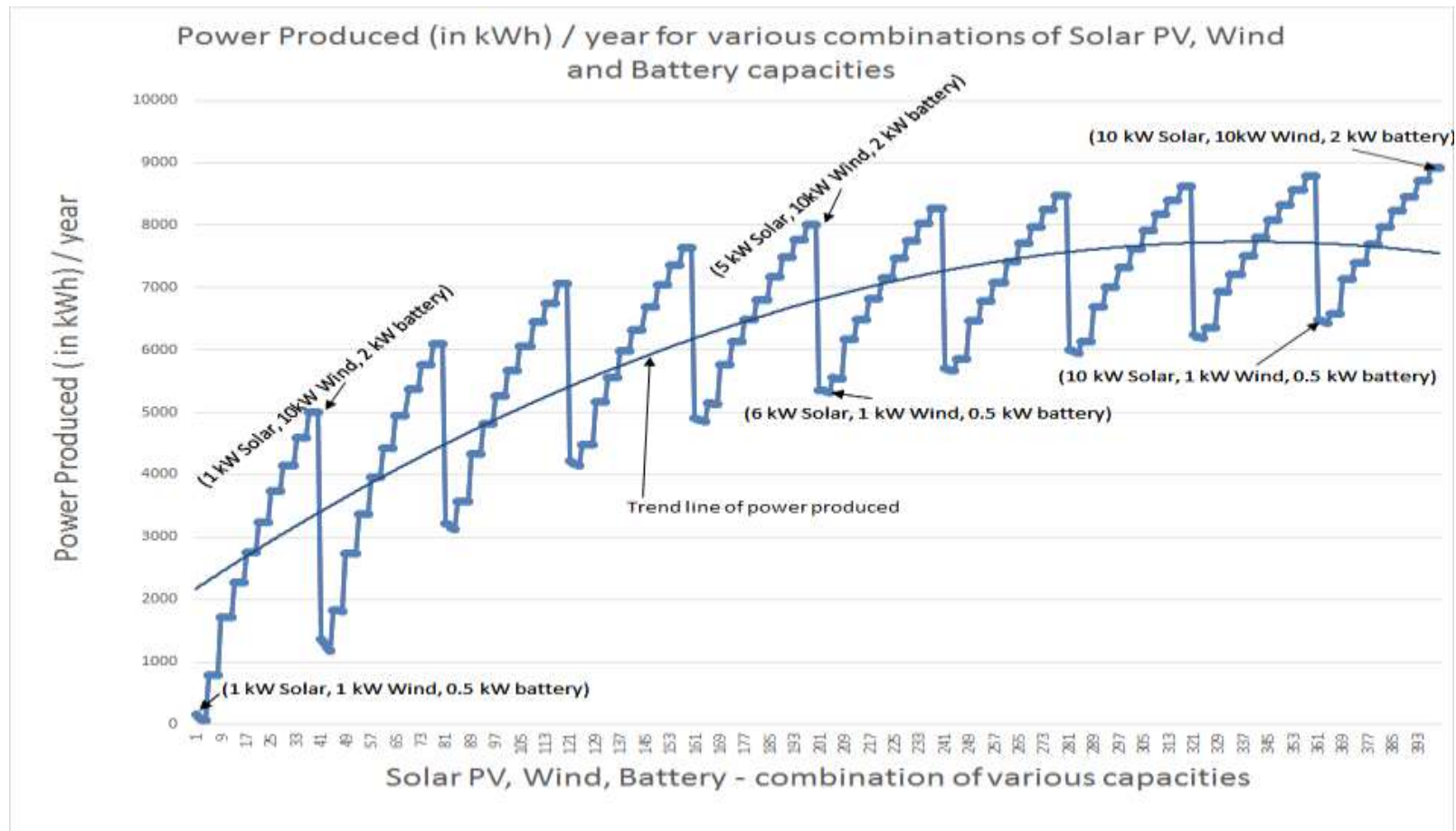


Figure 2.3 Trend line showing total power produced (in kWh) / per year for various combinations of capacities

In X-axis, each number represent a particular combination of PV, wind and battery capacity. 400 such combinations are considered. The Total units produced per year for each such combination is plotted. We can observe that the total units produced gets saturated and does not increase significantly beyond combination of capacities.

2.8.1 Monthly distribution of power generation

The main disadvantage of renewable energy systems is its uneven distribution, and hence very small quantities of power may be available during certain months of a year. Figure 2.4 shows the monthly power generation of individual sources – solar PV and wind for a particular combination of capacities (6 kW solar PV, 9 kW wind, 0.5 kW battery). We can observe that the wind power generation dips during March-April months, but at the same period the solar PV power generation increases. Similar dip in wind power generation can be seen during September which is partially compensated by increase in solar PV generation.

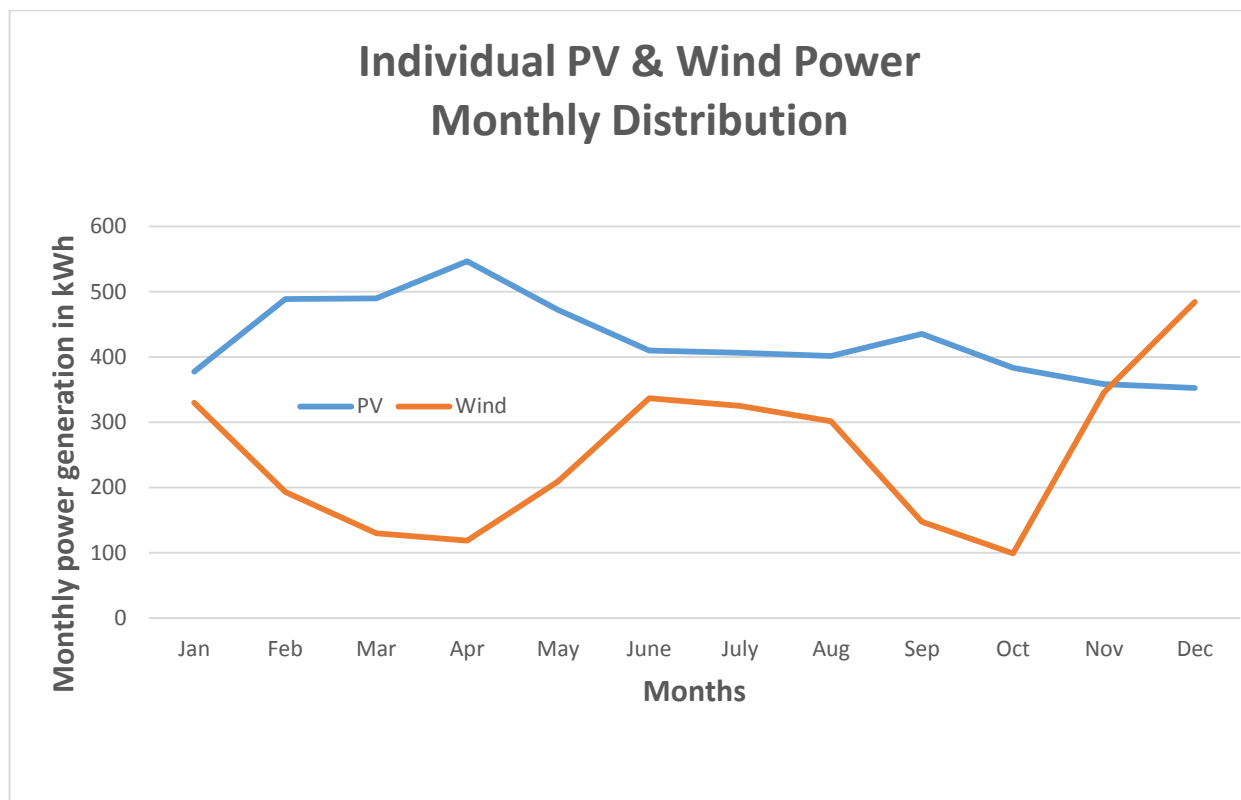


Figure 2.4 Individual PV & wind power generation - Monthly distribution

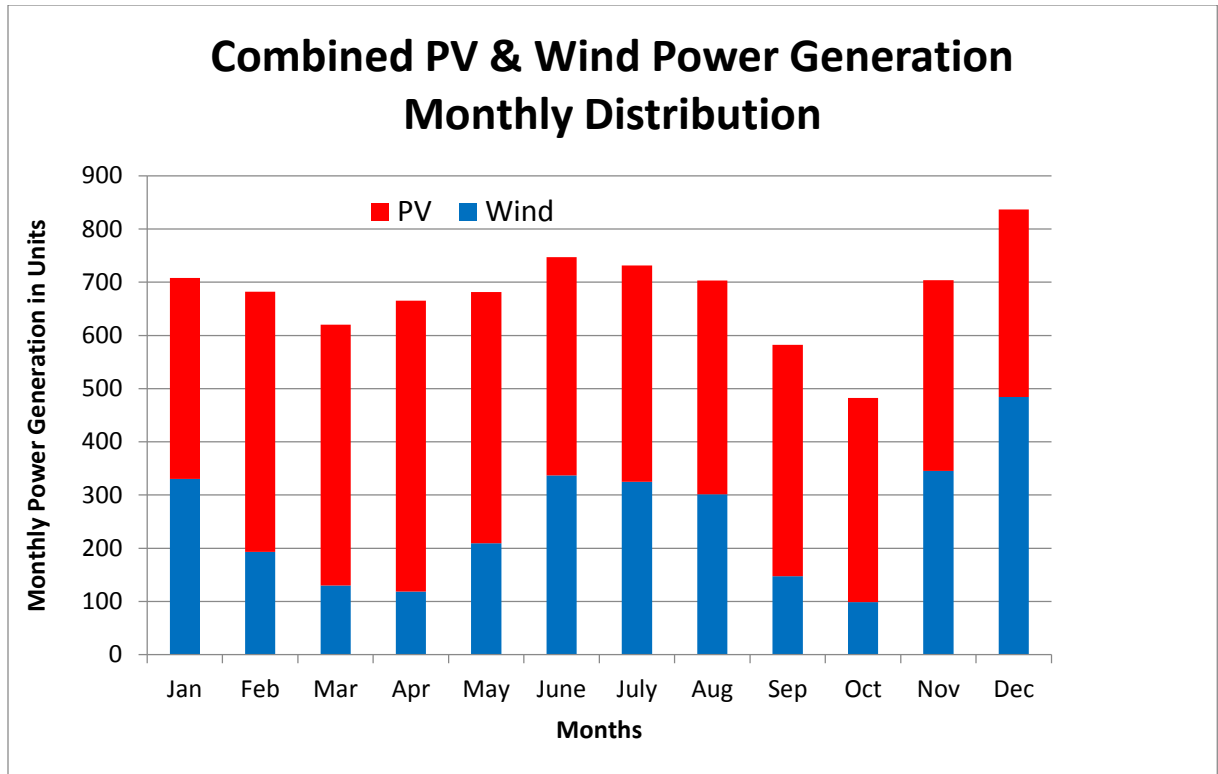


Figure 2.5 Monthly power generation of solar PV and wind

The above figure shows the monthly power generation in kWh for a particular combination of capacities (solar PV – 6 kW, wind – 9 kW, battery – 0.5 kW). The plot indicates the months in a year that we can expect decent share of power generation from PV and wind sources.

Figure 2.5 gives the combined monthly power generation of the hybrid power system. From the plot, we can find that when hybrid system is employed, the monthly power generation is fairly distributed throughout the year except in October when both the sources produce less power simultaneously. The solar and wind resources supplement each other. For instance, when the generation from wind is significantly low during March-April, the generation is supplemented by increased solar PV. Similarly, when the solar PV generation dips during November-December, the wind generation increases and compensates. Hence,

increasing capacity of any one power source separately does not help to increase overall power production significantly, and ultimately contributes to increase in cost of energy per kWh

2.8.2 Analysis of Cost of Energy Vs. Energy production

The sizing of various renewable sources leads to different costs of energy. The Cost of Energy per unit power produced is calculated based on total cost and total units generated throughout the year. The profile of Cost of energy and energy produced with respect to these combinations is given in Figure 2.6.

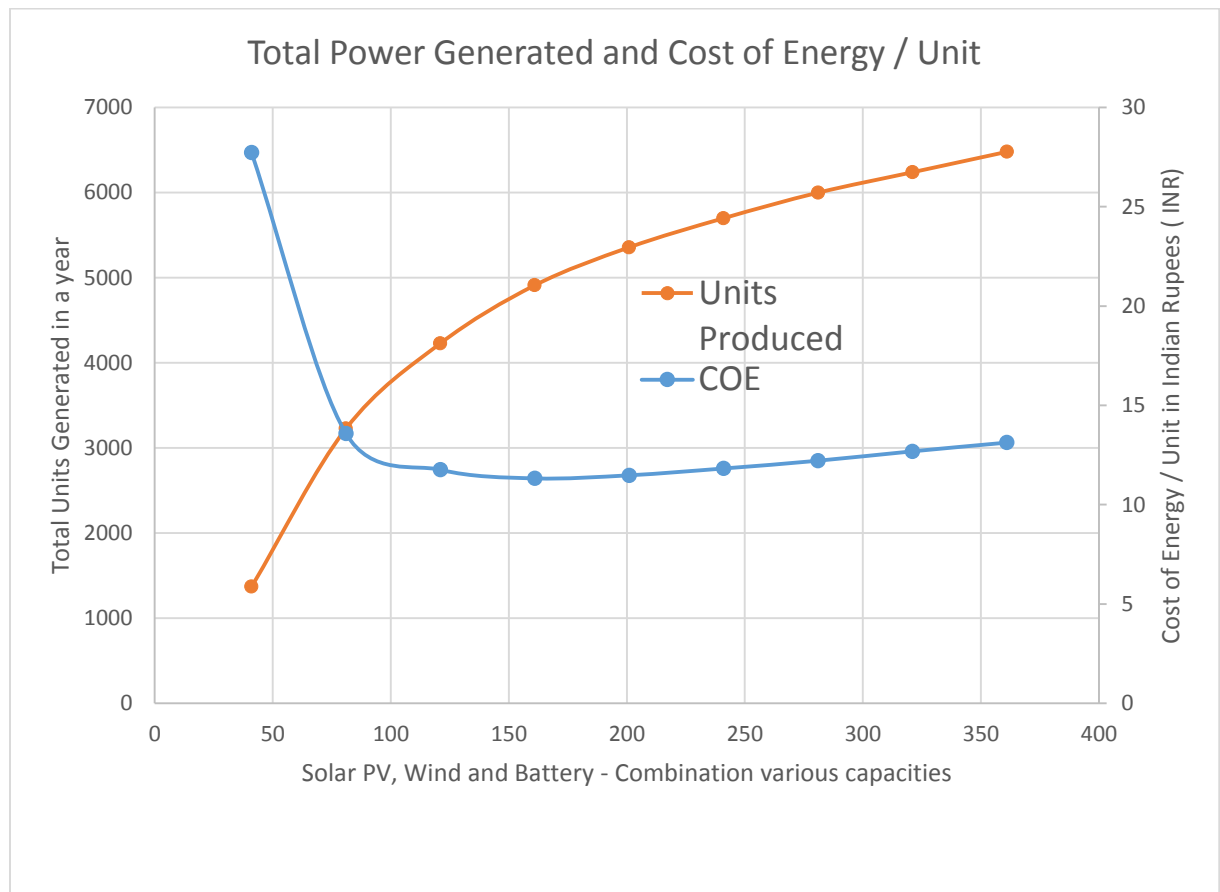


Figure 2.6 Comparison of trend of Cost of Energy and Units produced for various sizing combination of energy sources

Obviously, an increased sizing of energy sources leads to increase in energy production and simultaneously the capital / O&M cost also increases. With the increase in total power generation, the cost of energy per unit starts dropping and saturates to a value after certain limit beyond which there is no significant increase in energy production. Hence, this region forms the suitable combination with reasonably good production and minimum cost of energy.

2.8.3 Availability of power Vs. Cost of Energy

In case of renewable power sources, the availability of energy is intermittent. Hence, it is imperative to take a look at the availability also for these combinations.

Figure 2.7 shows the plot of Cost of Energy/kWh Vs. % availability of power for the year colour coded with the total units produced / year. The deep blue areas represent the highest power production band (7953 to 8920). We observe from the plot that the cost of energy ranges can be less than Rs. 25 per unit with 60 % availability in this maximum power band. Also in the power band of 6018 to 6985 units (light blue areas of the plot), the cost of energy is as low as Rs. 12-20 per unit with good availability of 40 – 55 % range.

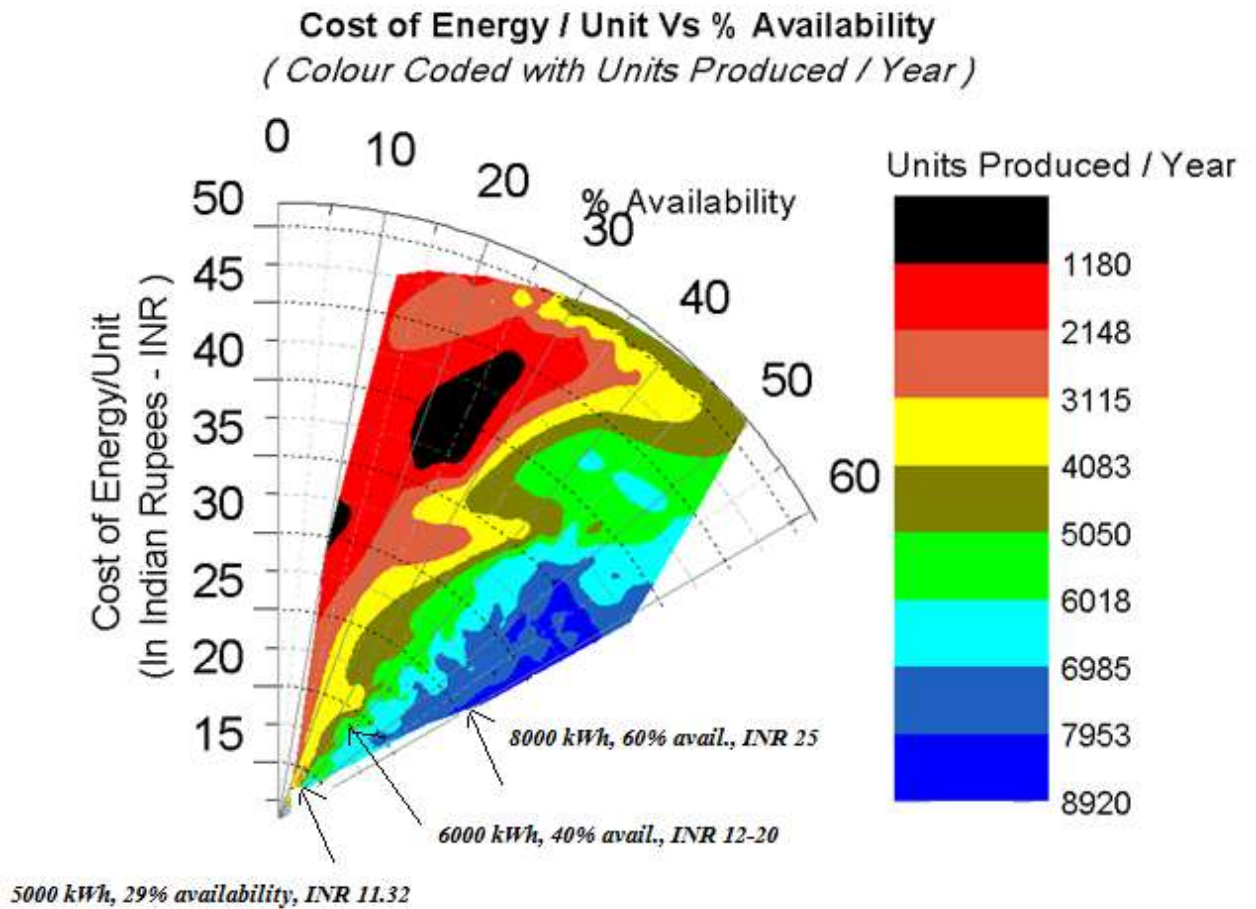


Figure 2.7 Effect of availability and Cost of energy [in Indian Rupees (INR)] colour coded with total power produced per year.

The deep blue areas represent combinations that produces maximum power. Please note the large variations in the Cost of Energy / unit from Rs. 12 up to Rs. 20. If we choose a wrong combination, we may end up with a low power production and high cost of energy. We may obtain higher power production, but at higher cost of energy. Thus, this analysis is crucial to determine the right combination of PV-wind capacities to obtain higher power at lower cost of energy. Also the availability of power in a year for the particular combination can also be determined. This plays an important role in deciding the battery capacity.

For instance, to produce approximately 6000 kWh per year, the best option is the combination of 8 kW solar PV , 1 kW wind and 1.5 kW storage battery for obtaining energy at cost of INR 12.73 per kWh with an availability of 40% .

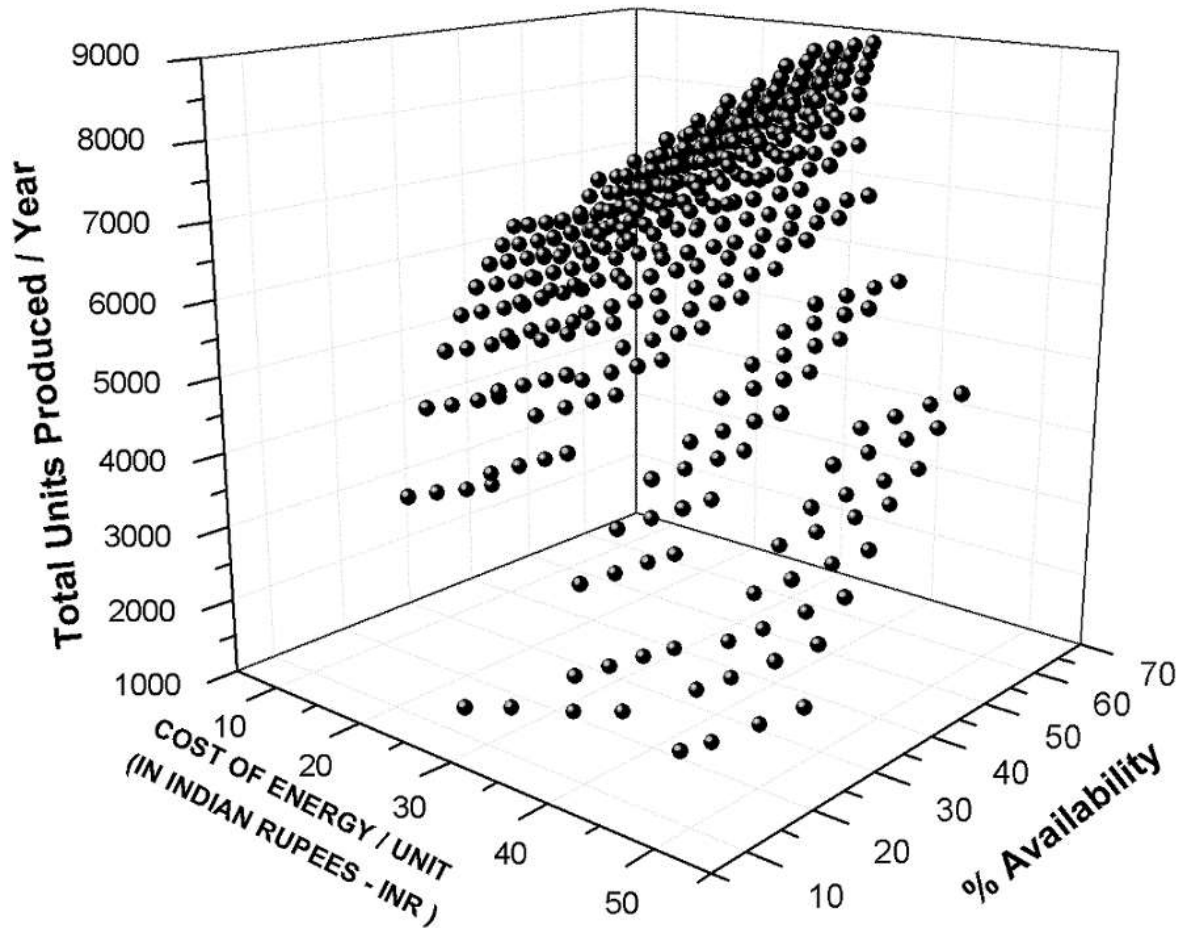


Figure 2.8 3-D Plot showing cost of energy / unit, % availability and total units produced / year.

This plot shows all the 400 combinations and their performance with respect to total power produced, cost of energy and the availability.

Similarly, to produce power at the lowest cost / kWh, we can select a combination of 5 kW solar PV, 1 kW wind and 0.5 kW battery. With the above

combination, we get the lowest cost of energy at INR 11.32 per kWh, but the total power produced in the year is around 5000 kWh with an availability of only 29%. The same is clearly represented in Figure 2.8.

2.9 Brackish Water RO plant as a variable load for Renewables based Hybrid Power System for increased power utilization

Modeling of hybrid renewable energy based with solar PV and wind turbines with a constant load is presented in the previous sections. This section proposes to use a brackish water desalination plant as a variable load coupled with hybrid power system and attempts to analyze the effect in power output from the system.

2.10 Simulation Methodology with desalination plant as load

The inputs and the simulation methodology are same as already explain in Section 2.7. We have used the hourly solar irradiance data measured in kWh/m²/day and wind speed data in m/s as inputs for simulation. The above data is used to calculate the power output available from PV and wind sources using the models as described in Section 2.

A Brackish water Reverse Osmosis (BWRO) plant with a capacity of 24 m³ / day is chosen as the load to be the system. This plant can operate at full load with 2 kW of power input and with reduced output up to a power input of 0.5 kW. Again, the power generated by renewables is calculated for every hour of the year. The algorithm used for the simulation is given in Figure 2.9.

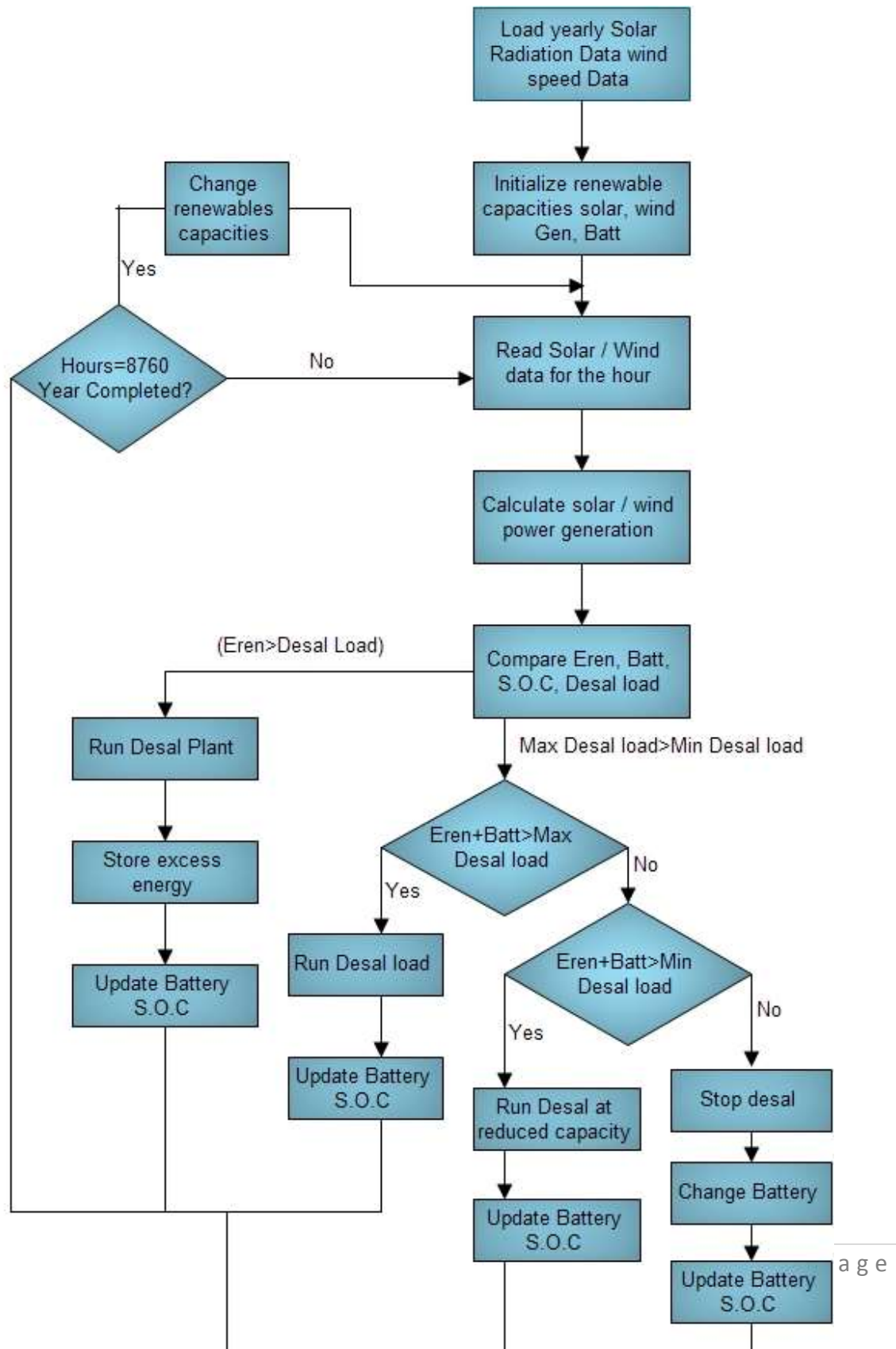


Figure 2.9 Proposed methodology of simulation

The power generated is utilized as per the following logic. When the power generated by the renewables is more than 2 kW, the plant will operate at full load producing rated output and excess power will be used to charge the battery. When the power generated is less than 2 kW and more than 0.5 kW, the plant will operate at lesser capacity. If the power generated is less than 0.5 kW, only batteries will keep charging and the plant will operate at lesser load using batteries until the battery is discharged to its maximum level beyond which the plant will shut down and only batteries will keep charging.

2.11 Results and discussions

The output of the simulation gives data on Total power output in kWh throughout the year for 400 combinations of solar PV, wind generator and battery capacity for the ranges mentioned in Section 3.3. The partial results of different configurations of hybrid power systems with constant load and with BWRO plant load is presented in Table 2.6. Complete data is given in Appendix – B.

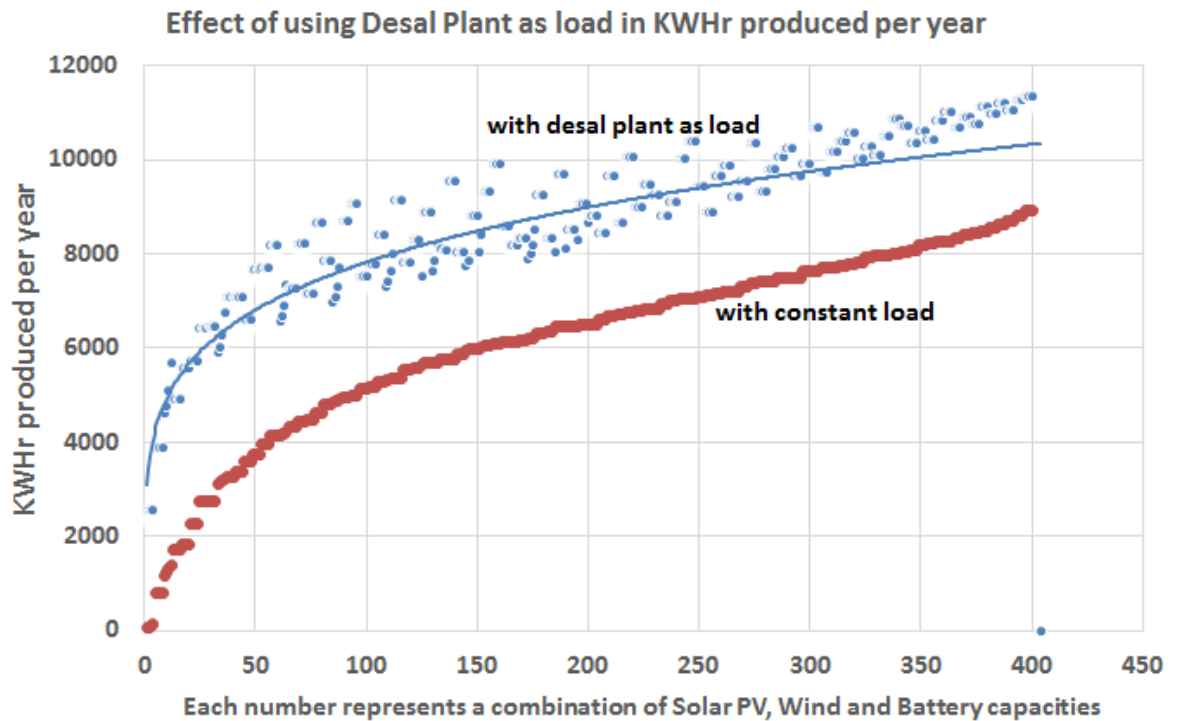
*Table 2.6 Partial list of different configurations of hybrid power systems and kWh/year generated with constant load and BWRO plant load
(Complete table given in Appendix – B)*

PV (kW)	Wind (kW)	Battery (kW)	kWh/year produced With constant load	KWh/year produced with desal. load	Water produced per year (in m³)
1	3	0.5	1712	4928	3240
1	4	2	2268	5738	2612
1	10	1	5000	9077	5457
2	1	2	1180	4628	5768
2	9	1.5	5760	9552	5811
3	1	0.5	3226	6743	6368
4	1	0.5	4228	7324	6708
4	10	2	7646	10678	6679
5	1	0.5	4910	7711	6906
5	5	2	6478	9066	5394
5	6	0.5	6806	9483	5731
5	10	2	8018	10861	6818
6	1	0.5	5356	8001	7039
7	1	0.5	5698	8221	7136
8	3	2	6700	8678	5160
9	2	0.5	6362	8326	7467
10	1	2	6440	8043	7327
10	2	0.5	6586	8440	7514
10	10	1	8912	11332	7173
10	10	1.5	8912	11332	7173
10	10	2	8912	11332	7173

From the results, we can see that there is a clear increase in the total kWh produced throughout the year. The increase is mainly due to direct utilization of renewables power generation to the maximum extent particularly when the power generated is low. In other case, this has to be used for charging the battery or will be wasted if the battery charge is already full. Hence the BWRO plant indirectly acts as a storage device tapping the generated energy to the maximum possible extent.

For example, in combination number 100, a solar PV of 5 kW, wind of 2 kW and battery of 1 kW capacities produces 5142 kWh/year with a constant load and 7520 kWh/year with BWRO plant as load. The average increase in kWh/year is around 25%.

Figure 2.10 shows the plot of kWh /year produced for various combinations of solar PV, wind and battery capacities in both cases (i.e.) with constant load and with desalination plant as a variable load. The constant load curve is same as the trend line already given in Figure 2.3. We can observe that there is a clear increase in the power produced with BWRO plant. Also we can see that the increase in power production is more predominant when the capacities of solar PV, wind and Batteries are in lower ranges. This is because of effective utilization of power during low power periods. At higher ranges, the increase becomes more or less steady.



*Figure 2.10 Plot showing increase in kWh/year produced with BWRO plant as load
The red plot shows the total power produced with a constant load for all 400 different combinations of PV, wind and batteries. The blue line indicates the trend line of total power produced with the variable desalination plant as load. The plot shows a definite increase in total power produced with desalination plant as a load.*

The production capacity of water at various combinations also can be found out using the above results. We have taken a specific energy consumption of 1.5 kW per m^3 of desalinated water production for the chosen BWRO plant. The daily water production for a particular combination of renewables (solar PV – 10 kW, wind generator – 5 kW) is shown in Figure 2.11. The total desalinated water production for the whole year for the above combination works out to 7768 m^3 and the average production per day is around 21.28 m^3 . This shows that with a suitably sized storage tank, we can deploy to proposed configuration easily to cater to desalinated water requirement of around $20 \text{ m}^3/\text{day}$.

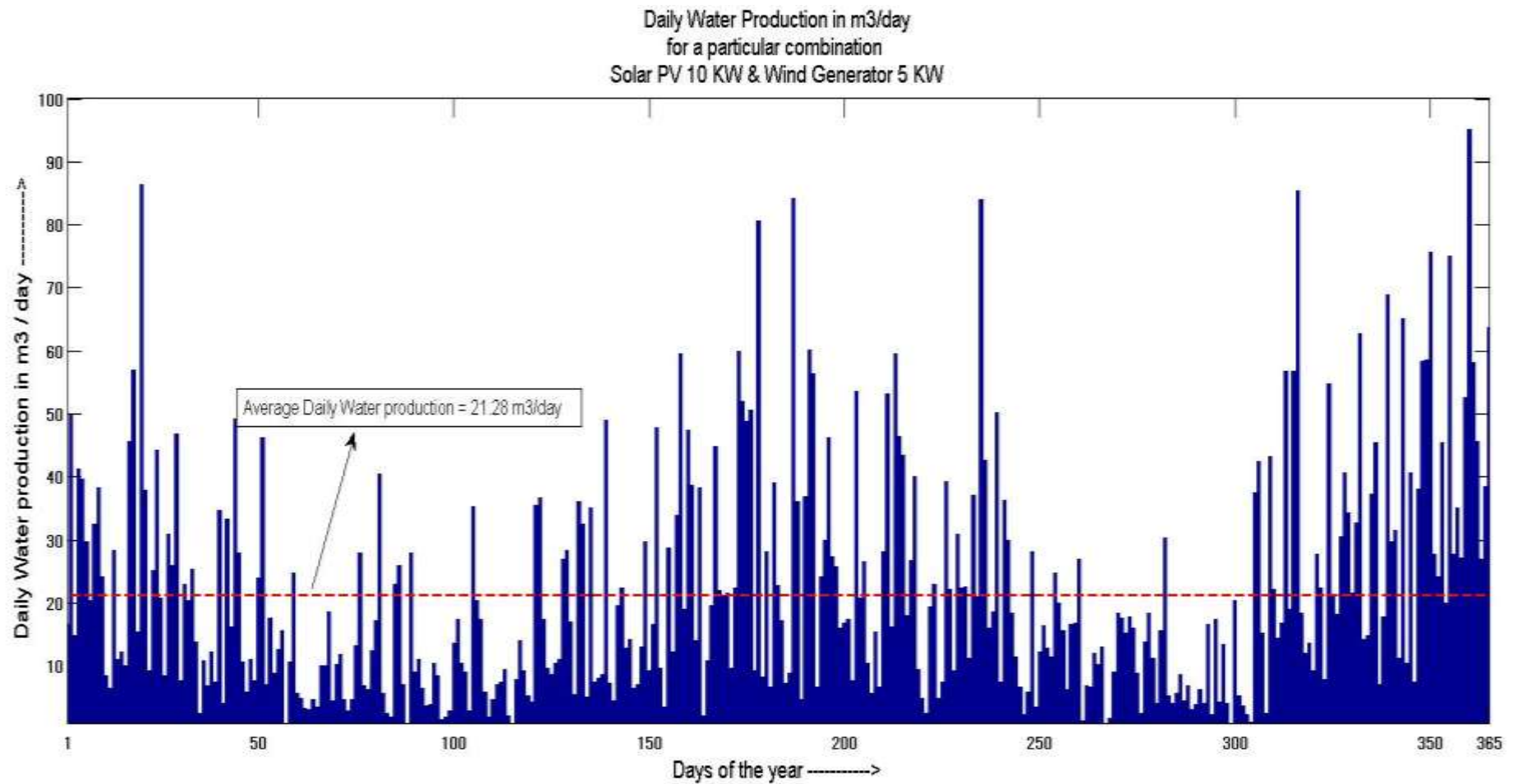


Figure 2.11 Daily water production throughout the year (in m³ /day)

The plot shows that there is always a minimum production of water for almost all days throughout the year, ensuring good availability. The average water production is around 21,000 Liters of water per day.

2.11.1 Cost of Water for various combinations of PV and wind capacities

The performance of the proposed configuration is analyzed for total water produced in a year and also the cost of water per m³ of water produced. This is done to ensure that the total amount of water produced during a year should be able to cater to the minimum requirements as desired. Apart from this, we also considered the availability of the power for running of the BWRO plant (i.e.) % of plant operating hours in a year.

The cost model of the various energy sources is developed considering the capital cost per kW capacity and the cost of desalination plant per m³ per day. The annualized capital costs are calculated by using the capital recovery factor which is calculated by taking the life span of systems and the interest rate into account. Also the operation and maintenance costs are included in the model. The annual total cost of the hybrid power system for a particular set of capacities of solar PV, wind and battery is finally calculated by summation of the individual costs. The formulae used for the cost model is as given below. Table 2.7 lists the description of symbols used and Table 2.8 gives the input parameters of simulation.

$$ACC = CC \times CRF \quad \dots \text{Eq.(2.12)}$$

$$\begin{aligned} ATC = & C(PV) \times [ACC(PV) + AMC(PV)] \\ & + C(W) \times [ACC(W) + AMC(W)] \\ & + C(B) \times [ACC(B) + AMC(B)] \\ & + C(D) \times [ACC(D) + AMC(D)] \quad \dots \text{Eq.(2.13)} \end{aligned}$$

Table 2.7 Symbols used in Cost model

Symbol	Description
CC	Capital cost/kW (in INR – Indian Rupees)
CRF	Capital recovery factor
ACC	Annualized capital cost (in INR)
AMC	Annual O&M cost (in INR)
ATC	Annualized Total cost (in INR)
C(PV)	PV Capacity (in kW)
C (W)	Wind plant capacity (in kW)
C (B)	Battery capacity (in kW)
C(D)	Desalination Plant capacity (in m ³ /day)
COE	Cost of Energy / kWh (in INR)

Table 2.8 Simulation input parameters

Parameter	Solar Photovoltaic	Wind Generator	Batteries	BWRO Plant
Capital Cost (in INR)	50000 per KW	180000 per KW	10656 per kW	250000 per m ³ /day
Life span	20 years	20 years	5 years	15 years

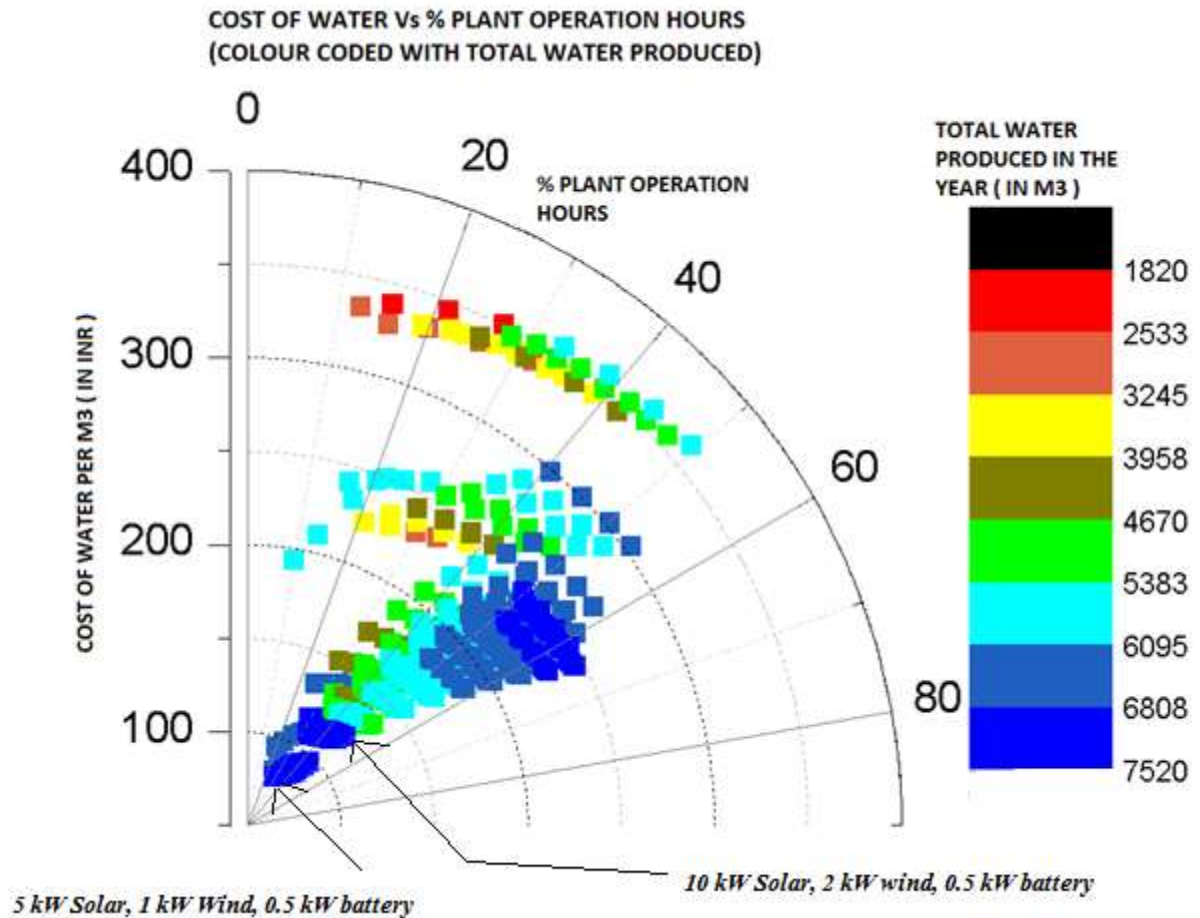


Figure 2.12 Cost of Water Vs % Plant Operation Hours
The deep blue band in the plot shows that the same total water production is achievable for various cost of water per 1000 liters (i.e.) around INR 80, around INR 110 and at INR 225 approximately. This is also spread in the availability of 20%, 40% and 60%. So this analysis is extremely crucial to make an informed decision.

We can observe from Figure 2.12 that the cost of water varies with selection of combination of solar PV and wind generator capacities. Also the total water produced for the whole year and the availability of plant also varies. The deep blue band in the plot shows that the same total water production is achievable

for various cost of water (i.e.) around INR 80, around INR 110 and at INR 225 approximately. This is due to increase in capital cost involved in various combination of the solar PV and wind generator capacities. But the total water production remains in same level. This only helps to increase the availability of the plant, but significantly increases the cost.

For an objective of lower cost of water, we can select the combination of solar 5 kW, wind 1 kW and battery 0.5 kW to produce a total of 6906 m³ of product water at a cost of INR 80 per 1000 liters. (Refer Table 2.6 - Combination no. 161) This comes with an availability of plant of around 28% which can be compensated by selecting suitable storage tanks.

Similarly, for a high production of water at around 7500 m³, we can select the combination of solar 10 kW, wind 2 kW and storage battery 0.5 kW to produce water at a cost of INR 116 per 1000 liters of water and the availability is around 54%. (Refer Table 2.6 – Combination no. 365).

The above knowledge enables us to select capacities on the basis of our actual requirements. We can fix up the total water required in the whole year and the maximum cost that can be afforded for producing this water. The system configuration can be selected for the necessary combination of PV-wind systems to meet our objective. Places where water cannot be stored to the required level and continuous availability of water is the main objective, the selection can be made accordingly, but at an increased cost.

2.12 Conclusion

In this chapter, modeling of renewable energy based desalination systems with solar PV and wind turbines along with battery storage system is carried out.

1. A methodology of selection of the capacities of various power sources of the hybrid power system is developed for obtaining the optimum configuration. The optimum configuration can be chosen based on our objectives.
2. From the results obtained, we can see that addition of capacities of PV panels or wind turbines or storage capacities separately does not help in reduction of the cost of energy. But, when the capacities of solar PV and wind turbines are supplemented with each other, we find that we are able to maintain the total kWh produced per year to meet the load requirements.
3. For an objective of around 6000 kWh per year power production, the best option is the combination of 8 kW solar PV , 1 kW wind and 1.5 kW storage battery for obtaining energy at cost of INR 12.73 per kWh with an availability of 40% .
4. But, if our objective is to have the system with minimum possible cost of energy / kWh, we can select a combination of 5 kW solar PV, 1 kW wind and 0.5 kW battery. With the above combination, we get the cost of energy at INR 11.32 per kWh, but the total power produced in the year is around 5000 kWh with an availability of only 29%.
5. For application of this hybrid power system for desalination purpose that requires a variable load of 2 kW, the necessity of energy storage battery is

reduced. There is an average increase in utilization of power generated by around 25%.

6. In the case of desalination plant as load, the hybrid power system can produce and store water in suitable tanks and hence the availability factor is not a major concern. For an objective of lower cost of water, we can select the combination of 5 kW solar PV, 1 kW wind and 0.5 kW battery to produce a total of 6906 m³ of product water at a cost of INR 80 per 1000 liters. This comes with an availability of plant of around 28% which can be compensated by selecting suitable storage tanks.
7. Similarly, for a high production of water at around 7500 m³, we can select the combination of 10 kW solar PV, 2 kW wind and 0.5 kW storage battery to produce water at a cost of INR 116 per 1000 liters of water and the availability is around 54%.

Chapter 3

3 MODELING OF RENEWABLES BASED HYBRID POWER SYSTEM WITH DESALINATION PLANT LOAD USING NEURAL NETWORK

3.1 Introduction

Hybrid power system is seen as a viable alternative to the conventional systems. Estimating the potential of these hybrid power systems for a selected site is a major input required for making informed decisions. Often, estimation of the kWh production is a very elaborate and tedious exercise due to lack of a reliable model for the same. This chapter proposed an Artificial Neural Network based model that can be used to easily estimate the total kWh/year for a given combination of solar PV, wind generator and battery. The variable load considered for the model is a desalination plant load. The data is modeled using Neural Network and validated. The proposed Neural Network model offers a reliable estimation on the total annual power generation for a given combination of solar PV, Wind generator and battery capacity.

3.2 Introduction to ANN

An Artificial Neural Network (ANN), simply referred to as a Neural Network, is essentially a computer program that is specifically modeled on the human brain. The ability of processing information and learning from the above processing is

also incorporated in the program [88]. Early artificial neural networks were inspired by biological nervous systems. The primary features of artificial neural networks are derived from two characteristics of the brain: the ability to 'learn' and to generalize from limited information [89]. In later years the development in ANN technology has evolved into an applied mathematical technique that has some similarities to the human brain [90] [91].

Figure 3.1 gives the simple artificial neural network. It is composed of a large number of highly interconnected processing elements (neurons) working in union to solve specific problems [92] [93] [94]. ANNs are more like human in the sense that they try to generalize and learn with examples they come across. An Artificial Neural network can be configured for a specific purpose application, like identification of patterns or classification of data, through a process of learning called training. Learning in human is basically by adjustment of the synaptic connections between the neurons. The ANN mimics the same.

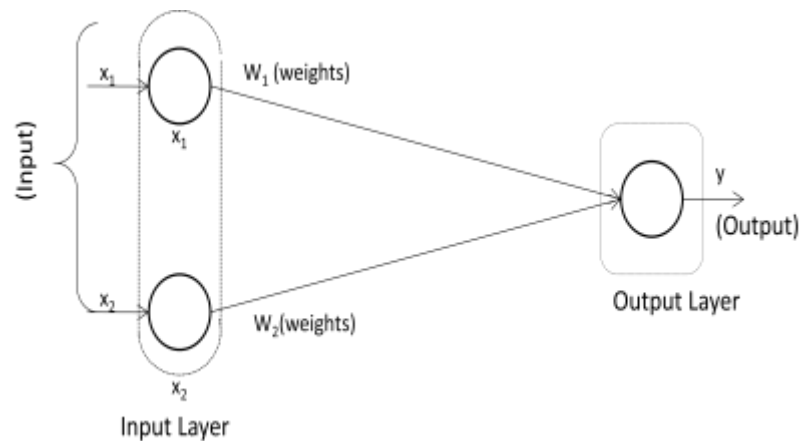


Figure 3.1 A simple Artificial Neural Network

Instead of using model of zeros and ones, the processing elements are interconnected with each other. The method of arrangement of these process elements and their connection weights decide the output of the network

3.3 Modeling the Biological Neuron

A biological neuron or a nerve cell consist of synapses, dendrites, the cell body (or hillock), and the axon. The synapses are elementary signal processing devices. The synapse converts a pre-synaptic signal into a chemical signal and then back into a post-synaptic electrical signal. The input signals are modified in magnitude by synapse parameters [95]. The modification is based on type of the synapse. The signal can be blocked or completely transmitted. The output signals from the synapse are summed up and transmitted through the dendrites up to the cell body. The cell produces the output signal that is transmitted to other neuron by means of axons. The total synaptic activity controls the frequency of firing and the synaptic activity is controlled by weights.

In general the function of the main elements can be given as:

Dendrite – Receives signals from other neurons;

Soma – Sums all the incoming signals and

Axon – When a particular amount of input is received, then the cell fires. It transmits signal through axon to other cells [96].

The basic function of a biological neuron is to receive inputs from other neurons and the received inputs are combined with each other in a nonlinear manner and give the final output.

The following are the basic characteristics of biological neuron inherited into the artificial neuron.

1. Signals are received by the processing elements. This element sums the weighted inputs.
2. The weight at the receiving end has the capability to modify the incoming signal.
3. The neuron fires (transmits output), when sufficient input is obtained.
4. The output produced from one neuron may be transmitted to other neurons.
5. The processing of information is found to be local.
6. The weights can be modified by experience.
7. Neurotransmitters for the synapse may be excitatory or inhibitory.
8. Both artificial and biological neurons have inbuilt fault tolerance.

Table 3.1 and Figure 3.2 indicate how the biological neural net is associated with the artificial neural net.

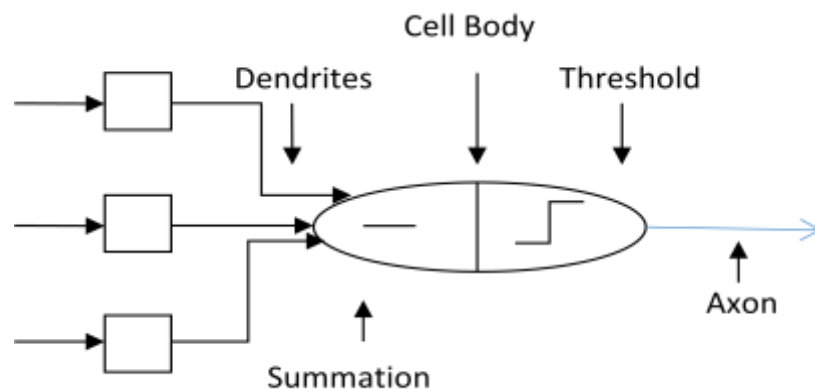


Figure 3.2 A simple model of Biological Neuron

Table 3.1 Associated Terminologies of Biological and Artificial Neural Net

Biological Neural Network	Artificial Neural Network
Cell Body	Neurons
Dendrite	Weights or interconnections
Soma	Net input
Axon	Output

3.4 Building Blocks of ANN

The basic building blocks of the artificial neural network are the network architecture, setting the weights and the activation function.

3.4.1 Network Architecture

The arrangement of neurons into layers and the pattern of connection within and in-between layer are generally called as the architecture. The neurons within a layer may or may not be interconnected [97]. The number of layers in the net can be defined as the number of layers of weighted interconnected links between the particular slabs of neurons. If two layers of interconnected weights are present, then the network has hidden layers.

There are various types of network architectures: feed forward, feedback, fully interconnected net, competitive net, etc. Figure 3.3 shows some of the very commonly used network architectures [98].

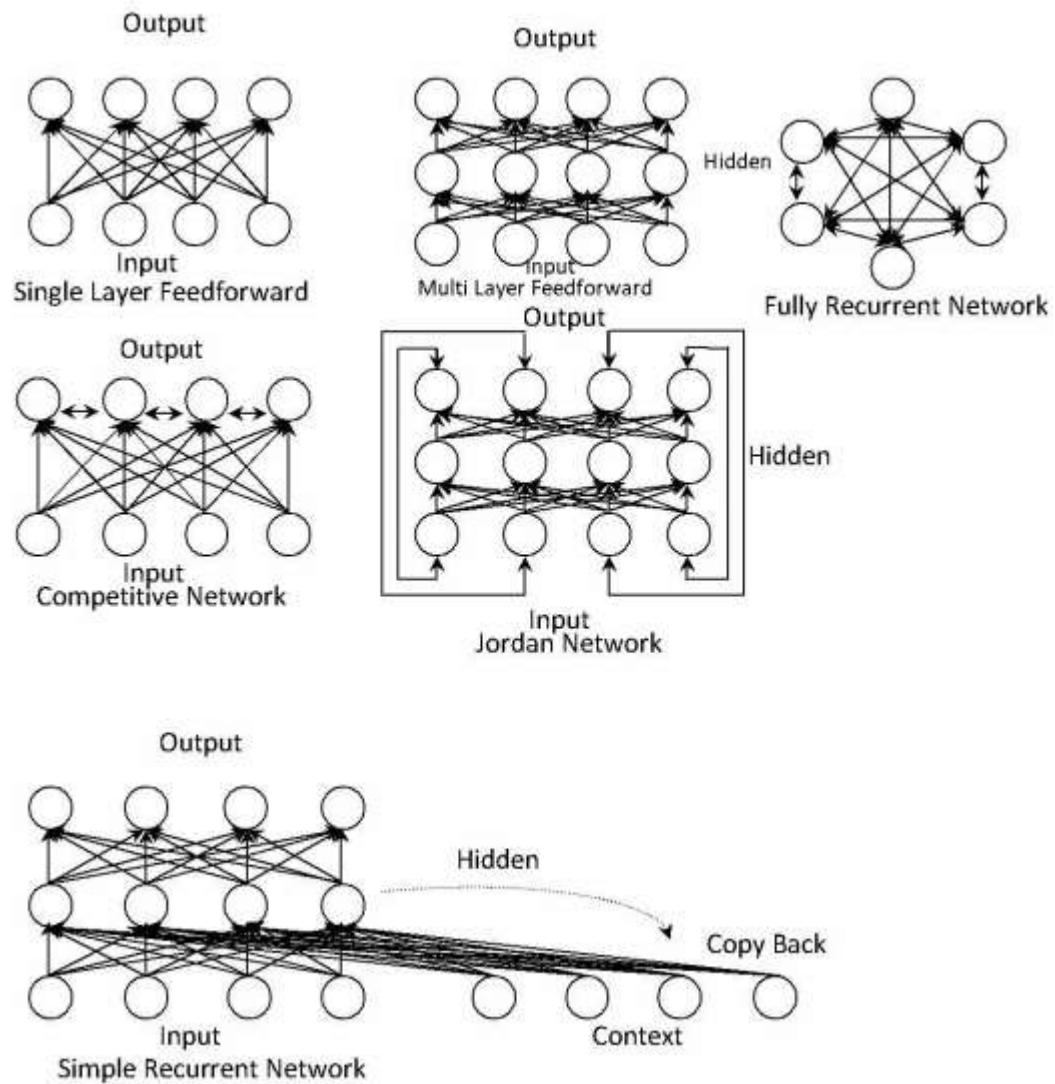


Figure 3.3 Some Artificial Neural Network Connection Structures

The Artificial neural networks (ANNs) as well as the actual biological neural networks have got a variety of shapes and they vary in terms of sizes in case of the feed forward network architectures. The input units are activated and these activated inputs become a particular value. These values are further propagated into the neural network. The process is continued till the weights of the all output nodes are found and fixed.

Some of the very common network architecture includes Feed Forward Net (both single layer and Multi-layer), Competitive Net, and Recurrent Net.

3.4.2 Setting the weights

The process of training or learning of neural network is by setting the weight values associated with individual connection. The weights are changed with the aim to obtain the expected output. This process is called the training of a network. The process that the network undergoes internally during the training is called learning. There are generally three different types of training namely supervised, unsupervised and reinforcement training [90] [99].

3.4.3 Activation Functions

The activation function is used to calculate the output response of a neuron. The sum of the weighted input signal is applied with an activation to obtain the response. For neurons in same layer, same activation functions are used. There may be linear as well as nonlinear activation functions. The nonlinear activation functions are used in a multilayer net [100].

3.5 Advantages of ANN:

Neural networks can easily bring out the trend, underlying meaning and implicit rules from data that are not precise. Systems and processes that are too difficult to be modeled using analytical techniques can be very easily and effectively modeled using neural networks. They can generalize and learn from the training set data and can accurately predict when new set of data is given. The neural network is a systematic approach to optimize a given problem. Once trained properly, neural networks can classify, estimate and do prediction [101] [102] [103].

3.6 ANN Vs Traditional statistical methods

In sharp contrast with the traditional methods, ANNs are data-driven methods. They are inherently self-adaptive methods with few prior assumptions on the models. Thus it can be applied to estimation and forecasting [104] [105]. ANNs need examples to learn and they can find out even small relationships underlying within the data which is otherwise very difficult to explain. Hence, ANN can be applied to solve very complex and non-linear problems. ANN can handle large set of input and output data [106] [107] [108] . This approach with learning ability can be applied to solve many practical problems where directly relationship between parameters are difficult to establish. The ANN method can produce results for all practical purposes which is very difficult using traditional statistical methods.

ANNs have the capacity to generalize and has got more flexible functional forms when compared with the traditional statistical methods [109] [110] [111] [112] [113] [114]. Almost all traditional statistical processes for time series

predictions like the Box-Jenkins [115] or ARIMA method [116] assume the system to be linear. Hence they may fail when applied for non linear systems [117] [118] [119] [120].

3.7 Back Propagation Network (BPN)

In this chapter, the Back propagation network is used to create a model to estimate the total power produced by the hybrid power system. Back propagation is a systematic method for training multi-layer artificial neural networks. It is basically a multi-layer forward network that uses gradient-descent algorithm based delta-learning rule [121]. This is commonly referred to as back propagation of errors rule. Back propagation provides a computationally efficient method for changing the weights in a feed forward network, with differentiable activation function units, to learn a training set of input-output [122]. Being a gradient descent method it minimizes the total squared error of the output computed by the net. The network uses supervised training for learning. [123] The network has to get itself trained based on the input patterns and should be able to respond in a similar manner for similar input patterns [124] [125]

3.7.1 Architecture

A multilayer feed forward back propagation network with three layers: one input layer X, one hidden layer Z and one output layer Y is shown in the Figure 3.4.

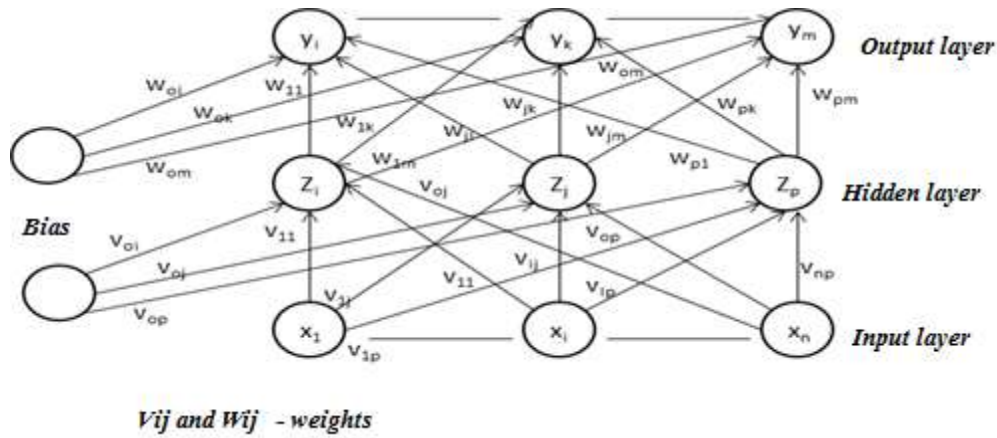


Figure 3.4 Architecture of Back Propagation Network

The output layer Y has \mathbf{w}_{ok} as bias input and hidden layer Z has \mathbf{v}_{ok} as bias input. The bias is used to trigger the neuron. From Figure 3.4, it is clear that the network has one input layer, one hidden layer and one output layer. The input layer is connected to the hidden layer and the hidden layer is connected to the output layer by means of interconnection weights. During the back propagation phase of learning, the signals are sent in the reverse direction [126]. The architecture of back propagation network resembles a multi-layered feed forward network. The increase in the number of hidden layers results in the computational complexity of the network. This may in turn lead to more convergence time and increased time to minimize the error. The bias may be provided for the hidden and the output layers [127].

3.7.2 Training Algorithm

The training algorithm of back propagation involves four stages, viz. initialization of weights, feed forward, back Propagation of errors, updation of the weights and biases.

During first stage which is the initialization of weights, some small random values are assigned. During feed forward stage each input unit (\mathbf{x}_i) receives an input signal and transmits this signal to each of the hidden units $\mathbf{z}_1 \dots \mathbf{z}_p$. Each hidden unit then calculates the activation function and sends its signal to each output unit \mathbf{y}_i . The output unit calculates the activation function to form the response of the net for the given input pattern [128] [129] [130].

During back propagation of errors, each output unit compares its computed activation \mathbf{y}_k with its target value \mathbf{t}_k to determine the associated error for that pattern with that unit. Based on the error, the factor $\delta_k(k = 1, \dots, m)$ is computed and is used to distribute the error at output unit \mathbf{y}_k back to all units in the previous layer. Similarly, the factor $\delta_j(j = 1, \dots, p)$ is computed for each hidden unit \mathbf{z}_j .

During final stage, the weight and biases are updated using the δ factor and the activation parameters.

The various parameters used in the training algorithm are as follows:

\mathbf{X} : Input training vector

$$\mathbf{X} = (\mathbf{x}_1 \dots, \mathbf{x}_j, \dots, \mathbf{x}_n)$$

\mathbf{t} : Output target vector

$$\mathbf{t} = (\mathbf{t}_1 \dots, \mathbf{t}_k, \dots, \mathbf{t}_m)$$

δ_k = error at output unit \mathbf{y}_k

δ_j = error at hidden unit \mathbf{z}_j

α = learning rate
 v_{oj} = bias on hidden unit j
 z_j = hidden unit j
 w_{ok} = bias on output unit k
 y_k = output unit k .

The training algorithm used in the back propagation network is as follows. The algorithm is given with the various phases:

Initialization of Weights

- Step 1 : Initialization of weight to randomly small values.
- Step 2 : Until we reach the stoppage criterion, remaining steps to be continued in loop.
- Step3 : Selection of a set inputs and outputs in training set to perform remaining steps

Feed Forward

- Step 4 : Input signal x_i fed to each input unit and which in turn transmits to other units of hidden layer.
- Step 5: For the hidden unit ($z_j, j = 1, \dots, p$), the input to the hidden unit is given by

$$z_{-inj} = v_{oj} + \sum_{i=1}^n x_i v_{ij} \quad \dots \text{Eq.(3.1)}$$

Then activation function is applied to get the output from hidden unit.

$$\mathbf{z}_j = \mathbf{f}(\mathbf{z}_{inj}) \quad \dots \text{Eq.(3.2)}$$

This signal is sent to all layers of output units.

Step 6 : For the output unit (\mathbf{y}_k , $k = 1, \dots, m$), the input to the output unit is given by

$$\mathbf{y}_{-ink} = \mathbf{w}_{ok} + \sum_{j=1}^p \mathbf{z}_j \mathbf{w}_{jk} \quad \dots \text{Eq.(3.3)}$$

Then, application of activation function gives the output signals.

$$\mathbf{y}_k = \mathbf{f}(\mathbf{y}_{-ink}) \quad \dots \text{Eq.(3.4)}$$

Back Propagation of Errors

Step 7 : Error in output is calculated using

$$\delta_k = (\mathbf{t}_k - \mathbf{y}_k) \mathbf{f}'(\mathbf{y}_{-ink}) \quad \dots \text{Eq.(3.5)}$$

Step 8 : The error is back propagated to the hidden layer using

$$\delta_{-inj} = \sum_{k=1}^m \delta_k \mathbf{w}_{jk} \quad \dots \text{Eq.(3.6)}$$

$$\delta_j = \delta_{-inj} \mathbf{f}'(\mathbf{z}_{-inj}) \quad \dots \text{Eq.(3.7)}$$

Updation of Weight and Biases

Step 9 : The weights are corrected based on the error in the hidden layer

$$\Delta \mathbf{w}_{jk} = \alpha \delta_k \mathbf{z}_j \quad \dots \text{Eq.(3.8)}$$

$$\text{Therefore, } \mathbf{w}_{jk}(\text{new}) = \mathbf{w}_{jk}(\text{old}) + \Delta \mathbf{w}_{jk}, \quad \dots \text{Eq.(3.9)}$$

$$\mathbf{w}_{ok}(\text{new}) = \mathbf{w}_{ok}(\text{old}) + \Delta \mathbf{w}_{ok} \quad \dots \text{Eq.(3.10)}$$

The input and hidden layer weights are corrected using the weight correction factors

$$\Delta v_{ij} = \alpha \delta_j x_i \quad \dots \text{Eq.(3.11)}$$

$$\Delta v_{oj} = \alpha \delta_j \quad \dots \text{Eq.(3.12)}$$

$$\text{Therefore, } v_{ij}(\text{new}) = v_{ij}(\text{old}) + \Delta v_{ij}, \quad \dots \text{Eq.(3.13)}$$

$$v_{oj}(\text{new}) = v_{oj}(\text{old}) + \Delta v_{oj} \quad \dots \text{Eq.(3.14)}$$

Step 10: The output response generated is checked for stopping criterion.

The stopping criterion can be anything like the targeted error or the number of training cycle.

3.8 Modeling hybrid Solar PV-Wind Power Scheme

The hybrid solar PV-Wind power scheme is already described in Chapter 2. The individual components of hybrid system is modeled. The solar irradiation and wind speed data for the selected site Kalpakkam is used. The total power produced in kWh per year is determined for various combination of capacities. The same is discussed in detail in Chapter 2.

The quick estimation of power generation that is generated by the hybrid power systems is required to evaluate the desired configuration of the system. This chapter proposes a neural network model of the hybrid power system to find out the total power generated for a year without going in for detailed analysis. The

model offers a good estimate of the total annual power generation with the capacities of solar PV, Wind generator and battery as input.

3.9 Proposed Neural Network Model

A neural network model is proposed to estimate the total kWh produced in a year for a given set of solar PV capacity, Wind generator capacity and storage battery capacity (in kW). A back propagation network with three layers: an input layer, a hidden layer and an output layer is proposed.

The input layer is composed of three nodes in inputs which are:

- i) Solar PV capacity
- ii) Wind generator capacity
- iii) Storage battery capacity

The hidden layer is composed of five nodes whose activation function is the hyperbolic tangent sigmoid transfer function. The output layer is composed of one node and this represents the required output (i.e.) the estimated total kWh produced in a year for a given set of capacities as input.

The neural network architecture is shown in Figure 3.5.

The configuration and the power generation data developed in Chapter 2 is chosen for neural network modeling. Complete data set given in Appendix-A. We have got 400 data sets for solar PV, Wind generator & Storage battery capacities as input and the total kWh produced for the year as output. This set is randomly divided into 3 sets of data:

1. Training data - 70% (280 data sets)
2. Validation data – 15 % (60 samples)
3. Test data – 15 % (60 samples)

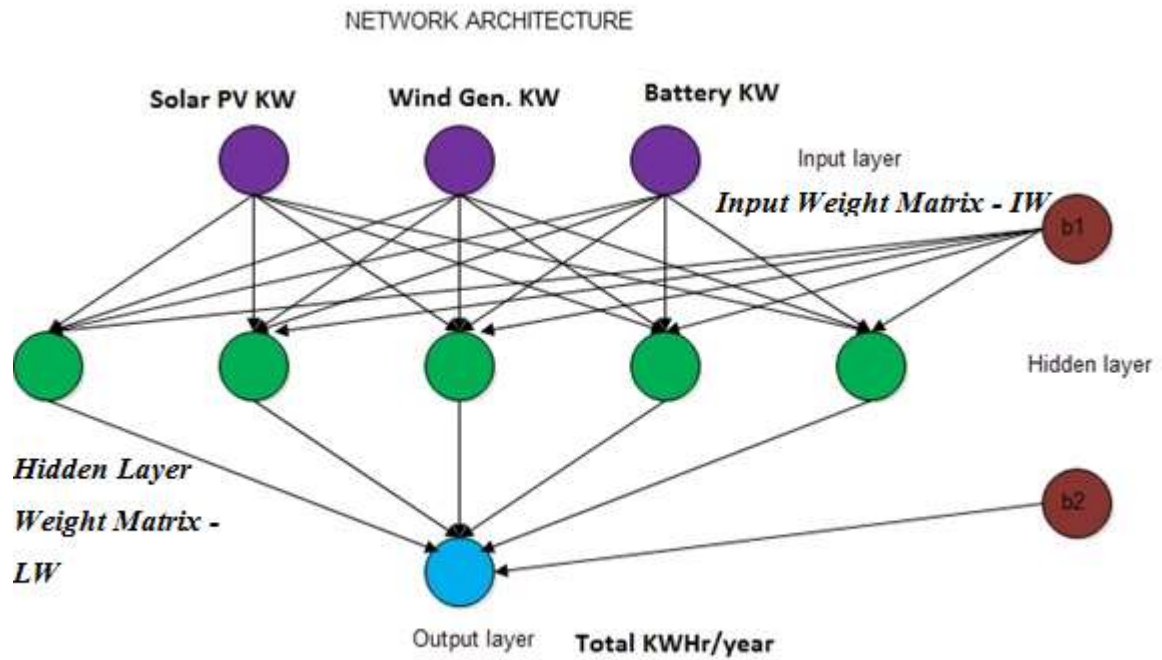


Figure 3.5 Proposed neural network architecture for estimation of total kWh produced per year

The input layer consists of capacities of solar PV, Wind generator and battery. 400 different combinations of such capacities are used. The output layer consists of total kWh produced throughout the year from respective input capacities. One hidden layer is used.

3.9.1 Training

The training data set is used for training of the chosen neural network. The training was carried out using training algorithm equation Eq 3.1 to 3.14.

The input values of solar PV kW, Wind kW and battery kW are taken from the selected data set for training. Initial bias values b_1 and b_2 are set to be 1. The input layer weight matrix – IW , connecting the input layer and hidden layer is initialized. Using this, all the nodes of hidden layers are calculated. Subsequently, the hidden layer weight matrix – LW and the hidden layer nodes are used to calculate the output layer node. This output is nothing but the total power (kWh) generated by the hybrid power system for the particular combination of capacities.

The predicted output is compared with the target value which is the power generated value in the training data set. The difference between the predicted and the required target value is the error. The error value is used to adjust the weight matrices (IW and LW) and the bias values (b_1 and b_2) and the output is predicted.

The above procedure is carried out for all the 280 training data sets. The weight values are adjusted using this data set during training according to the error calculated. The training is repeated for all the training data sets until the error becomes minimum. Each training cycle is called an epoch.

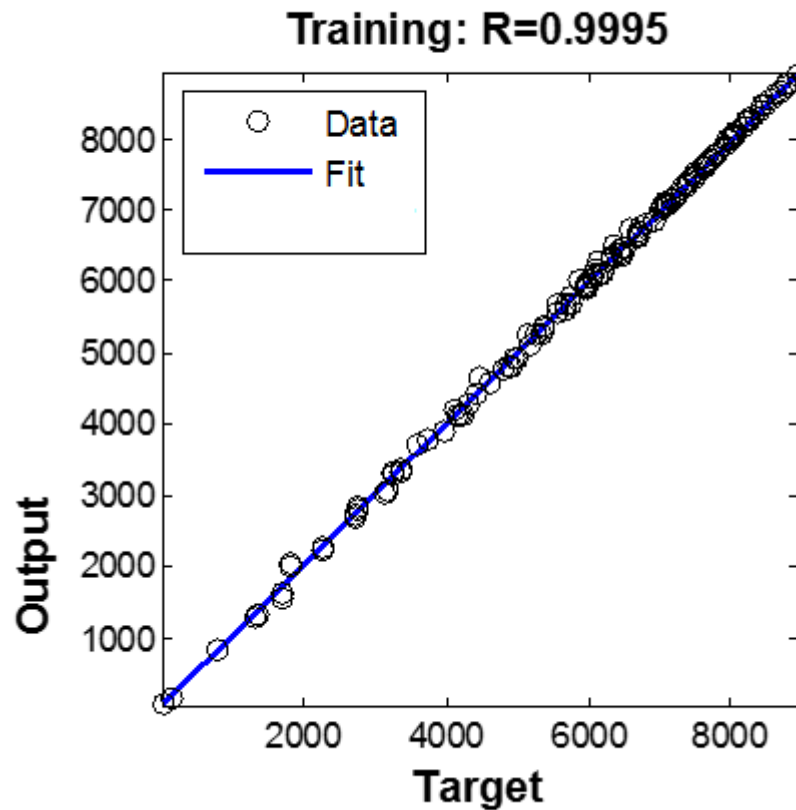


Figure 3.6 Regression plots of neural network model for training datasets

The regression value close to 1 shows that the network is effectively trained.

The performance of the proposed neural network model during training is shown in Figure 3.6. The predicted output is plotted against the required target values of the training data set. The plots show the regression value of the model during the training phase. The value of 0.9995 shows that the neural network model has undergone enough training so that the predicted value of the output is almost close to the actual value.

3.9.2 Validation and Verification:

The validation data set is used to measure the network generalization. This gives us information when to halt the training. 15% of the data i.e. 60 samples of data are chosen in random for the validation of the model. This data was presented as inputs to the neural network model to calculate the output. The predicted value of output is compared with the actual value to find out the error in prediction. If the error is high, the model is trained further.

Figure 3.7 shows the performance parameters of validation. The gradient refers to the derivate from all the data sets before calculating the update required for the weight matrices. The gradient in various training cycle called epochs is shown in the plot. The momentum update (μ) value is the training gain in each training cycle which helps the error to converge. The μ values during the entire training cycle is also shown in this plot. The validation fail check is done to ensure that the neural network is not over trained. The training is stopped with six validation check fails.

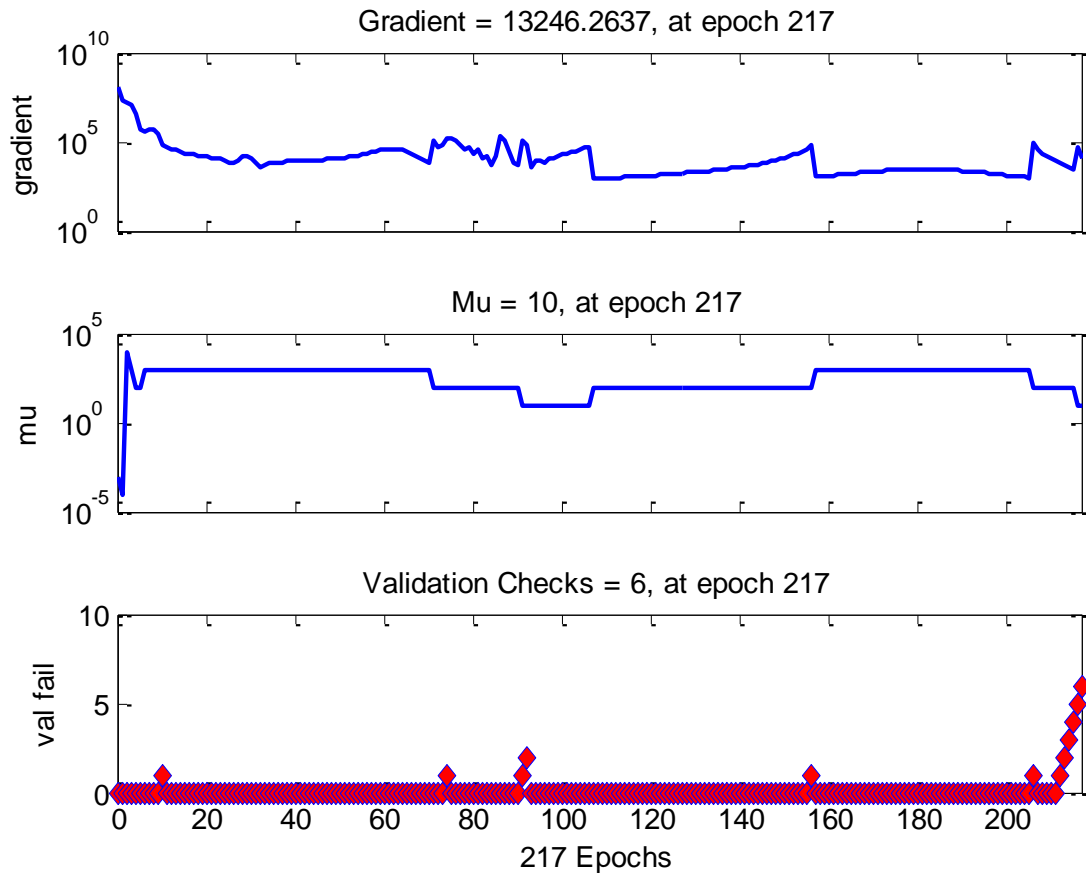


Figure 3.7 Validation checking of the neural network model

The performance of the model for the validation set of data is shown in Figure 3.8. The regression value (R) between the obtained output and the targeted value is 0.99942 which shows a high correlation and good validation of data.

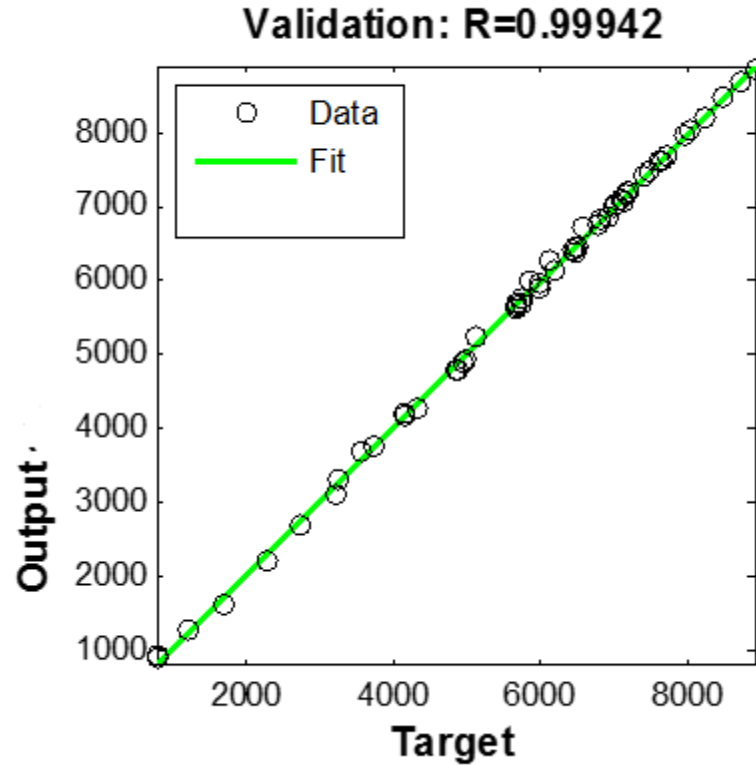


Figure 3.8 Regression plots of neural network model for validation datasets

3.9.3 Verification

The verification of the fitted neural network model was carried out using the test data set. The test data set consists of again 15% i.e. 60 samples. The test data set provides an independent measure of network performance after training. In the verification phase, the model is presented with completely a new set of input data which it has not encountered during the training. This set is not used during training and has no effect in training the network. This will indicate the performance of the model when it encounters a completely new set of input data.

Figure 3.9 shows the model performance for the test data set and also the overall data set which includes the training, validation and testing data sets. The regression values close to 1 indicates a very high level of correlation between the predicted value by the model and the actual value. This shows that the fitted model is accurate.

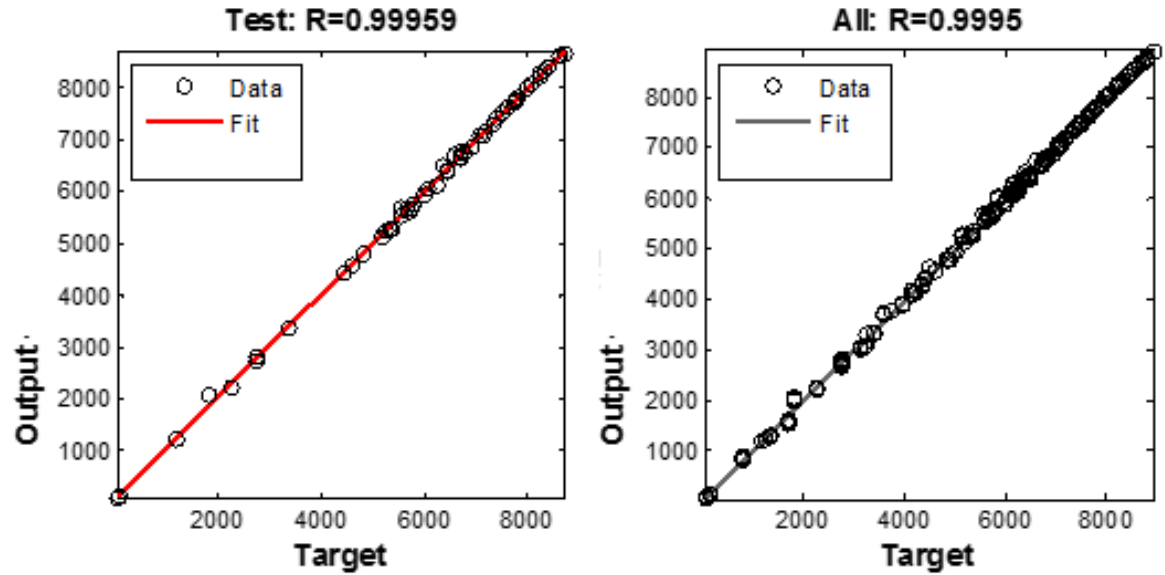


Figure 3.9 Regression plots of neural network model for verification testing and overall datasets

3.9.4 Neural network model

The neural network models the data into the relationship as given in equation 3.15.

kWh / year produced

$$= b2 + LW * \tanh [(b1 + IW * (\text{Inputs} - \text{solar PV kW}, \\ \text{Wind kW, Batt. kW}))]$$

... Eq.(3.15)

where

IW is the input weight matrix,

b1 is the bias for hidden layer,

LW is the hidden layer weight matrix and

b2 is the bias for the output layer.

The values of weight matrices and biases are given in Table 3.2. Using equation Eq. 3.15, we can instantly obtain the estimated total kWh produced in a year for a given capacity of solar PV, Wind generator and battery for the selected site.

Table 3.2 Values of Weight matrices and biases

IW Input Weight Matrix	b1 Bias for hidden layer	LW Hidden Layer Weight Matrix	b2 Bias for output layer
[-2.2208,-0.096177, -0.018034; -0.18876,0.31461,-.00066758; -1.8081,0.49754, 2.239; 6.3759, 0.5142, -0.010182; 1.7715 ,1.2849, -0.043931]	[-1.0518; -0.44379; 0.080092; 4.8492; 2.9711]	[-0.16632 -1.3172 -0.00112 0.16754 0.27026]	[-0.58362]

The regression values are close the one which indicates a very high correlation between the estimated kWh value and the actual one which in fact shows that the fitted NN model is accurate.

3.10 Conclusion

In this chapter, neural a network model of renewable energy based desalination systems using Solar PV and Wind turbines is developed. [131]

1. A neural network model is proposed for the above system with Solar PV, Wind generator and battery capacities as inputs and total kWh production per year as the output.
2. The proposed three layer architecture is trained to obtain the required performance. The model fitted gives very high regression value close to one indicating the accuracy of the NN model.
3. The weight matrices for the model is determined.
4. The model estimates the total power generated per year for a given capacity of Solar PV, Wind generator and Battery. The model equation and parameters are given in Eq. 3.15 and Table 3.2. The model predicts the unknown test data with regression of 0.99.

Chapter 4

4 HIGH STEP-UP CONVERTER IN CLOSED LOOP FOR RENEWABLE ENERGY APPLICATIONS

4.1 Introduction

Since a majority of small scale renewable energy sources (RES) including the solar PV modules gives the output voltage in the range of around 15 – 40 V DC, the output needs to be stepped up to suit the load requirements using a high voltage gain converter. The renewable sources inherently generate sudden variations in input voltage, a good output voltage profile even during such random variations in input conditions is essential. Such power converter enables deployment of hybrid renewable systems for standalone desalination applications. This chapter presents prototype development of a high step-up converter configuration with closed loop control. The converter topology is explained and the design of the circuit is elaborated. The converter for hybrid power system that can handle two input sources is developed and tested.

4.2 Background

The power-electronic technology plays a vital role in distributed generation and in integration of renewable energy sources into the electrical grid, and it is widely used and rapidly expanding as these applications become more integrated with the grid-based systems [132]. The increasing number of renewable energy sources

and distributed generators requires new strategies for the operation and management of the electricity grid in order to maintain or even to improve the power-supply reliability and quality [133] [134] [135].

Solar panels and other renewable energy sources have now become an important alternate source for the power generation. The scale of production is expected to reach to tens of Giga Watts in the future. Solar photovoltaic (PV) system and wind generators have got obvious advantages when compared to other renewable energy systems as this is silent, modular, easily transportable and quickly installed. Power can be generated in-situ, eliminating the need of long transmission lines. Also, small scale systems like terrestrial applications of photovoltaic panels supplement the other conventional power generation [136]. There are PV-AC modules that has got an integrated and compact DC-AC inversion circuit fitted to the suitable configuration and is usually at the back side of the PV panel [137] [138]. Such an arrangement protects the system from losing the power production due to shadow and at the same time offers easier method for installing the PV modules in line with the financial requirements [139] [140].

The required level of DC voltage can be obtained by connecting a series of PV panels. But this solution may not be suitable for low power applications where putting more PV devices will end up in higher capacities and also occupy large space making this option unviable [141] [142] [143]. Also high voltage generated from PV panels can be a safety issue in low power applications. Hence there is a serious need for efficient power electronic conversion systems for low power applications of the order of 100 W [144] [140]. The possible applications includes low power domestic solar PV system with one or two PV panels generating less than 40 V DC. [145] This voltage is required to be stepped up for use in domestic

appliances. Also, it can be used in integrated and compact mobile power units with possible applications in powering up of mobile devices, LED lamps and low mechanical power applications like pumping water and small desalination plant systems [146] [147] [148] [149].

In this chapter, a DC-DC converter with coupled inductor in closed loop operation with high step-up is proposed. The main concept is to obtain high step-up voltage from low voltage delivering devices like photovoltaic panels. The voltage step-up is achieved using the inductor coupling along with connection of capacitors and diodes. The input switch can isolate the power source during periods of non-operation and this feature ensures human safety as well as safety of other circuit components. The designed circuit is extended for hybrid sources with two inputs. The power from the individual input sources can be supplied to the load independently or simultaneously at the same time. The power converter can handle large variations in input voltage caused by changes in solar irradiation and wind speeds. The maximum power point tracking (MPPT) is also implemented for individual sources. The experimental hardware is designed for 100 W.

4.3 Description and modeling of the High Step-up Converter

The general schematic of a power generation system with a high step-up converter is shown in Figure 4.1. The solar PV or other renewable energy source acts as the input power source. This source is then connected to the high step-up converter to produce a sufficient DC voltage. The DC voltage is then fed to an

inverter circuit to get an AC output voltage for connecting with the load. In case of DC loads, the inverter is not necessary.

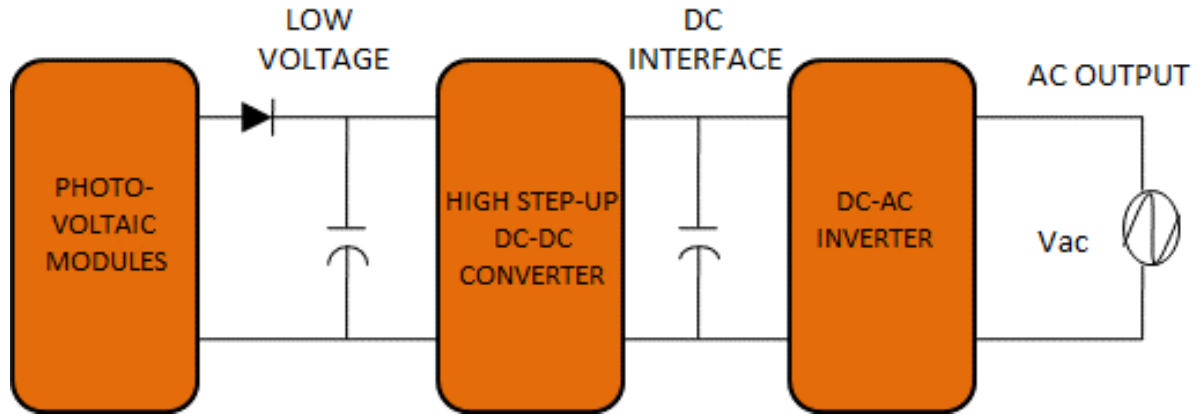


Figure 4.1 Schematic of renewables based generation system with a high step-up converter

The circuit configuration of the high step-up converter is shown in Figure 4.2. The circuit has got a coupled inductor T_1 , switch S_1 , capacitors C_1 and C_2 , diodes D_1 and D_2 . The voltage input V_{in} is connected to the primary winding N_1 of the coupled inductor T_1 . The primary winding N_1 is connected to a pair of capacitor C_1 and diode D_1 . Similarly, the secondary winding N_2 is connected to capacitor C_2 and diode D_2 . The coupled inductor T_1 has a turns ratio 'n' which is equal to N_2/N_1 . The converter shown a large step-up voltage-conversion ratio because of the connection of the two pairs of inductors, capacitor, and diode. The same is explained in subsequent sections.

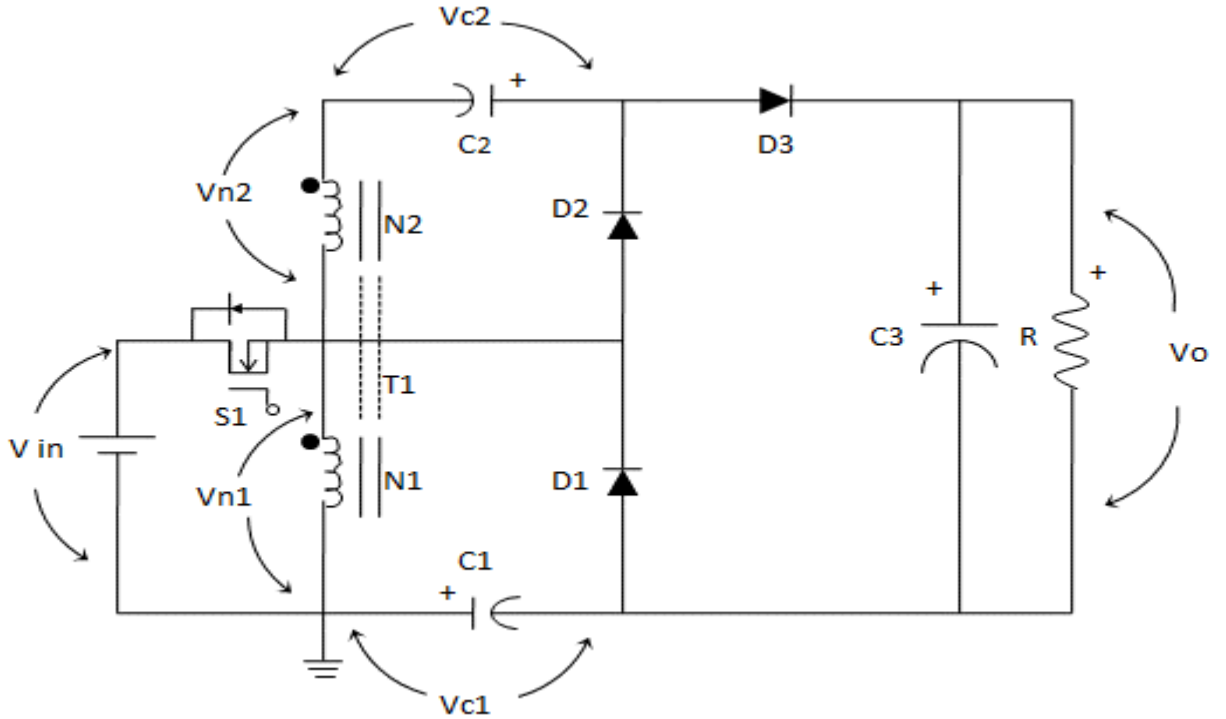


Figure 4.2 Circuit configuration of high step-up converter

Under steady state, the input voltage V_{in} is applied across N_1 winding of coupled inductor. This induces a voltage of n times of V_{in} with polarity as shown in *Figure 4.3* where n is the turns ratio of coupled inductor. Two circulating currents i_{c1} and i_{c2} are set up in the loops in directions shown in the same figure. The voltages V_{c1} , V_{c2} are also set up across the capacitors C_1 and C_2 due to the circulating currents in respective loops. The voltages across the capacitors have the polarity as per the respective current directions and it can be seen that they are in such a way to aid the incoming voltage. The stored energy of the inductor is recycled through the freewheeling diodes D_1 and D_2 to increase the efficiency.

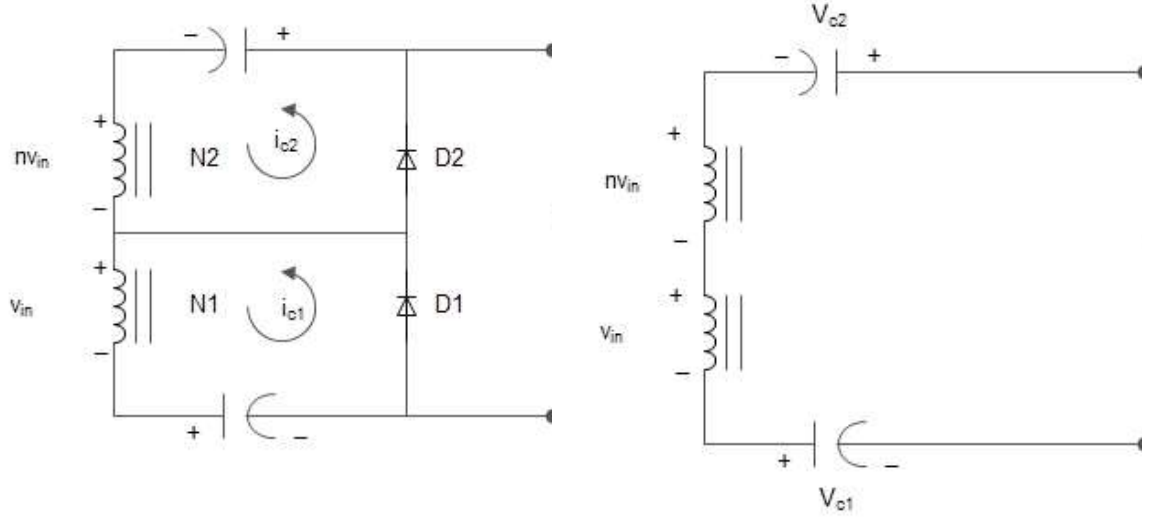


Figure 4.3 Diagram indicating the current and voltage polarities under steady state

From the *Figure 4.3*, the output voltage V_o is the sum of voltage drops across the capacitors C_1 & C_2 (V_{C1} & V_{C2}) and the coupled inductors N_1 & N_2 (V_{N1} & V_{N2}) with the input voltage V_{in} . This is given by the equation (4.1).

$$V_o = V_{in} + V_{n2} + V_{C2} + V_{C1} \quad \dots \text{Eq.(4.1)}$$

The voltage across capacitors C_1 and C_2 are obtained as follows:

$$V_{C1} = \frac{D}{1-D} V_{in} \quad \dots \text{Eq.(4.2)}$$

$$V_{C2} = \frac{nD}{1-D} V_{in} \quad \dots \text{Eq.(4.3)}$$

where D is the Duty cycle and n is the turn's ratio of the coupled inductor T_1 windings which is equal to N_2 / N_1 .

Substituting equations 4.2 and 4.3 in equation 4.1, we get

$$V_0 = V_{in} + nV_{in} + \frac{nD}{1-D} V_{in} + \frac{D}{1-D} V_{in} \quad \dots \text{Eq.(4.4)}$$

The overall voltage gain M is as follows:

$$M = \frac{V_0}{V_{in}} = \frac{1+n}{1-D} \quad \dots \text{Eq.(4.5)}$$

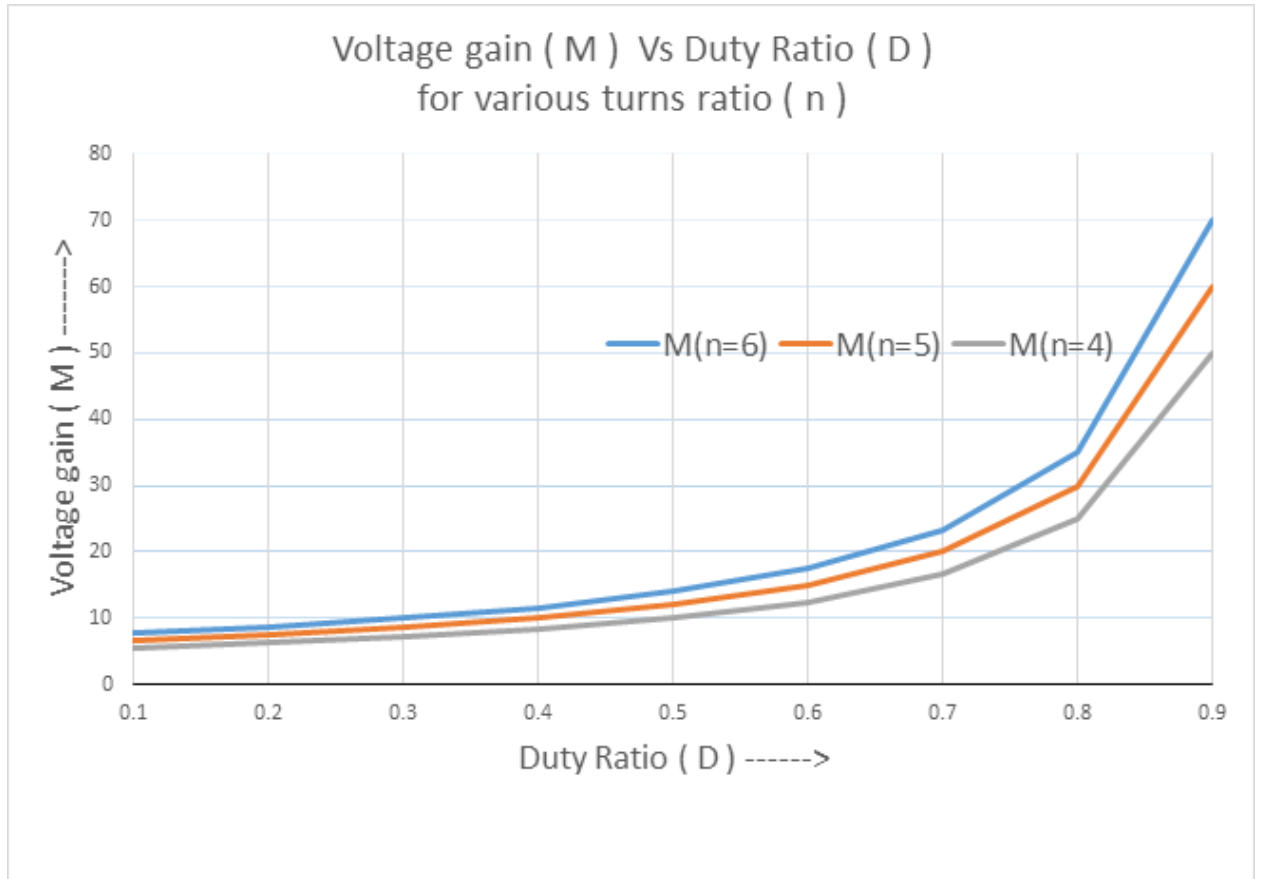


Figure 4.4 Voltage gain for various duty ratios with different values of n
From the plot we can see that with moderate duty ratios in the range of 0.4 to 0.6 and switching frequency $f_s = 50$ kHz, we are able to obtain the voltage gain in the range of 8 to 17. We have chosen the turns ratio of $n=5$.

To select the turns ratio of the coupled inductor, we have plotted the voltage gain against the duty ratios for various values of turns ratio using equation (4.5). The obtained plot is shown in Figure 4.4.

From the plot we can see that with moderate duty ratios in the range of 0.4 to 0.6 and switching frequency $f_s = 50$ kHz, we are able to obtain the voltage gain in the range of 8 to 17. We have chosen the turns ratio of $n=5$. Hence for $V_{in}=15$ V to 40 V and $V_0 = 200$ V; we need a voltage gain (M) up to 13 which is obtainable at a turns ratio of $n=5$ and a moderate duty ratio (D) of 0.55. The capacitor C_1 and C_2 are selected as 47 μ F and their equivalent series resistance (ESR) values are chosen as 4.203 Ohms from capacitor data sheet. The output capacitor C_3 is chosen as 220 μ F. The converter is designed for 100 W and hence the maximum load is also designed for 100 W. Hence at an output voltage of 200 V, the load resistor chosen is 400 Ohms.

Considering the efficiency of 80% under worst case for design considerations with minimum input voltage of $V_{in}=15$ V, the input power is 125 W and input current $I_{in}=8.33$ A for the rated output power of 100 W.

The magnetizing inductance L_m of the coupled inductor

$$L_m > \frac{DV_{in}T_s}{I_{in}} > 21.6 \mu H \quad \dots \text{Eq.(4.6)}$$

where $T_s = 1/f_s$.

We have chosen the magnetizing inductance L_m to be 30 μ H.

When the solar PV module is installed, there will be some output voltage at the terminals depending upon the solar irradiation levels. This voltage can be unsafe for both personnel and other systems. The floating active switch (S_1) is connected in series with the PV terminals. The switch isolates the DC current from the PV panel during periods of non-operation. The isolation for live power supply makes sure that no energy is transferred to output terminals un-intentionally.

The voltage output from the converter varies with respect to the input voltage which in turn depends upon the prevailing solar irradiation and wind speed conditions. Also, the output voltage varies with changes in the load. To maintain the required output voltage, we need to go for closed loop operation where the output voltage is constantly measured and controlled using the second order compensators such as proportional (P), proportional-integral (PI) and proportional-integral-derivative (PID) controllers.

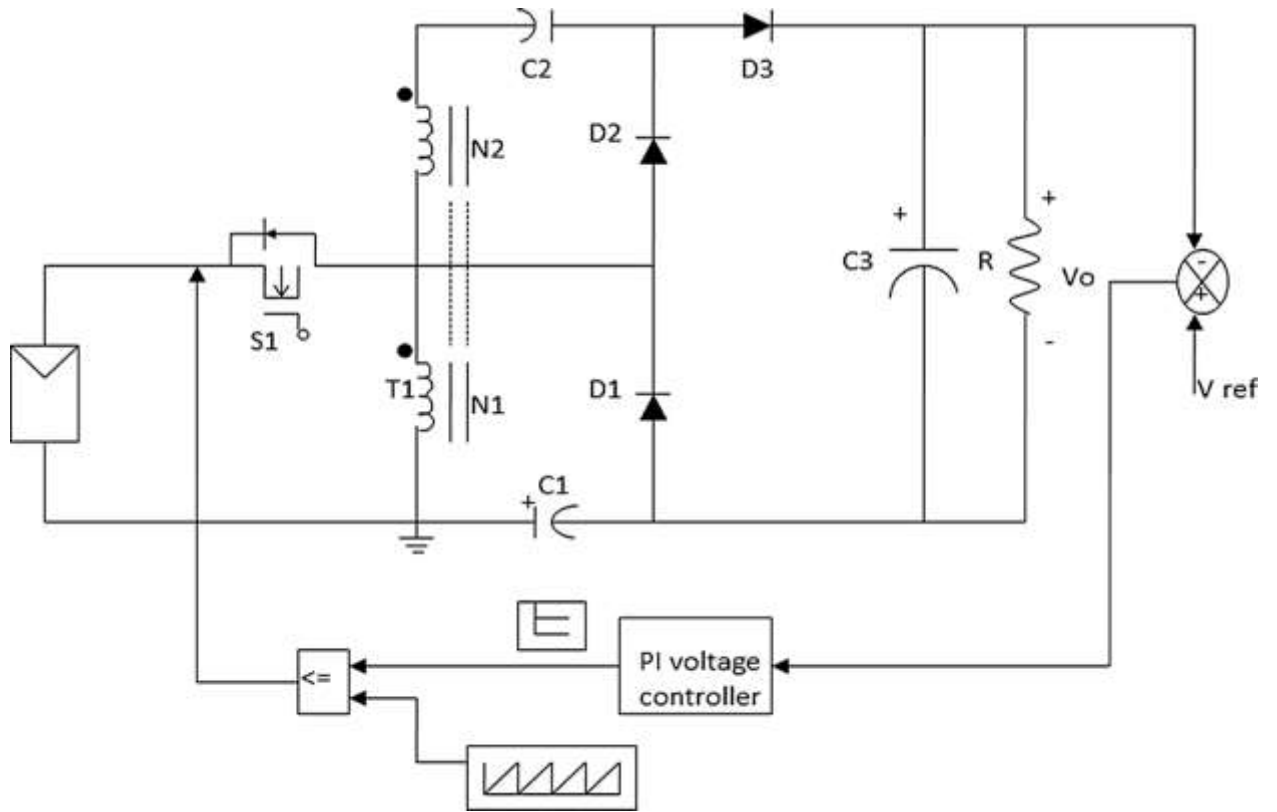


Figure 4.5 High step up dc-dc converter PV system in closed loop with PI controller.

The PI controller is implemented in closed as shown in Figure 4.5, because of its fast dynamic response and ability to achieve minimum steady state error $e_{tr} \approx 0$. In this the actual output voltage V_o and the desired output voltage V_{ref} is compared. Based on the error, the control signal is generated. The gate pulse for input switch S_1 is generated using this control signal to increase the duty ratio (D) and hence correct the error in output voltage. If the actual output voltage is less than the desired one, the duty ratio is increased. If the actual output voltage is more than the desired voltage, then the duty ratio is decreased. The pulse width modulated signals are generated by comparing the error signal with a saw tooth carrier waveform. Thus the desired output voltage is maintained.

4.4 Results - MATLAB Modeling and Simulation

The converter is modeled in MATLAB/Simulink to analyze and study the performance of the system. Figure 4.6 shows the MATLAB/Simulink model of high step-up DC-DC converter using PI controller.

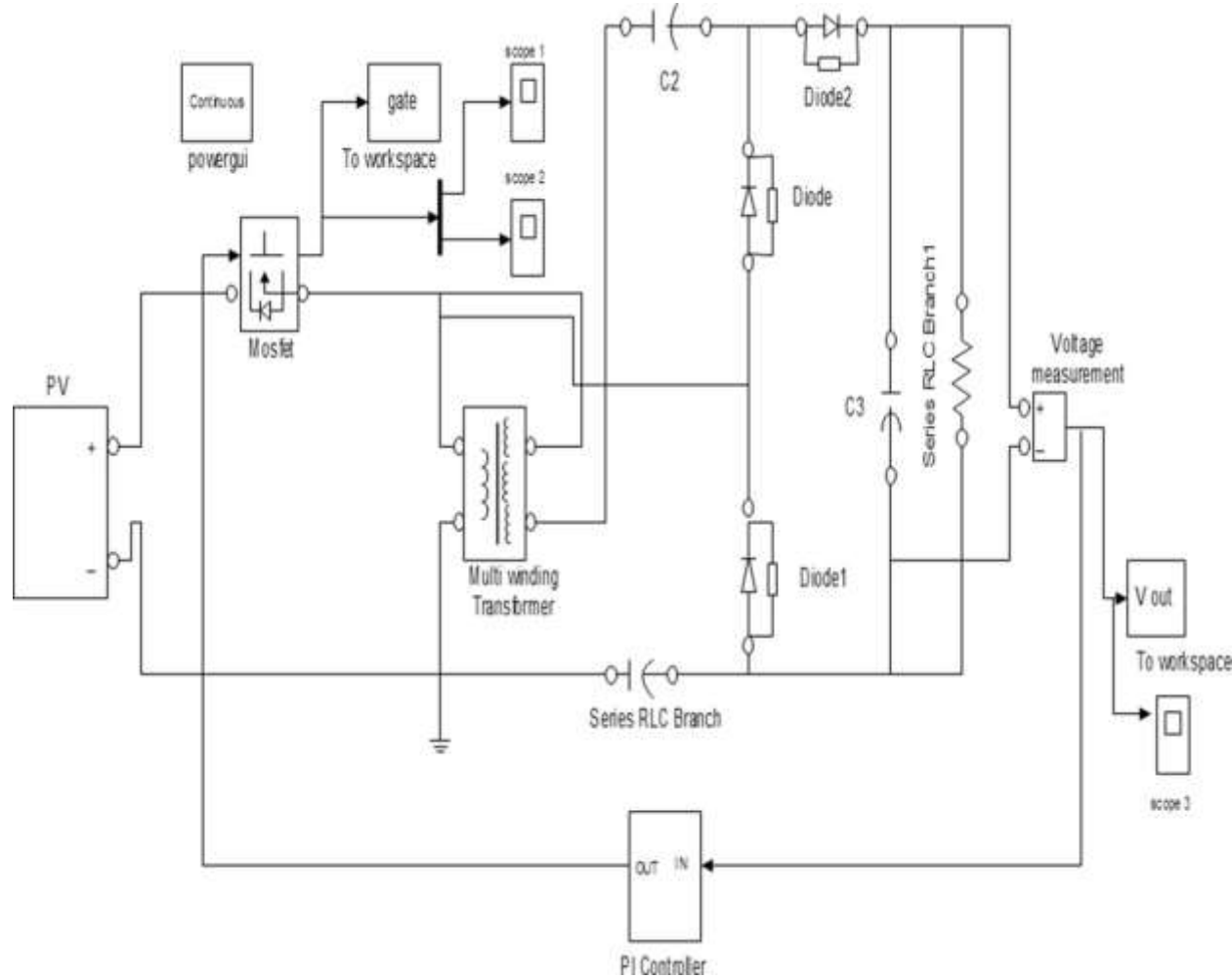


Figure 4.6 Model of high step-up DC-DC converter with closed loop PI controller

The open loop transfer function of the above system is obtained from equation (4.4) and is as given below:

$$G(s) = \frac{V_o(s)}{V_{in}(s)} = I + n + \left(\frac{D}{I-D}\right) \cdot \frac{1}{sC_1} + \left(\frac{nD}{I-D}\right) \cdot \frac{1}{sC_2} \quad \dots \text{Eq. (4.7)}$$

$$G(s) = \frac{[(1+n)(1-D)C_1C_2]S^2 + (C_1+C_2)S}{(1-D)S^2C_1C_2} \quad \dots \text{Eq. (4.8)}$$

With PI controller in the feedback loop, the feedback loop transfer function is given by

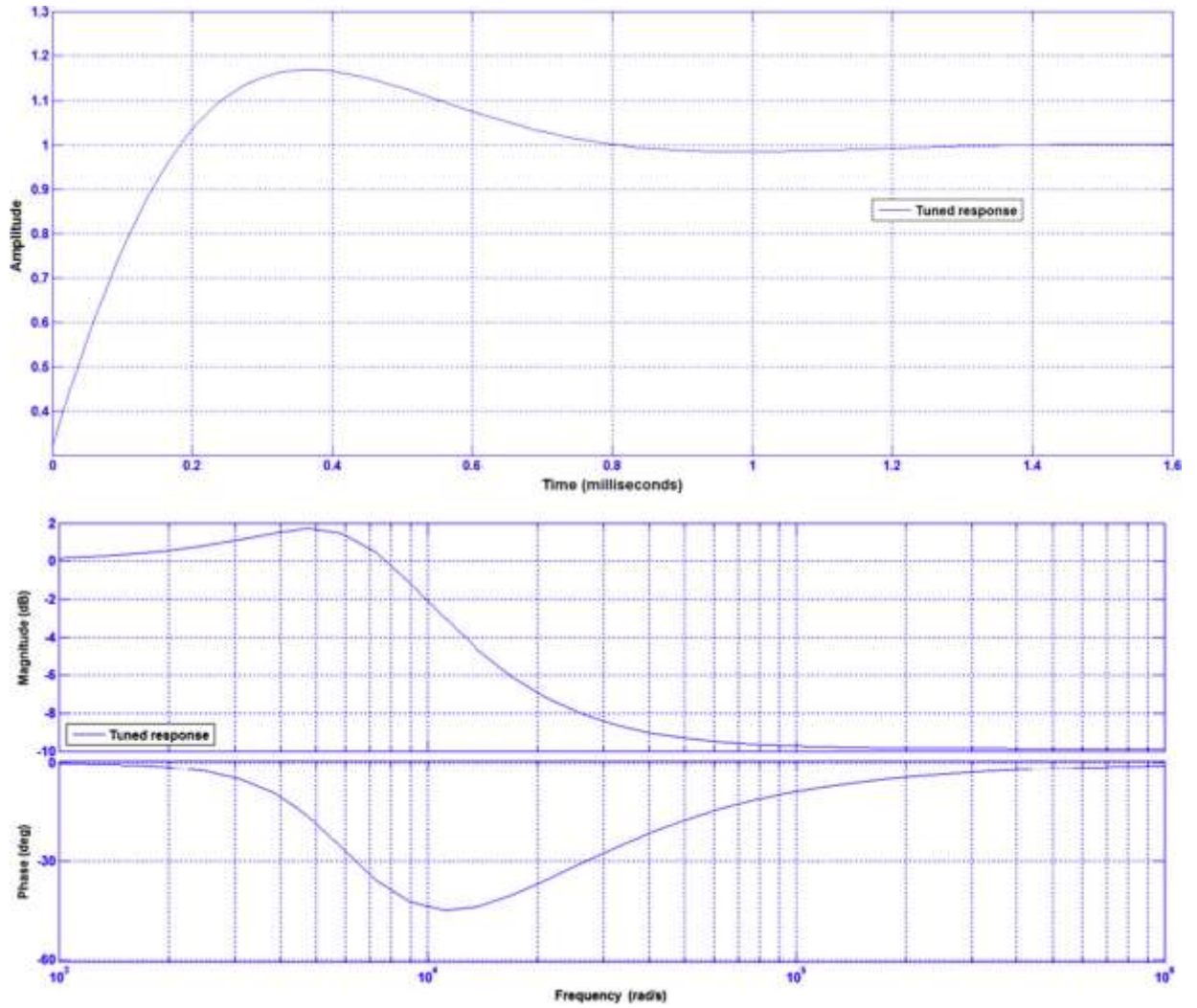
$$H(s) = K_p + \frac{K_i}{s} \quad \dots \text{Eq. (4.9)}$$

where K_p is the proportional constant and K_i is the integral constant.

Then the overall closed loop transfer function is given by

$$\text{T.F} = \frac{G(s)}{1+G(s) \cdot H(s)} \quad \dots \text{Eq. (4.10)}$$

The above model equations Eq. (4.7) – (4.10) represent the closed loop transfer function for the power converter. The system is tuned to find out the suitable values of proportional and integral constants (K_p & K_i). The step response of the converter and the bode plot is shown in Figure 4.7.



*Figure 4.7 Step response and Bode Plot for the converter in closed loop
The stable performance is obtained with less than 17% peak overshoot and rise time of less than 0.2 ms.*

The controller is tuned initially by increasing the K_p value till oscillations are set. Then K_i value is increased to obtain steady state with minimum error. The K_p and K_i values were set to 9.1 and 1.7 respectively. The stable performance with less than 17% peak overshoot and rise time of less than 0.2 ms.

The output voltage and current waveforms of capacitors and diodes are shown in Figure 4.8 and Figure 4.9 respectively. This shows that there is no extreme voltage stress across the components and high current through the components.

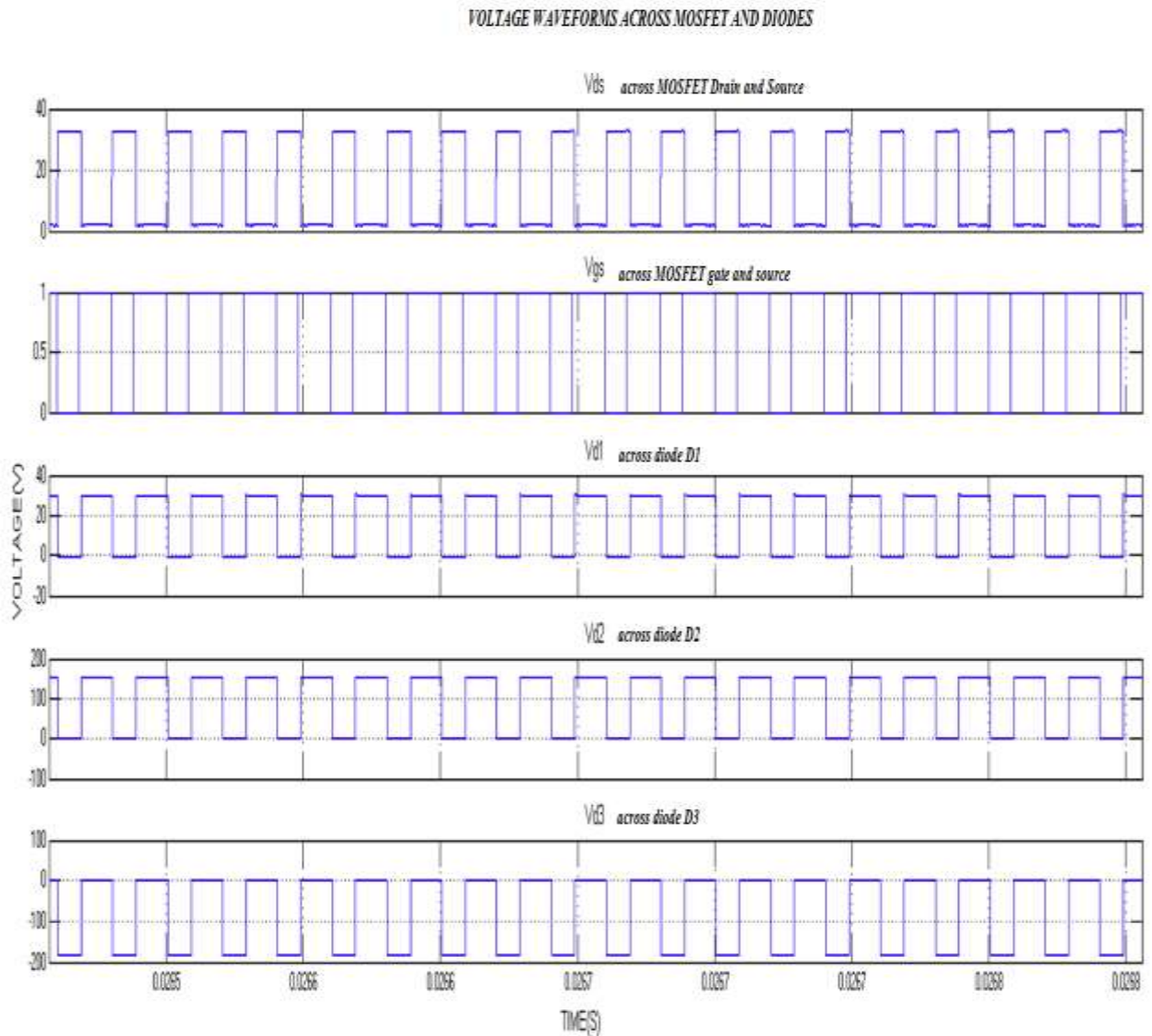


Figure 4.8 Output voltage waveforms of MOSFET and diodes of High step-up DC-DC converter using PI controller

The voltage across various components like the switch and diodes are within limits. There is no voltage stress and this ensures safety of the individual components.

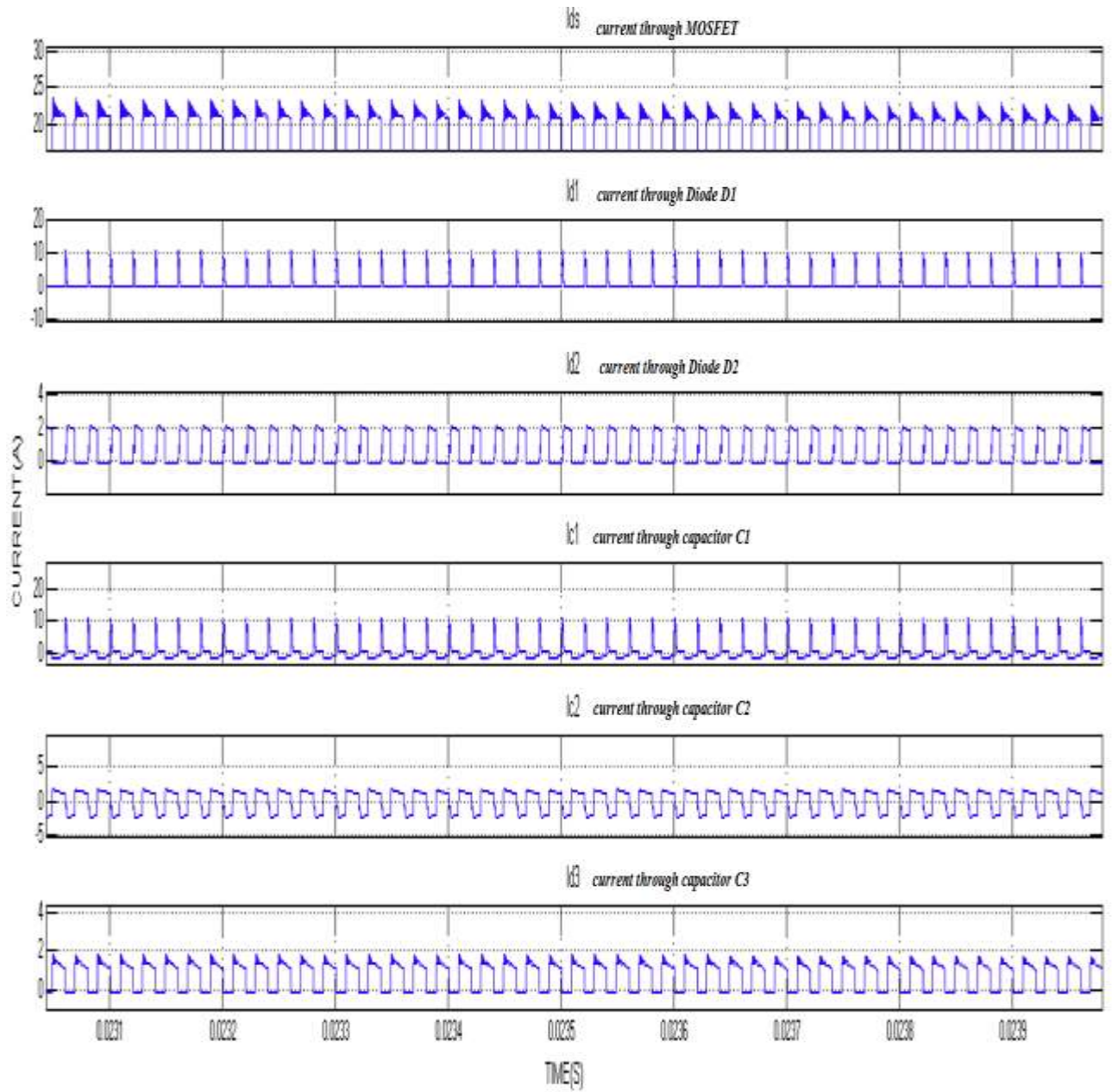
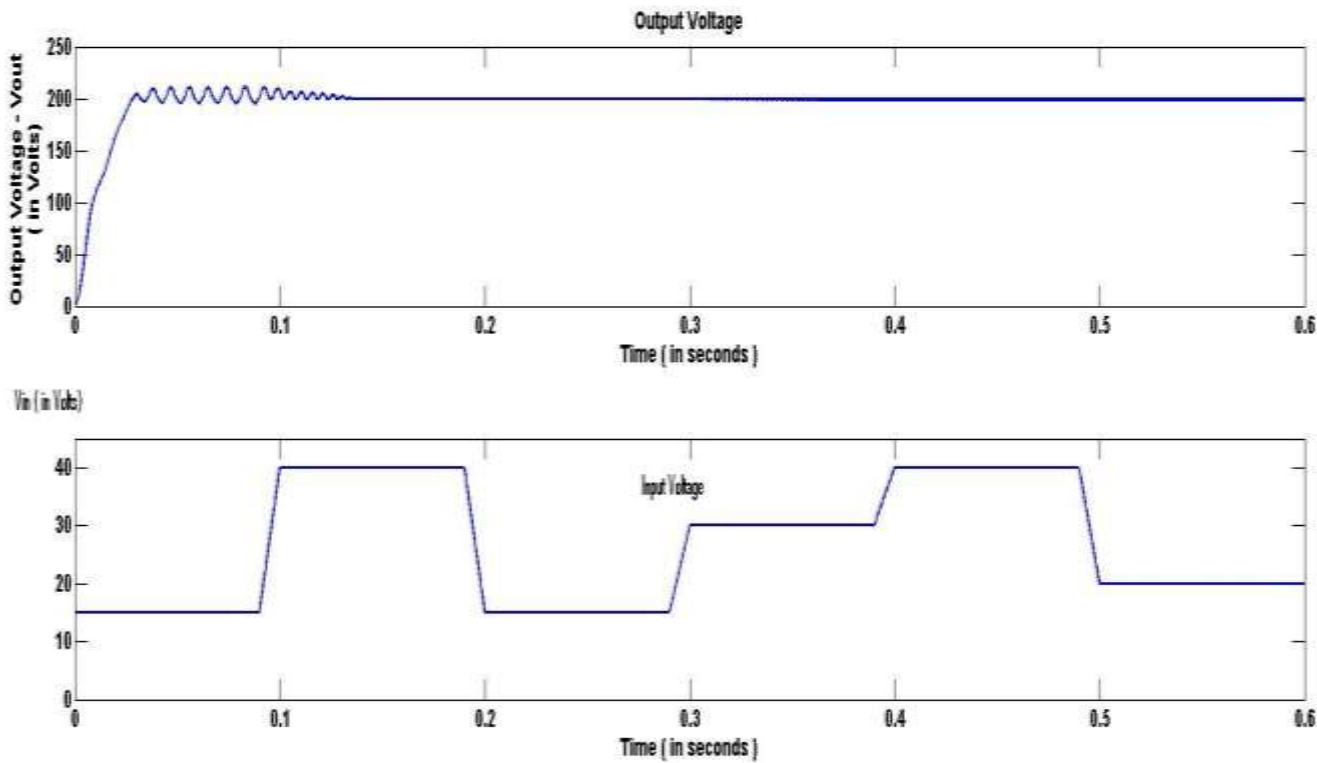


Figure 4.9 Output current waveforms of capacitors and diodes of High step-up DC-DC converter using PI controller

4.5 Performance with variation in input voltage:

The system is subjected to variation in input voltage to observe variation in output voltage to verify the response of the converter in closed loop. First the

converter was given with an input voltage that varies every 0.1 s within the range of 15 V to 40 V. The input and output voltage waveforms are shown in Figure 4.10. It is observed that after initial oscillation with maximum of around 5%, the output voltage settles down and further steady voltage variations does not affect the output voltage to great extent and gives a near straight line performance.



*Figure 4.10 Output voltage response for steady change in Input voltage
The output voltage waveform remains stable with large variations in input voltages which is expected from the output of renewable energy system.*

Further to verify the converter for application in renewable energy systems where variations of input voltage can be very much random based on Solar irradiations, cloud movement etc., a random voltage waveform is generated as input that

varies much faster in fraction of second within the range of 15 V to 40 V. This input voltage waveform was used to evaluate the performance of converter and the same is given in Figure 4.10. Under such harsh input voltage conditions also, the output voltage could be controlled easily within the band of $\pm 5\%$. We can observe response of the controller with slight overshoots for sudden rise or drop in input voltage and the oscillations damping in two or three cycles.

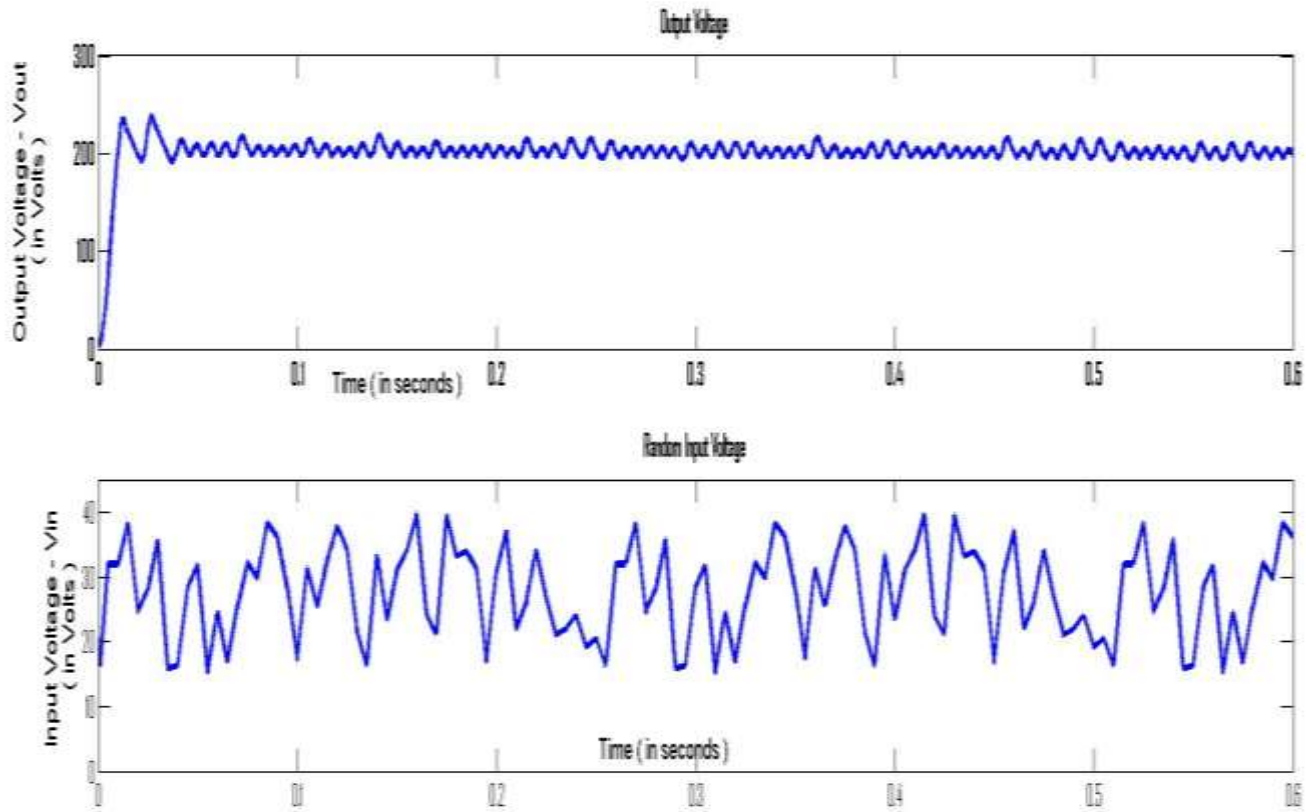


Figure 4.11 Output voltage response for Random Input voltage

The plot shows the almost stable output voltage with randomly varying input voltage conditions. This shows the performance of the designed power converter in closed loop.

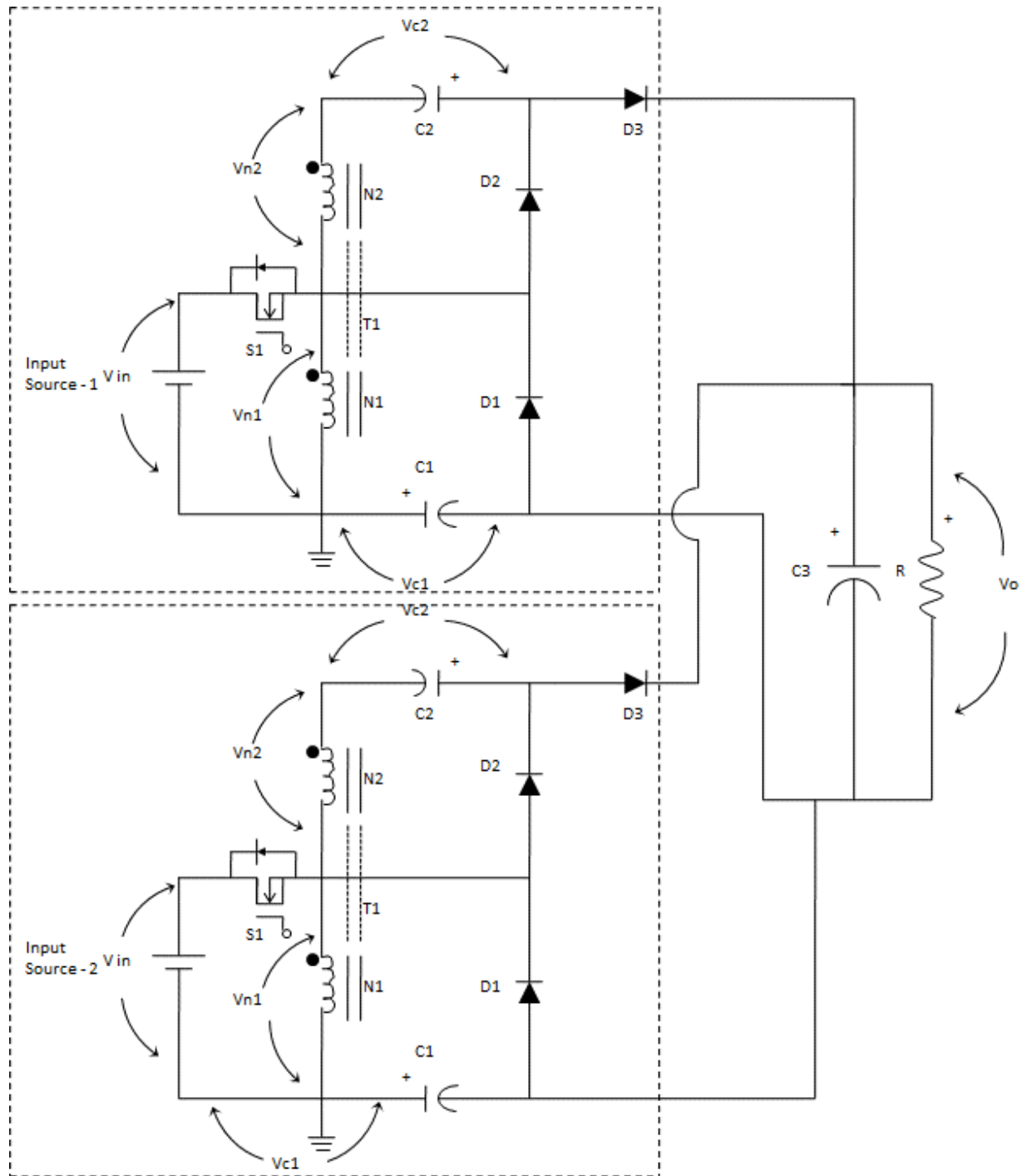


Figure 4.12 Hybrid power converter with two inputs

4.6 Experimental details and setup

A prototype was developed for experimental verification of the above design. The system consists of the power converter with provision for accepting inputs from two renewable sources viz. solar PV and wind generator. The output is connected to the load. The power circuit is designed with the configuration developed in previous section and the same is shown in Figure 4.12.

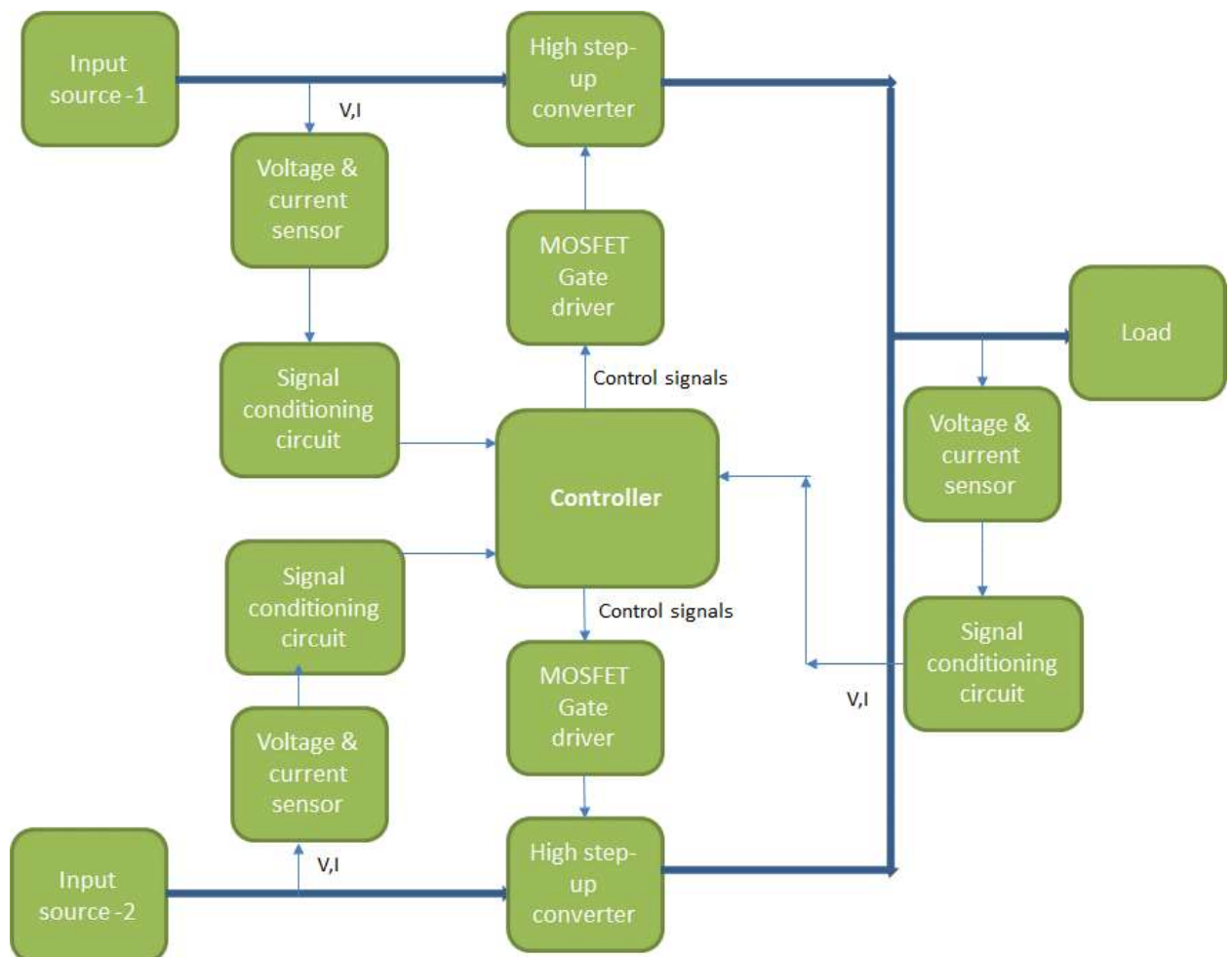


Figure 4.13 Block diagram of the hybrid power converter

The required control logic is implemented using the controller. The schematic block diagram is given in Figure 4.13. The solar panel output (input source -1) and the wind source output (input source -2) are connected with the power circuit through a miniature circuit breaker (MCB) for on/off control. The input voltage and current from both the sources are measured used voltage and current sensors. The sensor output is given as input to the controller through a signal conditioning circuit. The DC supply from sources is fed to the high step-up converter section that steps up the DC voltage. This output voltage is connected to the load. The output voltage and current is measured by the controller using sensors and signal conditioning circuits.

The major circuit components are chosen as per the design requirement and calculations elaborated in Section 4.3. The coupled inductor of 30 μH is used in the circuit. The capacitors in loop with inductors are chosen as 47 μF and the capacitor in the output side is of 220 μF . A variable resistance is used to load the system. The photographs of the experimental set up is shown in Figure 4.14.

The MOSFET device IRFP4468 is used as input switches S_1 and S_2 . TLP250 is the gate driver used for firing the above MOSFET. The voltage sensors and current sensors used in are circuit are LV25P and LTS25N – P respectively. The diodes used are MUR3060. The capacitors C_1 & C_2 used in the loop and the output capacitor C_3 are of electrolytic type with 450 V rating.

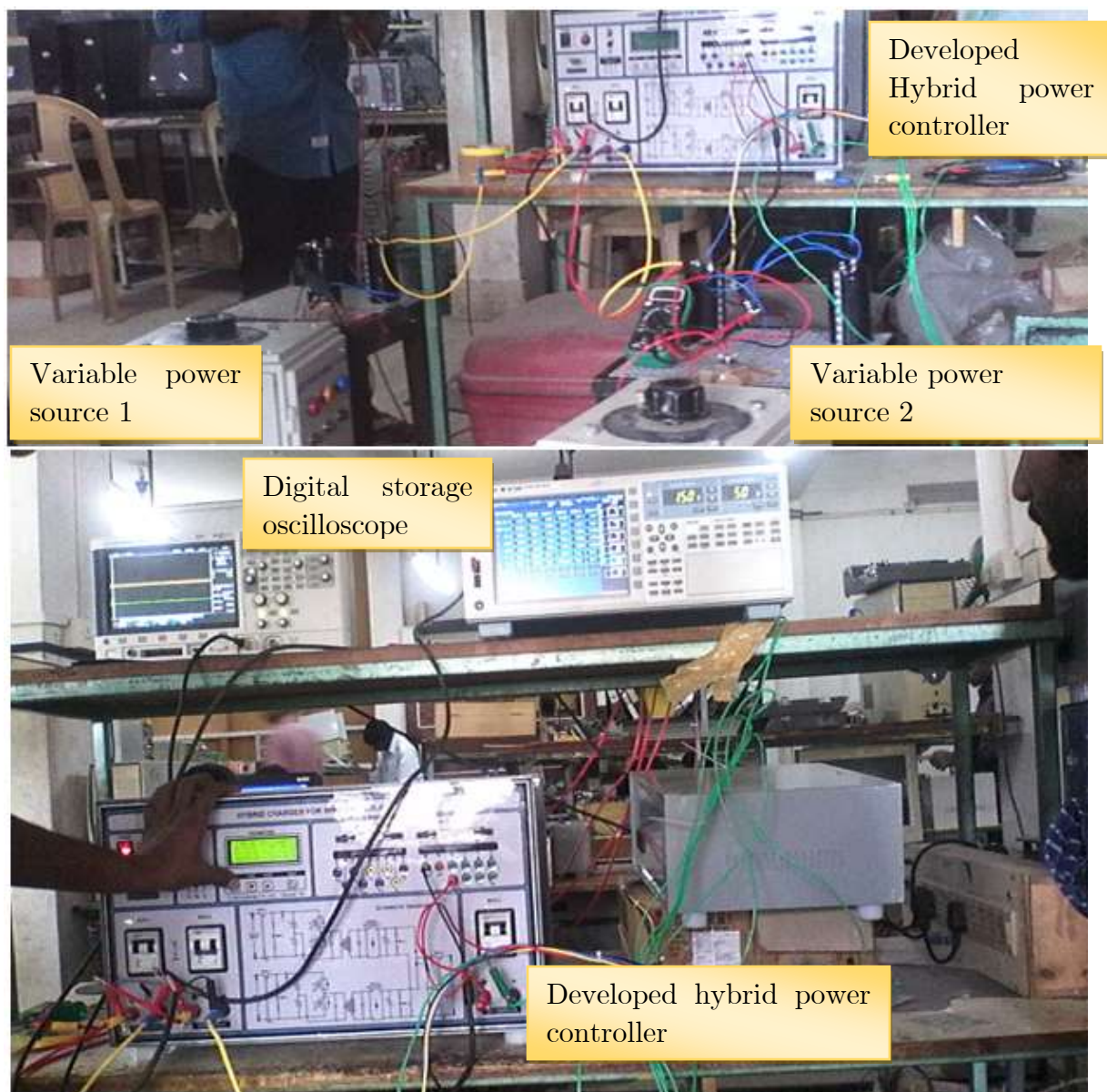


Figure 4.14 Photograph of experimental setup
It shows the developed power converter under testing using variable power sources. The input and output waveforms being recorded using DSO

1. Solar DC to DC Boost converter section

- a. Maximum Input voltage : 40V DC
- b. input current protection : 15A (Max)
- c. Output voltage : 325V DC (Max)
- d. Power rating : 200W

2. Wind DC to DC Boost converter section

- a. Maximum input voltage : 40V DC
- b. Input current protection : 15A (Max)
- c. Output voltage : 325V DC (Max)
- d. Power rating : 200W

3. Voltage and Current Sensor – Signal Conditions Outputs

- a. Solar Input voltage (Vsi) : 50V
- b. Solar Output voltage (Vo) : 325V / 5V
- c. Wind Input voltage (Vw1) : 50V / 5V
- d. Wind Output voltage (Vw0) : 325V / 5V
- e. Output voltage (Vo) : 350V/5V
- f. Solar Input current (Is) : 16A/5V
- g. Wind Input current (In) : 16A/5V
- h. Output current (Io) : 4A/5V

4. PWM Input

- a. PWM – Amplitude : 5V (TTL Input)
- b. PWM Frequency : 18KHZ (20KHZ – Max)

5. Power Circuit Details

- a. Solar Input capacitor (C1, C2) : 4700 μ F / 50V / E
- b. Wind Input capacitor (C3, C4) : 4700 μ F / 50V / E
- c. Solar Input capacitor (C5) : 47 μ F / 450V / E

- d. Wind Input capacitor (C6) : 47 μ F / 450V / E
- e. Output capacitor at μ CB3 : 330 μ F / 450V / E
- f. Setup Transformer Ratio : $\leq 1:10$
- g. MOSFET model name : IRFP4468
- h. Voltage sensor model name : LV25P
- I. Current sensor model name : LTS25N – P
- j. D1, D2 Diode model name : MUR3060
- k. Driver for MOSFET : TLP250

4.7 Errors associated with measurements:

The solar and wind output voltages and currents are measured the implement the MPPT algorithm. The voltage transducer as an overall accuracy of 0.9 % and the current transducer has an accuracy of 0.7 %. The power generated is calculated based on the voltage and current measured. These measurement error is propagated to the calculated power value. This value is measured for every time step.

But for the MPPT algorithm adopted, the absolute value of power is not important because we are checking only the direction of change in power i.e. if the power is increased or decreased from the previous instant. Hence the error in absolute value of power does not impact the functioning of the circuit.

4.8 Experimental results

The input voltages were varied from 15 V to 30 V to check the outputs at variable inputs to simulate the renewable power source conditions. It was observed that the output voltage could be maintained within 5 % of the set voltage of 200 V in loaded condition. When the output is kept open under no-load condition with around 30 V input in both the input sources, the maximum output voltage was 233 V.

The snapshots of Digital storage oscillator (DSO) with the readings at different input voltages of both sources are shown in Figure 4.15. The input voltages and currents are displayed in element 4 and element 5 of the DSO. The outputs voltages and currents are shown in element 2. We can see that the input voltages are varied from 15 V to around 30 V. The corresponding output voltages vary between 189 V up to 199 V and during open circuit goes to 233 V.

The typical voltage and current waveforms obtained in the DSO is shown in Figure 4.16. The observed output voltage and current waveform is smooth with near straight line performance irrespective of variations in input voltage and current waveforms.

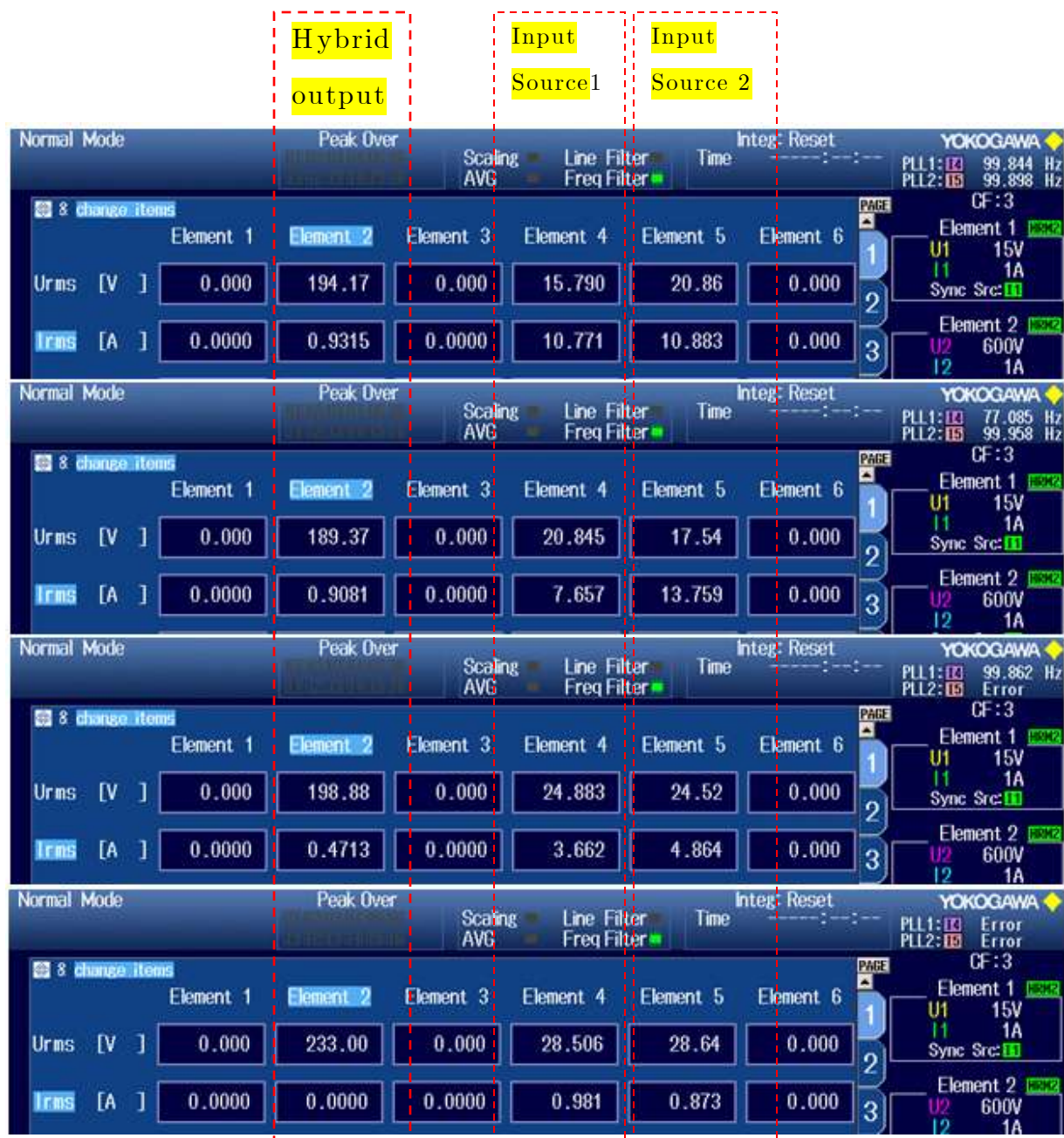


Figure 4.15 Snapshot of DSO displays showing output voltages at various input conditions

The input voltages were varied from 15 V to 30 V to check the outputs at variable inputs to simulate the renewable power source conditions. It can be observed that the output voltage could be maintained within 5% of the set voltage of 200 V in loaded condition. When the output is kept open under no-load condition with around 30 V input in both the input sources, the maximum output voltage was 233 V.

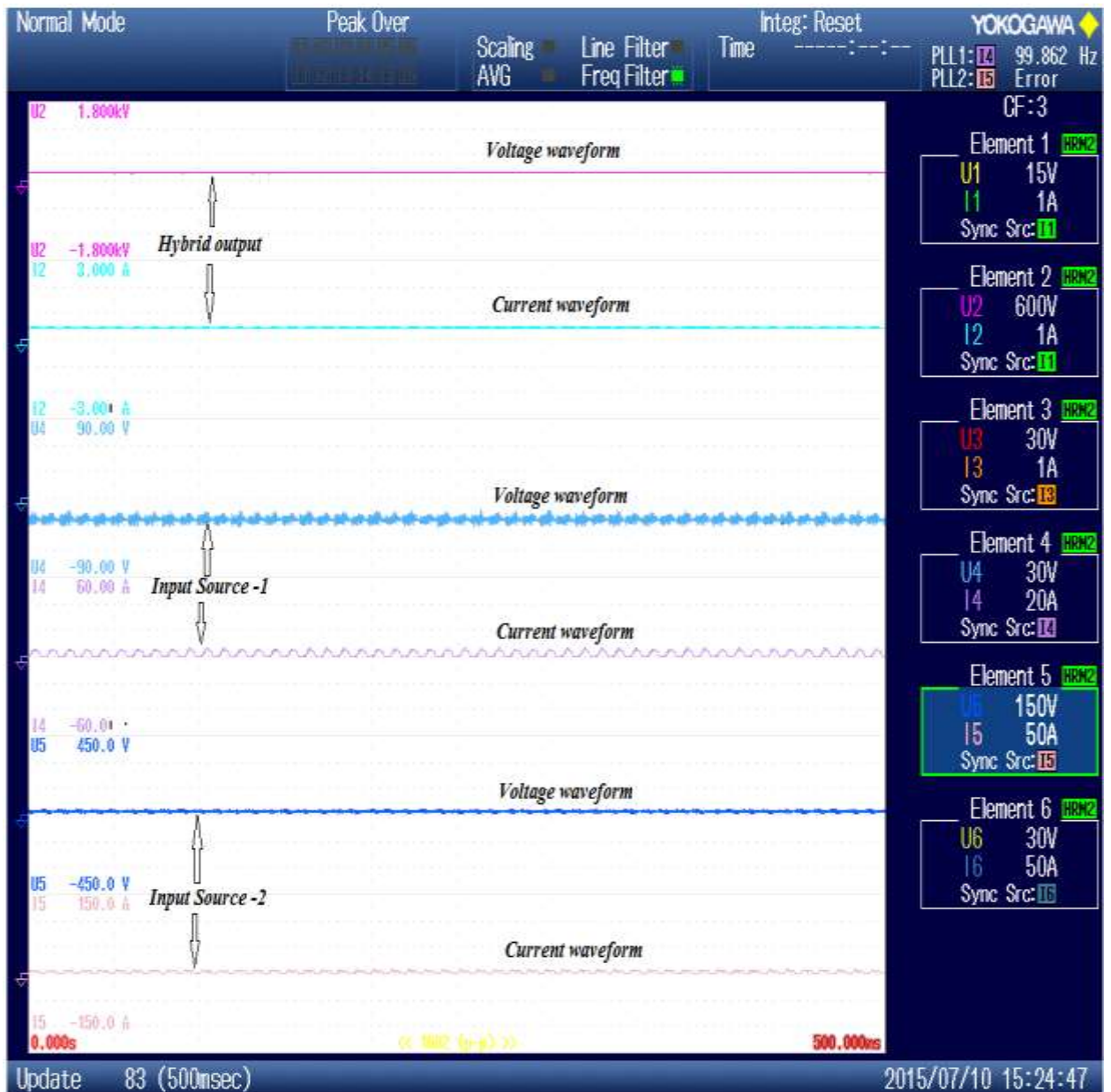


Figure 4.16 DSO waveforms of input and output voltages and currents
The hybrid output voltage and current waveforms are smooth and steady even with variations in input sources voltage and currents.

4.9 Conclusion

In this chapter, the development of a 100 W high step up dc-dc converter prototype with two input sources is presented. The converter is designed in closed loop to deliver an output voltage of around 200 V with variable input voltage in 15 V to 40 V range. The proposed configuration is suitable for application for renewable sources based systems [150].

- A prototype power converter configuration for the renewable energy application is developed.
- The circuit components and parameters are designed from the design equations Eq. 5.1 to Eq. 5.7. The turns ratio (n) of coupled inductor is chosen to be 5 for a moderate duty cycle of 0.4 to 0.6 to obtain the desired voltage ratio in the range of 8 to 17. The inductance of coupled reactor is designed for a value of 30 μH . Other capacitors and resistor values are also chosen using the design equations.
- The transfer function is derived for closed loop operation of the designed circuit. The controller is tuned and the proportionality constant K_p and integral constant K_i values are set at 9.1 and 1.7 respectively. We obtained the stable performance with less than 17% peak overshoot and rise time of less than 0.2 ms.
- The designed circuit is subjected to both steady and random input voltage variations and the output voltage is found to be within $\pm 5\%$ range.

Chapter 5

5 CONCLUSIONS AND FUTURE SCOPE OF WORK

The thesis deals with modeling of renewable energy based desalination systems with solar PV and wind turbines along with battery storage system. The hybrid power system is analyzed for application to a desalination plant with a variable load. The salient features of the work is summarized below.

A methodology of selection of the capacities of various power sources of the hybrid power system is presented for obtaining the optimum configuration. Use of hybrid PV-Wind systems for desalination has a unique advantage of reduction in energy storage battery capacity resulting in increased utilization of power generated and reduced cost.

A neural network modeling of renewable energy based desalination systems using Solar PV and Wind turbines has been carried out and the model estimates the annual power produced by a given configuration of hybrid power.

A prototype power converter suitable for application for hybrid renewable sources with solar and wind sources for desalination application is developed. The converter has high step up ratio and is designed in closed loop to deliver an output voltage of around 200 V with variable input voltage in 15 V to 40 V range.

This chapter summarizes the overall conclusions of this study and also discusses the future scope of work.

5.1 Summary of major findings

1. A methodology of selection of the capacities of various power sources of the hybrid power system is developed for obtaining the optimum configuration. The optimum configuration can be chosen based on the requirement.
2. From the results obtained, we can see that addition of capacities of PV panels or Wind turbines or storage capacities separately does not help in reduction of the cost of energy. But, when the capacities of Solar PV and Wind turbines are supplemented with each other, we find that we are able to maintain the total kWh produced per year to meet the load requirements.
3. For a requirement of around 6000 kWh per year power production, the best option obtained is the combination of 8 kW Solar PV , 1 kW Wind and 1.5 kW storage battery for obtaining energy at cost of INR 12.73 per kWh with an availability of 40% .
4. If the requirement is only the lowest cost of energy / kWh, we can select a combination of 5 kW Solar PV, 1 kW Wind and 0.5 kW battery. With the above combination, we get the lowest cost of energy at INR 11.32 per kWh, but the total power produced in the year is around 5000 kWh with an availability of only 29%.
5. In the case of desalination plant as load, the hybrid power system can produce and store water in suitable tanks and hence the availability factor is not a major concern. The necessity of energy storage battery is also reduced. For application of hybrid power system for desalination purpose

that requires a load of 2 kW, there is an average increase of around 25% in utilization of power generated, when used for desalination plant.

6. For lower cost of water, we can select the combination of 5 kW solar PV, 1 kW wind and 0.5 kW battery to produce a total of 6906 m³ of product water at a cost of INR 80 per 1000 liters. This comes with an availability of plant of around 28% which can be compensated by selecting suitable storage tanks.
7. Similarly, for a high production of water at around 7500 m³, we can select the combination of 10 kW solar PV, 2 kW wind and 0.5 kW storage battery to produce water at a cost of INR 116 per 1000 liters of water and the availability is around 54%.
8. A neural network model is developed for the above system with Solar PV, Wind generator and battery capacities as inputs and total kWh production per year as the output. The proposed three layer architecture is trained to obtain the required performance optimization. The network estimates the total power generated per year for a given capacity of Solar PV, Wind generator and Battery. The model equation and parameters are given in Eq. 3.15 and Table 3.2. The developed model predicts the unknown test data with regression of 0.99.
9. A prototype power converter configuration for the renewable energy application is developed. The circuit components and parameters are fixed from the design. The turns ratio (n) of coupled inductor is chosen to be 5 for a moderate duty cycle of 0.4 to 0.6 to obtain the desired voltage ratio in the range of 8 to 17. The transfer function is derived for closed loop operation of the designed circuit. The controller is tuned and the proportionality constant K_p and integral constant K_i values are set at 9.1

and 1.7 respectively. We obtained the stable performance with less than 17% peak overshoot and rise time of less than 0.2 ms.

10. The designed circuit is subjected to both steady and random input voltage variations and the output voltage is found to be within $\pm 5\%$ range.

5.2 Major contributions:

The following are the major contributions of this work:

1. A methodology of selection of the capacities of various power sources of the hybrid power system is developed for obtaining the optimum configuration. The optimum configuration can be chosen based on the requirement.
2. The desalination plant load helps in reducing the energy storage capacity requirements and hence offer better performance of the hybrid power system. Thus the load profile selected for the hybrid power system influences the performance of the system.
3. A neural network model is developed for the above system with Solar PV, Wind generator and battery capacities as inputs and total kWh production per year as the output.
4. A prototype power converter configuration for the renewable energy application is developed.

5.3 Directions for future scope of work

The small scale renewable energy based hybrid power system coupled with desalination plants will be the future of solution for co-generation of power and water especially in remote and isolated locations. The proposed future scope of work is aimed to make the technology perfect and ready to deliver for future market. Also, there is a potential in other similar areas of application.

1. The solar and wind resource data shall be collected for different places; sites with different potentials for solar energy and wind energy. The developed methodology presented in this thesis shall be applied to a variety of sites. This exercise can be done for remote locations and islands. By this, we will be able to map the energy potential of the region. This will enable the designers to take decisions on planning the infrastructure of that region.
2. The proposed configuration shall be installed at a site and tested for actual performance based on solar irradiation and wind speed in a particular year by actually connecting solar PV and wind generator.
3. The study shall be extended to other locally available renewable energy sources like biomass, tidal energy and ocean thermal energy. Also, the combination of solar thermal collectors based systems shall also be considered. The addition of such systems into the hybrid power will increase the complexity of analysis and hence need to be completely studied to increase the availability of energy on hourly basis in a day and also on yearly basis across various seasons.
4. Various dedicated load options like powering of remotely placed sensors, connecting water pumps, powering a mobile tower, residential applications

shall be considered. Different voltage configurations depending upon the application shall also be developed. An integrated supervisory controller to control both renewable sources and desalination plant can be developed. The integrated system shall control the parameters of Solar PV and Wind generator, power flow to and from the energy storage device and control the operation of the desalination plant.

5. Combining more than two hybrid energy sources need the power converters that can handle more inputs. The power converter that can accept more than two renewable power sources with varying nature shall be developed to enable such system. Also the power converters shall be able to operate at higher input voltages and handle high power levels which will eventually lead to scaling up of the capacity of hybrid power systems.

REFERENCES

- [1] "BP: Statistical Review of World Energy, Workbook (xlsx), London, 2016," June 2016.
- [2] "IEA - Key world energy statistics, 2015," 2015.
- [3] Varadi, P., "Sun Above the Horizon: Meteoric Rise of the Solar Industry", CRC Press," 2014.
- [4] Shiklomanov, Igor, "World fresh water resources," in *Water in Crisis: A Guide to the World's Fresh Water Resources*, P. H. Gleick, Ed., 1993.
- [5] "<http://www.wri.org/resources/maps/india-water-tool>," World Resources Institute, [Online]. Available: <http://www.wri.org/resources/maps/india-water-tool>.
- [6] Research, Pike, "Desalination Technology Markets-Global Demand Drivers, Technology Issues, Competitive Landscape and Market Forecasts.," 2010.
- [7] Yousef, R.M., "Desalination Technology Roadmap 2030, Information and Decision Support-Center for Future Studies.," 2007.
- [8] American Bar Organization, "WATER AND GREENHOUSE GASES: THE," *International Environmental and Resources Law*, vol. 19, no. 2, pp. 14-19, October 2016.
- [9] IEA ETSAP, IRENA, "Water Desalination Using Renewable Energy Technology Brief," ETSAP and IRENA, 2012.
- [10] Naveen Bhutani, Amit Purohit, Senthilmurugan S et.al., "Energy efficiency solutions for RO desalination plant," *Desalination and Water Treatment*, vol. 51, no. 27, 2013.
- [11] Greenpeace International, "Coal Impacts on Water," March 2014. [Online].

Available: <https://www.greenpeace.org/archive-international/en/campaigns/climate-change/coal/Water-impacts/>.

- [12] DOE, US, "The Water-Energy Nexus : Challenges and Opportunities," US DOE, June 2014.
- [13] Skaggs, R., Hibbard, KA., "Climate and Energy-Water-Land System Interactions: Technical Report to the U.S. Department of Energy in Support of the National Climate Assessment," Richland, WA: Pacific Northwest National Laboratory., 2012.
- [14] U.S. Department of Energy, January 2013. [Online]. Available: <http://cms.doe.gov/sites/prod/files/2014/12/f19/2011%20Portsmouth%20ASER.pdf>.
- [15] Wagman, D, "Water Issues Challenge Power Generators," *Power Magazine*, July 2013.
- [16] IRENA, "<http://www.irena.org/publications/2015/Jan/Renewable-Energy-in-the-Water-Energy--Food-Nexus>," January 2015. [Online]. Available: http://www.irena.org/documentdownloads/publications/irena_water_energy_food_nexus_2015.pdf.
- [17] UN Water, "The United Nations World Water Development Report 2014," *UN Water*, 2014.
- [18] Gulf News, "Dewa to Introduce Fuel Surcharge," 2011.
- [19] WRI , "Over Heating: Financial Risks from Water Constraints on Power Generation in Asia," 2010.
- [20] Greenpeace, "Water Hungry Coal: Burning South Africa's Water to Produce Electricity," 2012.
- [21] IEA, "World Energy Outlook 2005 Middle East and North Africa Insights,"

International Energy Agency (IEA), 2005.

- [22] IEA, "World Energy Outlook 2009,," International Energy Agency (IEA), 2009.
- [23] IEA, "World Energy Outlook 2012," OECD (Organisation for Economic Co-operation and Development), 2012.
- [24] The Guardian, "Fracking May be Causing Groundwater Pollution, says EPA Report", The Guardian, London," 2011.
- [25] Environment America, "Fracking by the Numbers," 2013.
- [26] Hadi, M., "Trace of Pollution Caused by Coal Mining Tracked in Kalimantan," 2014.
- [27] Groenewald, Y., "Coal's Hidden Water Cost to South Africa," 2012.
- [28] Luis G. Palacin, Fernando Tadeo, Cesar de Prada, Johanna Salazar, "Operation of desalination plants using renewable energies and hybrid control," *Desalination and Water Treatment*, vol. 25, pp. 119-126, 2011.
- [29] Noredine Ghaffour, Sabine Lattemann, Thomas Missimer, Kim Choon Ng, Shah Nawaz Sinha, Gary Amy, "Renewable energy-driven innovative energy-efficient desalination technologies," *Applied Energy*, vol. 136, pp. 1155-1165, 2014.
- [30] [Online]. Available: <https://www.slideshare.net>.
- [31] Sendhil Kumar Natarajan, K.S.Reddy, Tapas Kumar Mallick, "Heat loss characteristics of trapezoidal cavity receiver for solar linear concentrating system," *Applied Energy*, vol. 93, pp. 523-531, 2012.
- [32] JoachimKaufler, Robbert Pohl & HadiSader, "Seawater desalination (RO) as a wind powered industrial process - Technical and economical specifics," *Desalination and Water Treatment*, 2011.

- [33] Haijun, J., "Nuclear Seawater Desalination Plant Coupled with 200 MW Heating Reactor," in *International Symposium on the Peaceful Applications of Nuclear Technology.*, 2008.
- [34] Isaka, Mirei, IEA-ETSAP and IRENA, January 2013. [Online]. Available: https://www.iea-etsap.org/E-TechDS/PDF/I12IR_Desalin_MI_Jan2013_final_GSOK.pdf.
- [35] Kalogirou, S.A., "Seawater desalination using renewable energy sources, Energy & Combustion Science 31," Vols. 242-281, 2005.
- [36] Karim Mousa, Ali Diabat & Hassan Fath, "Optimal design of a hybrid solar-wind power to drive a small-size reverse osmosis desalination plant.," *Desalination and water treatment*, 2013.
- [37] Behnaz Rezaie, Bale V. R, Marc A. Rosen, "Exergy Assessment of a Solar-Assisted District Energy System," *The Open Fuels & Energy Science Journal*, vol. 11, no. 1, pp. 30-43, March 2018.
- [38] Senthil S, Senthilmurugan S, "Modelling, simulation and optimization - Reverse Osmosis Pressure Retarded Osmosis hybrid system," *Desalination*, vol. 389, pp. 78-97, July 2016.
- [39] Gude, V., "Renewable approaches for desalination, Renewable & Sustainable Energy Reviews 14," Vols. 2641-2654, 2010.
- [40] Zeji, D., "Applications of solar and wind energy sources to sea-water desalination-economical aspects, International conference on nuclear desalination," 2002.
- [41] Group, Oxford Business, "The Report Saudi Arabia Oxford Business Group Oxford," 2010.
- [42] E. Union, A guide to desalination system concepts, Euro-Mediterranean

Regional Programme for water Management (MEDA), 2008.

- [43] Al-Karaghoul, A.A., "Renewable Energy Opportunities in Water Desalination, Desalination, Trends and Technologies, Micheal Schorr," 2011.
- [44] Moilanen, Piia & Mroueh, Ulla-Maija, " Mobilising funding in the water sector: the potential for private sector participation and desalination in the levant region," 2018.
- [45] Papapetrou, M., "Roadmap for the development of desalination powered by renewable energy, Promotion of renewable energy for water desalination," 2010.
- [46] Gine, M. Zak, Amin Ghobeity, Mostafa, H., Sharqawy & Alexander Mitsos, "A review of hybrid desalination systems for co-production of power and water: analyses, methods, and considerations," *Desalination and Water Treatment*, 2013.
- [47] Karthikeyan, R., M. Afsar Hussain., Bale V. R and P.K. Nag, "Performance simulation of heat recovery steam generators in a co-generation system," *International Journal of Energy Research*, vol. 22, pp. 399-410, 1998.
- [48] Ahmed Hassan, Magdi El-Saadawi, Mohmoud Kandil & Mohammed Saeed, "Modeling and optimization of a hybrid power system supplying RO water desalination plant considering CO2 emissions," *Desalination and Water Treatment*, 2016.
- [49] Al-Karaghoul, "Solar and wind for water desalination in the Arab regions, Renewable and Sustainable Energy Reviews 13," Vols. 2397-2407, 2009.
- [50] Giridhar G, Dr., "Solar Energy and Solar Radiation Resource Assessment,"

in *Wind Turbine Technology and applicaitons*, 2015, pp. 535-541.

- [51] Delyannis, E., "Historic background of desalination and renewable energies," *Solar Energy*, 2003.
- [52] RAMBABU, K. "RENEWABLE ENERGY BASED SMALL HYBRID POWER SYSTEM," *International Journal of Electrical, Electronics and Data Communication*, vol. 2, no. 5, pp. 11-15, 2014.
- [53] Nagaraj, R., Thirugnanamurthy D., Manik Murthy Rajput, Panigrahi, B.K., "Techno-economic analysis of hybrid power system sizing applied to small desalination plants for sustainable operation," *International Journal of Sustainable Built Environment*, vol. 5, no. 2, pp. 269-276, 2016.
- [54] Nagaraj.R, Swaminathan.P,, "Feasibility Analysis of Eco-Friendly Hybrid Power Based R.O.for Remote Location," *Int.J.of Environmental Sciences*, vol. 1, no. 1, pp. 226 -232, 2012.
- [55] L., Garcia-Rodriguez, "Renewable energy applications in desalination: state of the art.Solar Energy," 2003.
- [56] Huneke, F., Henkel, J., Benavides González, J.A. et al, "Optimisation of hybrid off-grid energy systems by linear programming," *Energy,Sustainability and Society*, vol. 2, no. 7, 2012.
- [57] Thomson M, Infield D.A, "Photovoltaic-powered seawater reverse-osmosis system without batteries.," *Desalination*, 2003.
- [58] Tzen E, Perrakis K, Baltas P., "Design of a stand alone PV desalination system for rural areas.," *Desalination*, 1998.
- [59] Al Suleimani Z, Nair NR., "Desalination by solar powered reverse osmosis in a remote area of Sultanate of Oman," *Appl Energy*, 2000.
- [60] Habali SM, Saleh IA., "Design of stand-alone brackish water desalination

- wind energy system for Jordan," *Solar Energy*, 1994.
- [61] Miranda MS, Infield D., "A wind-powered seawater reverse osmosis system without batteries.," *Desalination*, 2003.
 - [62] Bakos G.C., "Feasibility study of a hybrid wind/hydropower-system for low cost electricity production," *Applied Energy*, pp. 599-608, 2002.
 - [63] Nagaraj, R., "Renewable energy based small hybrid power system for desalination applications in remote locations," in *2012 IEEE 5th India International Conference on Power Electronics (IICPE)*, Delhi, 2012.
 - [64] Cliff Dansoha, "The viability of renewable energy and energy storage as the power source for municipal-scale reverse osmosis desalination," *Desalination and Water Treatment*, 2015.
 - [65] Andrew, J., Pimm & Seamus, D., Garveya, "The economics of hybrid energy storage plant," *International Journal of Environmental Studies*, 2014.
 - [66] Ting-Long Pana, Hong-Shu Wana&Zhi-ChengJia, "Stand-alone wind power system with battery/supercapacitor hybrid energy storage," *International Journal of Sustainable Engineering*, 2014.
 - [67] Radian Belu, "Energy Storage Systems," *Encyclopedia of Energy Engineering and Technology*, 2015.
 - [68] Shaahid, S.M., &Elhadidy, M.A., "Optimal sizing of battery storage for stand-alone hybrid (Photo-voltaic+diesel) power systems," *International Journal of Sustainable Energy*, 2005.
 - [69] James, D., Van de Ven, "Increasing Hydraulic Energy Storage Capacity: Flywheel-Accumulator," *International Journal of Fluid Power*, 2009.
 - [70] Evans, A., Strezov, V., Evans, T.J., "Assessment of utility energy storage

- options fo increased renewable energy penetration," *Renew Sustain Energy Rev*, 2012.
- [71] Leadbetter, J., Swan, L., "Battery storage system for residential electricity peak demand shaving," *Energy Build*, 2012.
 - [72] Chen, H., Cong, T.N., Yang, W., Tan, C., Li, T., Ding, Y., "Progress in electrical energy storage sytem: a critical review," *Prog Nat Sci*, 2009.
 - [73] Baker, J., "New technology and possible advances in energy storage," *Energy Policy*, 2008.
 - [74] "www.doaj.org,"[Online].Available: <https://doaj.org/article/752d87f8eb0d4f3c8721dc50604e1b1e>.
 - [75] Thomson M., Infield D., "A photovoltaic-powered seawater reverse-osmosis system without batteries.," *Desalination*, 2003.
 - [76] E. Tzen, K. Perrakis, P. Baltas, "Design of a stand alone PV desalination system for rural areas," *Desalination*, vol. 119, no. 1-3, pp. 327-333, 1998.
 - [77] Al Suleimani Z, Nair NR., "Desalination by solar powered reverse osmosis in a remote area of Sultanate of Oman.Appl Energy," 2000.
 - [78] Habali SM, Saleh IA., "Design of stand-alone brackish water desalination wind energy system for Jordan.," 1994.
 - [79] Miranda MS, Infield D., "A wind-powered seawater reverse osmosis system without batteries.Desalination," 2003.
 - [80] G.C., Bakos, "Feasibility study of a hybrid wind/hydropower-system for low cost electricity production?,Applied Energy," 2002.
 - [81] Luque, Antonio and Steven Hegedus, Handbook of photovoltaic science and engineering, John Wiley & Sons, 2011.
 - [82] SC Gupta, Y Kumar, G Agnihotri, "Design of an autonomous renewable

- hybrid power system," *International Journal of Renewable Energy Technology*, vol. 2, no. 1, 2011.
- [83] [Online]. Available: <http://www.inderscience.com/>.
- [84] Bundesverband Solarwirtschaft, "Presiindex Photovoltaik Quartal 3," 2010.
- [85] M. Holger, B. Sebastian and Z. Wilfried, "Development of an Evaluation Methodology for the Potential of Solar-thermal Energy Use in the Food Industry," *Energy Procedia*, vol. 48, pp. 1194-1201, 2014.
- [86] The World Bank Group - Energy Unit, Transport and Water Department, "Technical and economic assessment of off-grid, mini-grid and grid electrification technologies annexes," 2006.
- [87] Solarbuzz (part of The NPD Group), "All battery index," 2010.
- [88] Haykin, Simon, "Neural Networks, A Comprehensive Foundation," 1994.
- [89] Hewitson, Bruce C. and Crane Robert G., "Looks and Uses in Hewitson Neural Nets: Applications in Geography," 1994.
- [90] Easson, Gregory L., "Integration of Artificial Neural Networks and Geographic Information Systems for Engineering Geological Mapping," *Doctoral Dissertation*, 1996.
- [91] "env.uregina.ca," [Online]. Available: <http://env.uregina.ca/huangg/publications.html>.
- [92] Sharma, Vidhi, "Neural Network Vs Human Brains," in *IJCA Proceedings on National Workshop-Cum-Conference on Recent Trends in Mathematics and Computing 2011 RTMC(12)*, 2012.
- [93] Stergiou, Chris, [Online]. Available: https://www.doc.ic.ac.uk/~nd/surprise_96/journal/vol1/cs11/article1.html.

- [94] [Online]. Available:
http://shodhganga.inflibnet.ac.in/bitstream/10603/19829/23/23_chapter%205.pdf.
- [95] [Online]. Available: <https://www.coursehero.com/file/p3f12k8/Areas-contributing-to-Artificial-neural-networks-Statistical-Pattern-recognition/>.
- [96] Dr. G.P.Rameshkumar, S.Samundeswari, "Neural Network, Artificial Neural Network (ANN) and Biological Neural Network (BNN) in Soft Computing," *INTERNATIONAL JOURNAL OF ENGINEERING SCIENCES & RESEARCH TECHNOLOGY*, vol. 3, no. 3, pp. 1159-1161, March 2014.
- [97] Dr.B.Karunanithi, Sweta Shriniwasan, Bogeshwaran.K, "Modelling of Vapour Liquid Equilibrium by Artificial Neural Networks," *International Journal of Computational Engineering Research (IJCER)*, vol. 4, no. 6, pp. 38-56, June 2014.
- [98] Jang Jyh-Shing Roger, Sun Chuen-Tsai, Mizutani Eiji, *Neuro-Fuzzy and Soft Computing. A Computational Approach to Learning and Machine Intelligence*, Prentice-Hall, 1997.
- [99] Obermeier Klaus K. and J & Barron anet J., "Time to get fired up," *Prentice Hall, Upper Saddle River*, 1989.
- [100] Dharmalingam M, "Artificial Neural Network Architecture for solving the double dummy bridge problem in contract bridge," *International Journal of Advanced Research in Computer and Communication Engineering*, vol. 2, no. 12, pp. 4683-4961, 2013.
- [101] Lai, "Intelligent Weather Forecasts," *3rd Int. Con. On Machine Learning and Cybernetics Shanghai*, 2004.

- [102] Baboo, S.S., and Shereef, I.D., "An Efficient Weather Forecast System Using Artificial Neural Network," *Int. J. of Env. Sci. & Dev.*, 2010.
- [103] Kadu, P.P., Wagh, K.P., Chatur, P.N., "A Review on Efficient Temperature Prediction using Back Propagation Neural Network," *Int. J. of Emerging Tech & Adv. Eng.*, pp. 52-55, 2012.
- [104] Sharda, R., "Neural Network for the MS/OR Analyst: An Application Bibliography Interfaces," pp. 166-130, 1994.
- [105] B. E. P. M. Y. H. Guoqiang Zhang, "Forecasting with artificial neural networks:: The state of the art," *International Journal of Forecasting*, vol. 14, no. 1, pp. 35-62, 1998.
- [106] White, H., "Learning in Artificial Neural Network:A Statistical Perspective Neural Computation I," pp. 425-466, 1989.
- [107] Ripley, B.D., "Statistical Aspect of Neural Network In : Barndroff-Nielsen, O.E., Jensen, J. L., Kendall, W.S., (Eds), Networks and Chaos-Statistical and Probabilistic Aspects," *Chopman & Hall*, pp. 40-123, 1993.
- [108] Cheng, B., Titterington, DM., "Neural Network : A Review from a Statistical Perspective," *Statistical Sci.*, pp. 2-54, 1994.
- [109] Irie, B., Miyake, S., "Capabilities of Three Layered Perceptrons," *In: Proc. Of the IEEE Int. Conf. on Neural Network I*, pp. 641-648, 1988.
- [110] Hornik, K., Stinchcombe, M., White, H., "Multilayer Feed Forward Network are Universal Approximators," *Neural Network*, pp. 359-366, 1989.
- [111] Cybenko, G., "Approximation by Superpositions of a Sigmoidal Function," *Mathematical Control Signal System2*, pp. 303-314, 1989.
- [112] Funahashi, K., "On the Approximate Realization of Continuous Map by Neural Network," *Neural Network 2*, pp. 183-192, 1989.

- [113] Hornik, K., "Approximation Capabilities of Multilayer Feed Forward Neural Network," *Neural Network*, pp. 251-257, 1991.
- [114] Hornik, K., "Some New Results on Neural Network Approximation," *Neural Network* 6, pp. 1069-1072, 1993.
- [115] Box, G.E.P., Jenkins, G.M., "TimeSeries Analysis : For Casting and Control," *Holden-Day, San Fransisco, C.A.*, 1976.
- [116] Pankratz, A., "Forecasting with Universalities Box-Jenkins Model : Concept and Cases John Wiley," 1983.
- [117] Granger, C.W.J., Terasvirta, T., "Modelling Non Linear Economic Relationship," *Oxford University Press, Oxford*, 1993.
- [118] Granger, C.W.T., Anderson, A.P., "An Introduction to Bilinear Time Series Models," *Vandenhoeck and Ruprecht, Gottingen*, 1978.
- [119] Tong, H., Lim, K.S., "Threshold Autoregressive, Limit cycles and Cyclical Data," *J. of the Roy, Statis.Soc.Series B*, pp. 245-292, 1980.
- [120] Guoqiang, Zhang, B., Eddy Patunio, Michaely, H.U., "Forecasting with Artificial Neural Network : The State of the Art," *Int. J. of Forecasting*, pp. 35-62, 1997.
- [121] [Online]. Available:
http://shodhganga.inflibnet.ac.in/bitstream/10603/58725/16/16_chapter%207.pdf.
- [122] Demuth Howard and Beale Mark, "Neural Network Toolbox User's Guide," *The MathWorks*, 2000.
- [123] Eldon R Rene, SM Maliyekkal, L Philip, T Swaminathan, "Back-propagation neural network for performance prediction in trickling bed air biofilter," *International Journal of Environment and Pollution*, vol. 28, no.

3, pp. 382-401.

- [124] Amutha, M. Moorthi and R., "Medical image compression using adaptive neural network," in *2012 International Conference on Emerging Trends in Science, Engineering and Technology (INCOSSET)*, Tiruchirappalli, 2012.
- [125] ME López, Eldon R Rene, Z Boger, MC Veiga, C Kennes, "Modelling the removal of volatile pollutants under transient conditions in a two-stage bioreactor using artificial neural networks," *Journal of Hazardous Materials*, vol. 324, pp. 100-109, Feb 2017.
- [126] Badri, Lubna, "Development of Neural Networks for Noise Reduction," *The International Arab Journal of Information Technology*, vol. 7, no. 3, pp. 289-294, July 2010.
- [127] K. Daqrouq, I. N. Abu-Isbeih and M. Alfauri, "Speech signal enhancement using neural network and wavelet transform," in *2009 6th International Multi-Conference on Systems, Signals and Devices*, Djerba, 2009.
- [128] Tapasya Pandit, Anil Dudy, "A FEED FORWARD ARTIFICIAL NEURAL NETWORK BASED SYSTEM TO MINIMIZE DOS ATTACK IN WIRELESS," *International Journal of Advances in Engineering & Technology*, vol. 7, no. 3, pp. 938-947, July 2014.
- [129] S. N. Sivanandam, S. N Deepa, Introduction to Neural Networks Using Matlab 6.0, Tata Mc-Graw Hill Education.
- [130] Sumathi, S., Ashok Kumar, L., Surekha, P., Solar PV and Wind Energy Conversion Systems : An Introduction to Theory, Modeling with MATLAB/SIMULINK, and the Role of Soft Computing Techniques, Springer International Publishing, 2015.
- [131] Nagaraj R, Thirugnanamurthy D, Rajput MM, "Modeling of Renewables

- based Hybrid Power System with Desalination Plant load using Neural Network," *Int. J of Distributed Generation & Alternate Energy*, vol. 34, no. 1, pp. 32-46, Dec 2018.
- [132] Farmad, H.S., & Biglar, S., "Integration of demand side management, distributed generation renewable energy sources and energy storage," Vols. 1,, no. No.4, 2012.
- [133] Oyedepo, S. O., Agbetuyi, A. F., & Odunfa, M. K., "Transmission network enhancement with renewable energy.," vol. 145, no. 5, 2014.
- [134] Sagar, K., & Goel, R., "Large scale grid amalgamation of renewable energy sources in indian power system.," vol. 3, no. 2, 2014.
- [135] [Online]. Available: <http://www.ijsetr.com>.
- [136] Rodriguez, C., & Amaratunga, G. A. J., "Long-lifetime power inverter for photovoltaic ac modules.," vol. 55, no. 7, 2008.
- [137] Shimizu, T., Wada, K., & Nakamura, N., "Flyback-type single-phase utility interactive inverter with power pulsation decoupling on the dc input for an ac photovoltaic module system.," vol. 21, no. 5, 2006.
- [138] Kjaer, S. B., Pedersen, J. K., & Blaabjerg, F., "A review of single-phase grid-connected inverters for photovoltaic modules.," vol. 41, no. 5, 2005.
- [139] Umeno, T. Takahashi, K., Ueno, F., Inoue, T., & Oota, I., "A new approach to low ripple-noise switching converters on the basis of switched-capacitor converters.," 1991.
- [140] Chen, S.-M., Liang, T.-J., Yang, L.-S., & Chen, J.-F., "A safety enhanced, high step-up DC-DC converter for AC photovoltaic module application.," vol. 27, no. 4, 2012.
- [141] Axelrod, B., Berkovich, Y., & Ioinovici, A., "Switched-capacitor/switched-

- inductor structures for getting transformerless hybrid dc-dc PWM converters.," vol. 55, no. 2, 2008.
- [142] Liang, T.-J., Chen, S.-M., Yang, L.-S., Chen, J.-F., & Ioinovici, A., "Ultra-large gain step-up switched-capacitor DC-DC converter with coupled inductor for alternative sources of energy.," vol. 59, no. 4, 2012.
- [143] Yang, L. S., & Liang, T. J., "Analysis and implementation of a novel bidirectional dc-dc converter.," vol. 59, no. 1, 2012.
- [144] Zhao, Q., & Lee, F. C., "High-efficiency, high step-up dc-dc converters.," vol. 18, no. 1, 2003.
- [145] Chen, S. M., Liang, T. J., Yang, L. S., & Chen, J. F., "A cascaded high step-up dc-dc converter with single switch for micro source applications.," vol. 26, no. 4, 2011.
- [146] Garcia-Valverde, R., Villarejo, J. A., Hosel, M., Madsen, M. V., Sondergaard, R. R., Jorgensen, M., et al., "Scalable single point power extraction for compact mobile and stand-alone solar harvesting power sources based on fully printed organic photovoltaic modules and efficient high voltage DC/DC conversion.," vol. 144, 2016.
- [147] R. Nagaraj, D. Thirugnanamurthy, Manik Murthy Rajput, B.K. Panigrahi, "Techno-economic analysis of hybrid power system sizing applied to small desalination plants for sustainable operation," *International Journal of Sustainable Built Environment*, vol. 5, no. 2, pp. 269-276, 2016.
- [148] Nagaraj, R., & Panigrahi, B. K., "Simulation and hardware implementation of FPGA based controller for hybrid power system.," *International Journal of Electrical Energy*, vol. 3, no. 2, 2015.
- [149] He, W. Li and X., "Review of Nonisolated High-Step-Up DC/DC

- Converters in Photovoltaic Grid-Connected Applications," *IEEE Transactions on Industrial Electronics*, vol. 58, no. 4, pp. 1239-1250, April 2011.
- [150] Nagaraj, R., Thiruganamurthy, D. & Rajput, M.M., "Modeling of high step-up converter in closed loop for renewable energy applications," *Environ Dev Sustain*, vol. 19, no. 6, p. 2475–2485, 2017.
- [151] Jang Jyh-Shing Roger, Sun Chuen-Tsai, Mizutani Eiji, "Neuro-Fuzzy Soft Computing, A Computational Approach to Learning and Machine Intelligence, Prentice Hall, Upper Saddle River," 1997.

Appendix - A

Table showing the performance of hybrid power system (cost of energy, % availability of power and total kWh produced for the year) with various capacity configurations of solar PV, wind and battery.

Combination No	PV kW	Wind kW	Battery kW	Cost of Energy (INR)	% availability	Total kWh produced per year
1	1	1	0.5	216	0.8	148
2	1	1	1	364	2.3	92
3	1	1	1.5	498	7.8	70
4	1	1	2	625	14.4	58
5	1	2	0.5	73	7.6	778
6	1	2	1	75	10.1	778
7	1	2	1.5	77	15.2	778
8	1	2	2	78	21.1	778
9	1	3	0.5	48	12.3	1712
10	1	3	1	48	15.6	1712
11	1	3	1.5	49	21.4	1712
12	1	3	2	50	27.1	1712
13	1	4	0.5	47	15.8	2268
14	1	4	1	47	20.0	2268
15	1	4	1.5	48	25.7	2268
16	1	4	2	49	31.6	2268
17	1	5	0.5	48	19.3	2754
18	1	5	1	48	23.7	2754
19	1	5	1.5	49	29.7	2754
20	1	5	2	49	35.3	2754
21	1	6	0.5	48	22.4	3244
22	1	6	1	48	27.5	3244
23	1	6	1.5	49	33.3	3244
24	1	6	2	49	38.7	3244
25	1	7	0.5	48	25.5	3732
26	1	7	1	49	30.8	3732

27	1	7	1.5	49	36.5	3732
28	1	7	2	50	41.8	3732
29	1	8	0.5	50	28.4	4144
30	1	8	1	50	33.6	4144
31	1	8	1.5	50	39.3	4144
32	1	8	2	51	44.6	4144
33	1	9	0.5	50	31.0	4600
34	1	9	1	50	36.2	4600
35	1	9	1.5	51	42.2	4600
36	1	9	2	51	47.2	4600
37	1	10	0.5	51	33.6	5000
38	1	10	1	51	38.9	5000
39	1	10	1.5	52	44.4	5000
40	1	10	2	52	49.5	5000
41	2	1	0.5	28	10.1	1368
42	2	1	1	30	13.7	1314
43	2	1	1.5	33	18.1	1226
44	2	1	2	36	21.9	1180
45	2	2	0.5	34	16.6	1818
46	2	2	1	35	20.6	1818
47	2	2	1.5	36	24.6	1818
48	2	2	2	37	28.2	1814
49	2	3	0.5	32	21.1	2738
50	2	3	1	32	25.6	2738
51	2	3	1.5	33	29.9	2738
52	2	3	2	33	33.6	2738
53	2	4	0.5	33	24.9	3374
54	2	4	1	34	29.4	3374
55	2	4	1.5	34	33.8	3374
56	2	4	2	34	37.9	3374
57	2	5	0.5	35	28.2	3962
58	2	5	1	35	32.8	3962
59	2	5	1.5	35	37.6	3962
60	2	5	2	36	41.4	3962
61	2	6	0.5	37	31.0	4428
62	2	6	1	37	35.8	4428
63	2	6	1.5	37	40.5	4428
64	2	6	2	37	44.6	4428

65	2	7	0.5	38	34.1	4940
66	2	7	1	38	38.8	4940
67	2	7	1.5	38	43.4	4940
68	2	7	2	39	47.4	4940
69	2	8	0.5	39	36.2	5364
70	2	8	1	40	41.0	5364
71	2	8	1.5	40	45.9	5364
72	2	8	2	40	49.8	5364
73	2	9	0.5	41	38.6	5760
74	2	9	1	41	43.3	5760
75	2	9	1.5	41	48.2	5760
76	2	9	2	42	52.0	5760
77	2	10	0.5	43	40.7	6106
78	2	10	1	43	45.6	6106
79	2	10	1.5	43	50.2	6106
80	2	10	2	43	54.1	6106
81	3	1	0.5	14	20.2	3226
82	3	1	1	14	23.7	3194
83	3	1	1.5	15	27.2	3146
84	3	1	2	15	30.4	3124
85	3	2	0.5	19	25.4	3580
86	3	2	1	20	29.2	3580
87	3	2	1.5	20	32.6	3578
88	3	2	2	20	35.7	3576
89	3	3	0.5	22	29.1	4332
90	3	3	1	22	33.3	4330
91	3	3	1.5	22	37.1	4328
92	3	3	2	23	40.4	4328
93	3	4	0.5	25	32.1	4816
94	3	4	1	25	36.3	4816
95	3	4	1.5	25	40.1	4816
96	3	4	2	25	43.8	4816
97	3	5	0.5	27	34.8	5262
98	3	5	1	27	39.1	5262
99	3	5	1.5	28	43.0	5262
100	3	5	2	28	46.6	5262
101	3	6	0.5	30	37.3	5670
102	3	6	1	30	41.7	5670

103	3	6	1.5	30	45.7	5670
104	3	6	2	30	49.4	5670
105	3	7	0.5	32	39.4	6060
106	3	7	1	32	44.0	6060
107	3	7	1.5	32	48.0	6060
108	3	7	2	32	51.7	6060
109	3	8	0.5	34	41.5	6446
110	3	8	1	34	46.0	6446
111	3	8	1.5	34	50.3	6446
112	3	8	2	34	54.0	6446
113	3	9	0.5	36	43.7	6748
114	3	9	1	36	48.0	6748
115	3	9	1.5	36	52.3	6748
116	3	9	2	36	55.9	6748
117	3	10	0.5	38	45.3	7054
118	3	10	1	38	49.9	7054
119	3	10	1.5	38	54.1	7054
120	3	10	2	38	57.7	7054
121	4	1	0.5	12	25.5	4228
122	4	1	1	12	28.7	4190
123	4	1	1.5	13	32.1	4168
124	4	1	2	13	34.9	4154
125	4	2	0.5	17	30.1	4480
126	4	2	1	17	33.5	4480
127	4	2	1.5	17	36.6	4480
128	4	2	2	18	39.5	4478
129	4	3	0.5	19	33.4	5174
130	4	3	1	19	37.1	5174
131	4	3	1.5	20	40.7	5174
132	4	3	2	20	43.8	5174
133	4	4	0.5	22	36.0	5564
134	4	4	1	23	39.8	5564
135	4	4	1.5	23	43.2	5564
136	4	4	2	23	46.6	5564
137	4	5	0.5	25	38.4	5980
138	4	5	1	25	42.3	5980
139	4	5	1.5	25	46.3	5980
140	4	5	2	26	49.4	5980

141	4	6	0.5	27	40.6	6316
142	4	6	1	28	44.5	6316
143	4	6	1.5	28	48.5	6316
144	4	6	2	28	51.9	6316
145	4	7	0.5	30	42.8	6694
146	4	7	1	30	46.8	6694
147	4	7	1.5	30	50.7	6694
148	4	7	2	30	54.2	6694
149	4	8	0.5	32	44.6	7036
150	4	8	1	32	48.6	7036
151	4	8	1.5	32	53.0	7036
152	4	8	2	32	56.3	7036
153	4	9	0.5	34	46.6	7362
154	4	9	1	34	50.7	7362
155	4	9	1.5	34	54.7	7362
156	4	9	2	34	58.0	7362
157	4	10	0.5	36	48.1	7646
158	4	10	1	36	52.3	7646
159	4	10	1.5	36	56.4	7646
160	4	10	2	36	59.7	7646
161	5	1	0.5	11	28.9	4910
162	5	1	1	12	31.8	4888
163	5	1	1.5	12	35.2	4868
164	5	1	2	12	37.9	4848
165	5	2	0.5	16	32.9	5142
166	5	2	1	16	36.2	5142
167	5	2	1.5	16	39.3	5140
168	5	2	2	16	42.2	5136
169	5	3	0.5	18	36.2	5756
170	5	3	1	19	39.6	5756
171	5	3	1.5	19	43.0	5756
172	5	3	2	19	46.0	5756
173	5	4	0.5	21	38.5	6138
174	5	4	1	21	42.2	6138
175	5	4	1.5	22	45.6	6138
176	5	4	2	22	48.8	6138
177	5	5	0.5	24	40.7	6478
178	5	5	1	24	44.4	6478

179	5	5	1.5	24	48.1	6478
180	5	5	2	25	51.2	6478
181	5	6	0.5	26	42.9	6806
182	5	6	1	27	46.5	6806
183	5	6	1.5	27	50.3	6806
184	5	6	2	27	53.6	6806
185	5	7	0.5	28	44.8	7174
186	5	7	1	29	48.7	7174
187	5	7	1.5	29	52.5	7174
188	5	7	2	29	55.8	7174
189	5	8	0.5	31	46.5	7484
190	5	8	1	31	50.4	7484
191	5	8	1.5	31	54.4	7484
192	5	8	2	31	57.8	7484
193	5	9	0.5	33	48.4	7774
194	5	9	1	33	52.1	7774
195	5	9	1.5	33	56.2	7774
196	5	9	2	33	59.5	7774
197	5	10	0.5	35	49.8	8018
198	5	10	1	35	53.8	8018
199	5	10	1.5	35	57.6	8018
200	5	10	2	35	61.0	8018
201	6	1	0.5	11	31.3	5356
202	6	1	1	12	34.0	5346
203	6	1	1.5	12	37.2	5330
204	6	1	2	12	39.9	5316
205	6	2	0.5	16	35.1	5550
206	6	2	1	16	38.2	5548
207	6	2	1.5	16	41.1	5548
208	6	2	2	16	43.8	5548
209	6	3	0.5	18	38.0	6166
210	6	3	1	18	41.3	6166
211	6	3	1.5	18	44.6	6166
212	6	3	2	19	47.4	6166
213	6	4	0.5	21	40.2	6496
214	6	4	1	21	43.8	6496
215	6	4	1.5	21	47.1	6496
216	6	4	2	22	50.1	6496

217	6	5	0.5	24	42.5	6820
218	6	5	1	24	45.9	6820
219	6	5	1.5	24	49.6	6820
220	6	5	2	24	52.5	6820
221	6	6	0.5	26	44.5	7164
222	6	6	1	26	48.1	7164
223	6	6	1.5	26	51.7	7164
224	6	6	2	26	54.9	7164
225	6	7	0.5	28	46.3	7480
226	6	7	1	28	50.1	7480
227	6	7	1.5	28	53.7	7480
228	6	7	2	29	57.1	7480
229	6	8	0.5	30	48.0	7756
230	6	8	1	30	51.7	7756
231	6	8	1.5	31	55.5	7756
232	6	8	2	31	58.9	7756
233	6	9	0.5	32	49.6	8034
234	6	9	1	32	53.4	8034
235	6	9	1.5	33	57.2	8034
236	6	9	2	33	60.5	8034
237	6	10	0.5	34	50.9	8264
238	6	10	1	35	55.0	8264
239	6	10	1.5	35	58.6	8264
240	6	10	2	35	61.9	8264
241	7	1	0.5	12	33.2	5698
242	7	1	1	12	36.0	5688
243	7	1	1.5	12	38.8	5670
244	7	1	2	13	41.4	5664
245	7	2	0.5	16	36.8	5860
246	7	2	1	16	39.8	5860
247	7	2	1.5	16	42.5	5860
248	7	2	2	16	45.1	5860
249	7	3	0.5	18	39.6	6464
250	7	3	1	18	42.9	6464
251	7	3	1.5	19	45.9	6464
252	7	3	2	19	48.6	6462
253	7	4	0.5	21	41.8	6776
254	7	4	1	21	45.2	6776

255	7	4	1.5	21	48.3	6776
256	7	4	2	22	51.3	6776
257	7	5	0.5	23	43.9	7082
258	7	5	1	24	47.1	7082
259	7	5	1.5	24	50.8	7082
260	7	5	2	24	53.5	7082
261	7	6	0.5	26	45.7	7410
262	7	6	1	26	49.2	7410
263	7	6	1.5	26	52.7	7410
264	7	6	2	26	55.8	7410
265	7	7	0.5	28	47.4	7718
266	7	7	1	28	51.2	7718
267	7	7	1.5	28	54.7	7718
268	7	7	2	29	57.8	7718
269	7	8	0.5	30	49.1	7976
270	7	8	1	30	52.6	7976
271	7	8	1.5	31	56.3	7976
272	7	8	2	31	59.7	7976
273	7	9	0.5	32	50.8	8256
274	7	9	1	32	54.4	8256
275	7	9	1.5	32	58.0	8256
276	7	9	2	33	61.4	8256
277	7	10	0.5	34	52.1	8474
278	7	10	1	34	55.8	8474
279	7	10	1.5	35	59.4	8474
280	7	10	2	35	62.8	8474
281	8	1	0.5	12	34.8	5998
282	8	1	1	12	37.3	5986
283	8	1	1.5	13	40.0	5974
284	8	1	2	13	42.4	5954
285	8	2	0.5	16	38.3	6140
286	8	2	1	16	41.1	6140
287	8	2	1.5	16	43.5	6138
288	8	2	2	17	46.2	6138
289	8	3	0.5	18	40.9	6700
290	8	3	1	19	44.0	6700
291	8	3	1.5	19	47.0	6700
292	8	3	2	19	49.6	6700

293	8	4	0.5	21	43.0	7006
294	8	4	1	21	46.1	7006
295	8	4	1.5	21	49.2	7006
296	8	4	2	22	52.2	7004
297	8	5	0.5	24	45.0	7318
298	8	5	1	24	48.1	7318
299	8	5	1.5	24	51.6	7318
300	8	5	2	24	54.5	7318
301	8	6	0.5	26	46.8	7618
302	8	6	1	26	50.2	7618
303	8	6	1.5	26	53.6	7618
304	8	6	2	26	56.6	7618
305	8	7	0.5	28	48.4	7918
306	8	7	1	28	52.1	7918
307	8	7	1.5	28	55.4	7918
308	8	7	2	29	58.7	7918
309	8	8	0.5	30	50.2	8172
310	8	8	1	30	53.6	8172
311	8	8	1.5	31	57.1	8172
312	8	8	2	31	60.4	8172
313	8	9	0.5	32	51.7	8404
314	8	9	1	32	55.1	8404
315	8	9	1.5	33	58.7	8404
316	8	9	2	33	62.0	8404
317	8	10	0.5	34	52.8	8626
318	8	10	1	34	56.4	8626
319	8	10	1.5	35	60.0	8626
320	8	10	2	35	63.3	8626
321	9	1	0.5	13	36.3	6238
322	9	1	1	13	38.5	6214
323	9	1	1.5	13	41.1	6206
324	9	1	2	13	43.5	6196
325	9	2	0.5	16	39.4	6362
326	9	2	1	17	42.1	6362
327	9	2	1.5	17	44.5	6362
328	9	2	2	17	46.9	6360
329	9	3	0.5	19	42.0	6926
330	9	3	1	19	44.9	6926

331	9	3	1.5	19	47.8	6926
332	9	3	2	19	50.4	6926
333	9	4	0.5	21	44.1	7210
334	9	4	1	21	47.1	7210
335	9	4	1.5	22	50.0	7210
336	9	4	2	22	52.9	7210
337	9	5	0.5	24	46.0	7504
338	9	5	1	24	49.0	7504
339	9	5	1.5	24	52.3	7504
340	9	5	2	24	55.1	7504
341	9	6	0.5	26	47.7	7802
342	9	6	1	26	50.9	7802
343	9	6	1.5	26	54.3	7802
344	9	6	2	27	57.4	7802
345	9	7	0.5	28	49.3	8078
346	9	7	1	28	52.9	8078
347	9	7	1.5	29	55.9	8078
348	9	7	2	29	59.3	8078
349	9	8	0.5	30	50.8	8316
350	9	8	1	31	54.3	8316
351	9	8	1.5	31	57.7	8316
352	9	8	2	31	60.9	8316
353	9	9	0.5	32	52.3	8566
354	9	9	1	33	55.8	8566
355	9	9	1.5	33	59.2	8566
356	9	9	2	33	62.6	8566
357	9	10	0.5	34	53.5	8794
358	9	10	1	34	57.2	8794
359	9	10	1.5	35	60.6	8794
360	9	10	2	35	63.9	8794
361	10	1	0.5	13	37.5	6478
362	10	1	1	13	39.5	6466
363	10	1	1.5	14	42.0	6454
364	10	1	2	14	44.1	6440
365	10	2	0.5	17	40.4	6586
366	10	2	1	17	43.0	6586
367	10	2	1.5	17	45.4	6586
368	10	2	2	17	47.6	6586

369	10	3	0.5	19	43.0	7132
370	10	3	1	19	45.8	7132
371	10	3	1.5	19	48.6	7132
372	10	3	2	19	51.1	7132
373	10	4	0.5	22	44.9	7396
374	10	4	1	22	47.7	7396
375	10	4	1.5	22	50.7	7396
376	10	4	2	22	53.5	7396
377	10	5	0.5	24	46.8	7696
378	10	5	1	24	49.6	7696
379	10	5	1.5	24	52.9	7696
380	10	5	2	24	55.7	7696
381	10	6	0.5	26	48.3	7964
382	10	6	1	26	51.7	7964
383	10	6	1.5	27	54.8	7964
384	10	6	2	27	57.9	7964
385	10	7	0.5	28	49.9	8226
386	10	7	1	29	53.4	8226
387	10	7	1.5	29	56.6	8226
388	10	7	2	29	59.7	8226
389	10	8	0.5	31	51.5	8454
390	10	8	1	31	54.8	8454
391	10	8	1.5	31	58.3	8454
392	10	8	2	31	61.4	8454
393	10	9	0.5	32	53.0	8712
394	10	9	1	33	56.2	8712
395	10	9	1.5	33	59.7	8712
396	10	9	2	33	63.0	8712
397	10	10	0.5	35	54.2	8912
398	10	10	1	35	57.6	8912
399	10	10	1.5	35	61.0	8912
400	10	10	2	35	64.2	8912

Appendix - B

Table showing the power utilized with various combinations of hybrid power with constant load and with desalination plant as load.

Combination no.	PV kW	Wind kW	Battery kW	Total kWh per year		Water produced m3/year
				Total kWh per year With constant load	with desal load	
1	1	1	0.5	148	2557	3240
2	1	1	1	92	2557	2463
3	1	1	1.5	70	2557	2005
4	1	1	2	58	2557	1825
5	1	2	0.5	778	3901	2640
6	1	2	1	778	3901	2628
7	1	2	1.5	778	3901	2620
8	1	2	2	778	3901	2612
9	1	3	0.5	1712	4928	3240
10	1	3	1	1712	4928	2463
11	1	3	1.5	1712	4928	2005
12	1	3	2	1712	4928	1825
13	1	4	0.5	2268	5738	2640
14	1	4	1	2268	5738	2628
15	1	4	1.5	2268	5738	2620
16	1	4	2	2268	5738	2612
17	1	5	0.5	2754	6459	3294
18	1	5	1	2754	6459	3292
19	1	5	1.5	2754	6459	3291
20	1	5	2	2754	6459	3288
21	1	6	0.5	3244	7087	3825
22	1	6	1	3244	7087	3825
23	1	6	1.5	3244	7087	3825

24	1	6	2	3244	7087	3825
25	1	7	0.5	3732	7673	4306
26	1	7	1	3732	7673	4306
27	1	7	1.5	3732	7673	4306
28	1	7	2	3732	7673	4306
29	1	8	0.5	4144	8185	4724
30	1	8	1	4144	8185	4724
31	1	8	1.5	4144	8185	4724
32	1	8	2	4144	8185	4724
33	1	9	0.5	4600	8652	5115
34	1	9	1	4600	8652	5115
35	1	9	1.5	4600	8652	5115
36	1	9	2	4600	8652	5115
37	1	10	0.5	5000	9077	5457
38	1	10	1	5000	9077	5457
39	1	10	1.5	5000	9077	5457
40	1	10	2	5000	9077	5457
41	2	1	0.5	1368	5667	5768
42	2	1	1	1314	5111	5768
43	2	1	1.5	1226	4773	5768
44	2	1	2	1180	4628	5768
45	2	2	0.5	1818	5585	6051
46	2	2	1	1818	5583	6051
47	2	2	1.5	1818	5581	6051
48	2	2	2	1814	5571	6051
49	2	3	0.5	2738	6404	3778
50	2	3	1	2738	6404	3407
51	2	3	1.5	2738	6404	3182
52	2	3	2	2738	6404	3085
53	2	4	0.5	3374	7088	3723
54	2	4	1	3374	7088	3722
55	2	4	1.5	3374	7088	3721
56	2	4	2	3374	7088	3714
57	2	5	0.5	3962	7702	4269
58	2	5	1	3962	7702	4269
59	2	5	1.5	3962	7702	4269
60	2	5	2	3962	7702	4269
61	2	6	0.5	4428	8228	4725

62	2	6	1	4428	8228	4725
63	2	6	1.5	4428	8228	4725
64	2	6	2	4428	8228	4725
65	2	7	0.5	4940	8716	5134
66	2	7	1	4940	8716	5134
67	2	7	1.5	4940	8716	5134
68	2	7	2	4940	8716	5134
69	2	8	0.5	5364	9153	5485
70	2	8	1	5364	9153	5485
71	2	8	1.5	5364	9153	5485
72	2	8	2	5364	9153	5485
73	2	9	0.5	5760	9552	5811
74	2	9	1	5760	9552	5811
75	2	9	1.5	5760	9552	5811
76	2	9	2	5760	9552	5811
77	2	10	0.5	6106	9918	6102
78	2	10	1	6106	9918	6102
79	2	10	1.5	6106	9918	6102
80	2	10	2	6106	9918	6102
81	3	1	0.5	3226	6743	6368
82	3	1	1	3194	6277	6368
83	3	1	1.5	3146	6026	6368
84	3	1	2	3124	5912	6368
85	3	2	0.5	3580	6619	6612
86	3	2	1	3580	6613	6612
87	3	2	1.5	3578	6606	6612
88	3	2	2	3576	6601	6612
89	3	3	0.5	4332	7281	4495
90	3	3	1	4330	7281	4185
91	3	3	1.5	4328	7281	4018
92	3	3	2	4328	7281	3942
93	3	4	0.5	4816	7862	4413
94	3	4	1	4816	7862	4409
95	3	4	1.5	4816	7862	4404
96	3	4	2	4816	7862	4401
97	3	5	0.5	5262	8396	4854
98	3	5	1	5262	8396	4854
99	3	5	1.5	5262	8396	4854

100	3	5	2	5262	8396	4854
101	3	6	0.5	5670	8868	5242
102	3	6	1	5670	8868	5242
103	3	6	1.5	5670	8868	5242
104	3	6	2	5670	8868	5242
105	3	7	0.5	6060	9306	5597
106	3	7	1	6060	9306	5597
107	3	7	1.5	6060	9306	5597
108	3	7	2	6060	9306	5597
109	3	8	0.5	6446	9701	5912
110	3	8	1	6446	9701	5912
111	3	8	1.5	6446	9701	5912
112	3	8	2	6446	9701	5912
113	3	9	0.5	6748	10062	6204
114	3	9	1	6748	10062	6204
115	3	9	1.5	6748	10062	6204
116	3	9	2	6748	10062	6204
117	3	10	0.5	7054	10401	6467
118	3	10	1	7054	10401	6467
119	3	10	1.5	7054	10401	6467
120	3	10	2	7054	10401	6467
121	4	1	0.5	4228	7324	6708
122	4	1	1	4190	6884	6708
123	4	1	1.5	4168	6661	6708
124	4	1	2	4154	6567	6708
125	4	2	0.5	4480	7167	6934
126	4	2	1	4480	7167	6934
127	4	2	1.5	4480	7165	6934
128	4	2	2	4478	7161	6934
129	4	3	0.5	5174	7774	4883
130	4	3	1	5174	7774	4589
131	4	3	1.5	5174	7774	4440
132	4	3	2	5174	7774	4378
133	4	4	0.5	5564	8302	4778
134	4	4	1	5564	8302	4778
135	4	4	1.5	5564	8302	4777
136	4	4	2	5564	8302	4774
137	4	5	0.5	5980	8799	5182

138	4	5	1	5980	8799	5182
139	4	5	1.5	5980	8799	5182
140	4	5	2	5980	8799	5182
141	4	6	0.5	6316	9240	5535
142	4	6	1	6316	9240	5535
143	4	6	1.5	6316	9240	5535
144	4	6	2	6316	9240	5535
145	4	7	0.5	6694	9650	5866
146	4	7	1	6694	9650	5866
147	4	7	1.5	6694	9650	5866
148	4	7	2	6694	9650	5866
149	4	8	0.5	7036	10019	6160
150	4	8	1	7036	10019	6160
151	4	8	1.5	7036	10019	6160
152	4	8	2	7036	10019	6160
153	4	9	0.5	7362	10360	6433
154	4	9	1	7362	10360	6433
155	4	9	1.5	7362	10360	6433
156	4	9	2	7362	10360	6433
157	4	10	0.5	7646	10678	6679
158	4	10	1	7646	10678	6679
159	4	10	1.5	7646	10678	6679
160	4	10	2	7646	10678	6679
161	5	1	0.5	4910	7711	6906
162	5	1	1	4888	7319	6906
163	5	1	1.5	4868	7080	6906
164	5	1	2	4848	6985	6906
165	5	2	0.5	5142	7520	7118
166	5	2	1	5142	7520	7118
167	5	2	1.5	5140	7517	7118
168	5	2	2	5136	7517	7118
169	5	3	0.5	5756	8093	5140
170	5	3	1	5756	8093	4879
171	5	3	1.5	5756	8092	4720
172	5	3	2	5756	8092	4657
173	5	4	0.5	6138	8597	5013
174	5	4	1	6138	8597	5013
175	5	4	1.5	6138	8597	5011

176	5	4	2	6138	8597	5011
177	5	5	0.5	6478	9066	5395
178	5	5	1	6478	9066	5395
179	5	5	1.5	6478	9066	5395
180	5	5	2	6478	9066	5394
181	5	6	0.5	6806	9483	5731
182	5	6	1	6806	9483	5731
183	5	6	1.5	6806	9483	5731
184	5	6	2	6806	9483	5731
185	5	7	0.5	7174	9877	6044
186	5	7	1	7174	9877	6044
187	5	7	1.5	7174	9877	6044
188	5	7	2	7174	9877	6044
189	5	8	0.5	7484	10227	6322
190	5	8	1	7484	10227	6322
191	5	8	1.5	7484	10227	6322
192	5	8	2	7484	10227	6322
193	5	9	0.5	7774	10558	6585
194	5	9	1	7774	10558	6585
195	5	9	1.5	7774	10558	6585
196	5	9	2	7774	10558	6585
197	5	10	0.5	8018	10861	6818
198	5	10	1	8018	10861	6818
199	5	10	1.5	8018	10861	6818
200	5	10	2	8018	10861	6818
201	6	1	0.5	5356	8001	7039
202	6	1	1	5346	7632	7039
203	6	1	1.5	5330	7406	7039
204	6	1	2	5316	7302	7039
205	6	2	0.5	5550	7807	7240
206	6	2	1	5548	7806	7240
207	6	2	1.5	5548	7804	7240
208	6	2	2	5548	7804	7240
209	6	3	0.5	6166	8346	5334
210	6	3	1	6166	8346	5088
211	6	3	1.5	6166	8346	4938
212	6	3	2	6166	8346	4868
213	6	4	0.5	6496	8820	5205

214	6	4	1	6496	8820	5204
215	6	4	1.5	6496	8820	5203
216	6	4	2	6496	8820	5202
217	6	5	0.5	6820	9266	5564
218	6	5	1	6820	9266	5564
219	6	5	1.5	6820	9266	5564
220	6	5	2	6820	9266	5564
221	6	6	0.5	7164	9667	5880
222	6	6	1	7164	9667	5880
223	6	6	1.5	7164	9667	5880
224	6	6	2	7164	9667	5880
225	6	7	0.5	7480	10044	6177
226	6	7	1	7480	10044	6177
227	6	7	1.5	7480	10044	6177
228	6	7	2	7480	10044	6177
229	6	8	0.5	7756	10384	6444
230	6	8	1	7756	10384	6444
231	6	8	1.5	7756	10384	6444
232	6	8	2	7756	10384	6444
233	6	9	0.5	8034	10704	6696
234	6	9	1	8034	10704	6696
235	6	9	1.5	8034	10704	6696
236	6	9	2	8034	10704	6696
237	6	10	0.5	8264	11000	6922
238	6	10	1	8264	11000	6922
239	6	10	1.5	8264	11000	6922
240	6	10	2	8264	11000	6922
241	7	1	0.5	5698	8221	7136
242	7	1	1	5688	7846	7136
243	7	1	1.5	5670	7637	7136
244	7	1	2	5664	7537	7136
245	7	2	0.5	5860	8027	7334
246	7	2	1	5860	8027	7334
247	7	2	1.5	5860	8025	7334
248	7	2	2	5860	8023	7334
249	7	3	0.5	6464	8532	5481
250	7	3	1	6464	8532	5231
251	7	3	1.5	6464	8532	5091

252	7	3	2	6462	8531	5025
253	7	4	0.5	6776	8986	5351
254	7	4	1	6776	8986	5351
255	7	4	1.5	6776	8986	5350
256	7	4	2	6776	8986	5349
257	7	5	0.5	7082	9421	5688
258	7	5	1	7082	9421	5688
259	7	5	1.5	7082	9421	5688
260	7	5	2	7082	9421	5687
261	7	6	0.5	7410	9809	5991
262	7	6	1	7410	9809	5991
263	7	6	1.5	7410	9809	5991
264	7	6	2	7410	9809	5991
265	7	7	0.5	7718	10178	6281
266	7	7	1	7718	10178	6281
267	7	7	1.5	7718	10178	6281
268	7	7	2	7718	10178	6281
269	7	8	0.5	7976	10510	6539
270	7	8	1	7976	10510	6539
271	7	8	1.5	7976	10510	6539
272	7	8	2	7976	10510	6539
273	7	9	0.5	8256	10822	6785
274	7	9	1	8256	10822	6785
275	7	9	1.5	8256	10822	6785
276	7	9	2	8256	10822	6785
277	7	10	0.5	8474	11112	7007
278	7	10	1	8474	11112	7007
279	7	10	1.5	8474	11112	7007
280	7	10	2	8474	11112	7007
281	8	1	0.5	5998	8405	7215
282	8	1	1	5986	8031	7215
283	8	1	1.5	5974	7837	7215
284	8	1	2	5954	7740	7215
285	8	2	0.5	6140	8192	7408
286	8	2	1	6140	8192	7408
287	8	2	1.5	6138	8192	7408
288	8	2	2	6138	8189	7408
289	8	3	0.5	6700	8679	5603

290	8	3	1	6700	8679	5354
291	8	3	1.5	6700	8679	5225
292	8	3	2	6700	8678	5160
293	8	4	0.5	7006	9120	5461
294	8	4	1	7006	9120	5461
295	8	4	1.5	7006	9120	5461
296	8	4	2	7004	9120	5459
297	8	5	0.5	7318	9545	5786
298	8	5	1	7318	9545	5786
299	8	5	1.5	7318	9545	5786
300	8	5	2	7318	9545	5785
301	8	6	0.5	7618	9921	6080
302	8	6	1	7618	9921	6080
303	8	6	1.5	7618	9921	6080
304	8	6	2	7618	9921	6080
305	8	7	0.5	7918	10283	6363
306	8	7	1	7918	10283	6363
307	8	7	1.5	7918	10283	6363
308	8	7	2	7918	10283	6363
309	8	8	0.5	8172	10609	6614
310	8	8	1	8172	10609	6614
311	8	8	1.5	8172	10609	6614
312	8	8	2	8172	10609	6614
313	8	9	0.5	8404	10915	6855
314	8	9	1	8404	10915	6855
315	8	9	1.5	8404	10915	6855
316	8	9	2	8404	10915	6855
317	8	10	0.5	8626	11200	7072
318	8	10	1	8626	11200	7072
319	8	10	1.5	8626	11200	7072
320	8	10	2	8626	11200	7072
321	9	1	0.5	6238	8532	7277
322	9	1	1	6214	8171	7277
323	9	1	1.5	6206	7993	7277
324	9	1	2	6196	7904	7277
325	9	2	0.5	6362	8326	7467
326	9	2	1	6362	8325	7467
327	9	2	1.5	6362	8323	7467

328	9	2	2	6360	8320	7467
329	9	3	0.5	6926	8796	5688
330	9	3	1	6926	8796	5448
331	9	3	1.5	6926	8796	5329
332	9	3	2	6926	8796	5269
333	9	4	0.5	7210	9229	5551
334	9	4	1	7210	9229	5550
335	9	4	1.5	7210	9229	5549
336	9	4	2	7210	9229	5547
337	9	5	0.5	7504	9643	5864
338	9	5	1	7504	9643	5864
339	9	5	1.5	7504	9643	5864
340	9	5	2	7504	9643	5864
341	9	6	0.5	7802	10014	6153
342	9	6	1	7802	10014	6153
343	9	6	1.5	7802	10014	6153
344	9	6	2	7802	10014	6153
345	9	7	0.5	8078	10367	6429
346	9	7	1	8078	10367	6429
347	9	7	1.5	8078	10367	6429
348	9	7	2	8078	10367	6429
349	9	8	0.5	8316	10689	6676
350	9	8	1	8316	10689	6676
351	9	8	1.5	8316	10689	6676
352	9	8	2	8316	10689	6676
353	9	9	0.5	8566	10990	6911
354	9	9	1	8566	10990	6911
355	9	9	1.5	8566	10990	6911
356	9	9	2	8566	10990	6911
357	9	10	0.5	8794	11270	7126
358	9	10	1	8794	11270	7126
359	9	10	1.5	8794	11270	7126
360	9	10	2	8794	11270	7126
361	10	1	0.5	6478	8660	7327
362	10	1	1	6466	8311	7327
363	10	1	1.5	6454	8123	7327
364	10	1	2	6440	8043	7327
365	10	2	0.5	6586	8440	7514

366	10	2	1	6586	8438	7514
367	10	2	1.5	6586	8438	7514
368	10	2	2	6586	8435	7514
369	10	3	0.5	7132	8901	5773
370	10	3	1	7132	8901	5540
371	10	3	1.5	7132	8901	5415
372	10	3	2	7132	8901	5362
373	10	4	0.5	7396	9326	5626
374	10	4	1	7396	9326	5626
375	10	4	1.5	7396	9326	5626
376	10	4	2	7396	9326	5623
377	10	5	0.5	7696	9735	5934
378	10	5	1	7696	9735	5934
379	10	5	1.5	7696	9735	5934
380	10	5	2	7696	9735	5934
381	10	6	0.5	7964	10097	6218
382	10	6	1	7964	10097	6218
383	10	6	1.5	7964	10097	6218
384	10	6	2	7964	10097	6218
385	10	7	0.5	8226	10444	6490
386	10	7	1	8226	10444	6490
387	10	7	1.5	8226	10444	6490
388	10	7	2	8226	10444	6490
389	10	8	0.5	8454	10759	6731
390	10	8	1	8454	10759	6731
391	10	8	1.5	8454	10759	6731
392	10	8	2	8454	10759	6731
393	10	9	0.5	8712	11056	6963
394	10	9	1	8712	11056	6963
395	10	9	1.5	8712	11056	6963
396	10	9	2	8712	11056	6963
397	10	10	0.5	8912	11332	7173
398	10	10	1	8912	11332	7173
399	10	10	1.5	8912	11332	7173
400	10	10	2	8912	11332	7173